Applied Mathematics and Computation 440 (2023) 127629

Contents lists available at ScienceDirect

Applied Mathematics and Computation

journal homepage: www.elsevier.com/locate/amc

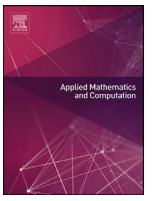

A simple and general framework for the construction of thermodynamically compatible schemes for computational fluid and solid mechanics

Rémi Abgrall[a], Saray Busto[b,*], Michael Dumbser[c]

[a] Institute of Mathematics, University of Zürich, Winterthurerstrasse 190, Zürich CH-8057, Switzerland
[b] Departamento de Matemática Aplicada I, Universidade de Vigo, Campus As Lagoas Marcosende s/n, Vigo E-36310, Spain
[c] Laboratory of Applied Mathematics, DICAM, University of Trento, via Mesiano 77, Trento I-38123, Italy

ARTICLE INFO

Article history:
Available online 11 November 2022

Keywords:
Hyperbolic and thermodynamically compatible (HTC) systems with extra conservation law
Entropy inequality
Nonlinear stability in the energy norm
Thermodynamically compatible finite volume schemes
Thermodynamically compatible discontinuous Galerkin schemes
Unified first order hyperbolic formulation of continuum mechanics

ABSTRACT

We introduce a simple and general framework for the construction of thermodynamically compatible schemes for the numerical solution of overdetermined hyperbolic PDE systems that satisfy an *extra conservation law*. As a particular example in this paper, we consider the general Godunov-Peshkov-Romenski (GPR) model of continuum mechanics that describes the dynamics of nonlinear solids and viscous fluids in one single unified mathematical formalism.

A main peculiarity of the new algorithms presented in this manuscript is that the *entropy inequality* is solved as a primary evolution equation instead of the usual total energy conservation law, unlike in most traditional schemes for hyperbolic PDE. Instead, total energy conservation is obtained as a mere *consequence* of the proposed thermodynamically compatible discretization. The approach is based on the general framework introduced in Abgrall (2018) [1]. In order to show the universality of the concept proposed in this paper, we apply our new formalism to the construction of three different numerical methods. First, we construct a thermodynamically compatible finite volume (FV) scheme on collocated Cartesian grids, where discrete thermodynamic compatibility is achieved via an edge/face-based correction that makes the numerical flux thermodynamically compatible. Second, we design a first type of high order accurate and thermodynamically compatible discontinuous Galerkin (DG) schemes that employs the same edge/face-based numerical fluxes that were already used inside the finite volume schemes. And third, we introduce a second type of thermodynamically compatible DG schemes, in which thermodynamic compatibility is achieved via an *element-wise* correction, instead of the *edge/face-based* corrections that were used within the compatible numerical fluxes of the former two methods. All methods proposed in this paper can be proven to be nonlinearly stable in the energy norm and they all satisfy a discrete entropy inequality *by construction*. We present numerical results obtained with the new thermodynamically compatible schemes in one and two space dimensions for a large set of benchmark problems, including inviscid and viscous fluids as well as solids. An interesting finding made in this paper is that, in numerical experiments, one can observe that for smooth isentropic flows the particular formulation of the new schemes in terms of entropy density, instead of total energy density, as primary

* Corresponding author.
E-mail addresses: remi.abgrall@math.uzh.ch (R. Abgrall), saray.busto@unitn.it (S. Busto), michael.dumbser@unitn.it (M. Dumbser).

https://doi.org/10.1016/j.amc.2022.127629

state variable leads to approximately twice the convergence rate of high order DG schemes for the entropy density.

1. Introduction

The seminal paper *An interesting class of quasilinear systems* published by Godunov in 1961 established for the first time the connection between symmetric hyperbolicity in the sense of Friedrichs [2] and thermodynamic compatibility, see [3]. Godunov showed that, for hyperbolic systems which have an underlying variational formulation, the total energy conservation law is an *extra conservation law* that can be obtained as a *consequence* of all the other equations via their suitable linear combination at the aid of the so-called thermodynamic dual variables, which are the partial derivatives of the total energy potential with respect to the conservative variables. The formalism introduced by Godunov was rediscovered independently 10 years later by Friedrichs and Lax [4]. Important contributions to the subject were also made by Boillat [5] and Ruggeri [6]. In [6] the thermodynamic dual variables were denoted as the so-called *main field*, while other works refer to them as the *Godunov variables*, see e.g. [7].

The results obtained in the original paper of Godunov [3] apply to the Euler equations of gas dynamics, to the shallow water equations and other simple inviscid hyperbolic systems in conservation form and without involution constraints. In subsequent work Godunov and Romenski extended the theory of symmetric hyperbolic and thermodynamically compatible (SHTC) systems to a much wider class of mathematical models, including magnetohydrodynamics [8], nonlinear hyperelasticity [9], compressible multi-phase flows [10,11] and even relativistic fluid and solid mechanics, see [12,13]. An extension to continuum mechanics with torsion was made in Peshkov et al. [14], while a connection of SHTC systems with Hamiltonian continuum mechanics was recently established in [15]. A rather general presentation of the overall formalism can be found in [16], and [17].

Usually in SHTC systems the entropy density is the *primary evolution variable*, while the conservation law for the total energy density is the *extra conservation law*, since it can be obtained as a *consequence* by a suitable linear combination of all the other evolution equations. The total energy potential has a privileged role in SHTC systems, because it is used in the Lagrangian of the underlying variational principle from which all SHTC systems can be derived. For other recent and very interesting hyperbolic and thermodynamically compatible systems based on an augmented Lagrangian approach for the derivation of hyperbolic models of dispersive systems via variational principles, see e.g. [18,19].

Most of the existing entropy preserving and entropy-stable schemes are built on the seminal ideas of Tadmor [20]. They discretize the total energy conservation directly and obtain a discrete compatibility with the entropy inequality as a consequence, mimicking the ideas of Friedrichs and Lax [4] on the discrete level. Also numerical schemes which are discretely compatible with kinetic energy preservation for the Euler equations fall into the larger class of schemes that satisfy additional extra conservation laws of the governing PDE system at the discrete level. Important contributions to the development of kinetic energy compatible and entropy compatible finite difference schemes for hyperbolic PDE that make use of skew symmetric forms and/or a discrete summation by parts (SBP) property can be found, for example, in the papers of Ducros et al. [21,22], Fisher et al. [23,24], Carpenter and Nordström et al. [25–28], Pirozzoli [29,30], Sjögreen and Yee [31–33] and in Reiss and Sesterhenn [34]. Without pretending completeness of the following overview, important recent developments on high order entropy-compatible schemes can be found, for example, in the work of Mishra and collaborators [35–37], Gassner et al., [38–42], Shu and collaborators [43,44] and in Chandrashekar and Klingenberg [45], Ray et al. [46], Ray and Chandrashekar [47], Chan and Taylor [48], Chan et al. [49], Gaburro et al. [50], while entropy-compatible schemes for non-conservative hyperbolic systems were presented in Fjordholm and Mishra [51].

A simple and general framework for the construction of compatible numerical methods which satisfy extra conservation laws at the discrete level was very recently put forward by Abgrall and collaborators in [1,52–55] and will also be the basis of the schemes presented in this paper.

In Lagrangian hydrodynamics thermodynamically compatible schemes have been developed in order to obtain the total energy conservation as a consequence of a compatible discretization of the equations of continuity, momentum and internal energy, see Caramana and R.Loubère [56], Bauera et al. [57], Maire et al. [58]. However, these schemes apply only to hydrodynamics and not to the GPR model of continuum mechanics treated in this paper.

Up to now, finite volume and discontinuous Galerkin methods that discretize directly the entropy inequality and which are able to obtain the total energy conservation law as a consequence of the compatible discretization of all the other equations are still quite rare. First progress in this direction has been recently made in Busto et al. [59–61], where a novel family of thermodynamically compatible finite volume schemes was introduced for turbulent shallow water flows, for the Euler and MHD equations, as well as for the GPR model of continuum mechanics. In [60,61] the entropy density was solved as primary evolution variable and the total energy conservation law was obtained as a consequence. These ideas have recently also been extended to high order discontinuous Galerkin finite element schemes, see [62]. A common building block in all

methods presented in [59–62] is the use of a path integral in order to obtain a thermodynamically compatible numerical flux for the underlying inviscid Euler or shallow water subsystem. This path integral was discretized at the aid of suitable numerical quadrature formulas, which, however, can lead to a small source of total energy conservation errors if the number of quadrature points was not large enough, see [61] for a detailed analysis. It is therefore the main objective of the present paper to construct thermodynamically compatible finite volume and discontinuous Galerkin schemes for the Euler equations and for the GPR model of continuum mechanics that do *not need* the approximate computation of a path integral in order to obtain a thermodynamically compatible flux. In this paper, we make use of the new concept of a direct discretization of the *entropy inequality* with appropriate non-negative production term in order to obtain the discrete total energy conservation law as a consequence. Our method can therefore be seen as a *dual scheme* with respect to traditional entropy-conserving and entropy-stable methods, where total energy is discretized and the entropy inequality is obtained as a consequence. A major innovation and special property of the new family of schemes presented in this paper is that they do *not* need the Godunov parametrization of the flux of the underlying Euler subsystem in terms of a generating potential, in contrast to the methods presented previously in Busto et al. [59–62], which were all explicitly relying on the Godunov parametrization in terms of a generating potential.

The rest of this paper is organized as follows: in Section 2, we present the governing PDE system treated in this manuscript, namely the first order hyperbolic GPR model of continuum mechanics supplemented with a thermodynamically compatible parabolic vanishing viscosity regularization. The next three sections are devoted to the introduction of three different but related thermodynamically compatible numerical schemes for the discretization of the GPR model. To facilitate the reader, the presentation of the three different schemes is organized in increasing level of complexity:

1. In Section 3 a new thermodynamically compatible cell centered finite volume method is presented. The readers who are only interested in FV schemes are invited to focus on this section.
2. In Section 4 we introduce a first DG scheme (DG scheme of type I) that employs the same thermodynamically compatible *edge/face-based* fluxes for the Euler subsystem as the one used in the finite volume method presented in Section 3. As such, the FV method and the DG schemes of type I are related to each other. The readers who are interested in a straightforward extension of finite volume schemes to the DG framework are invited to focus on Sections 3 and 4.
3. In Section 5 we propose a second DG scheme (DG scheme of type II) which is completely different from the previous two methods as it establishes thermodynamic compatibility directly in a genuinely multi-dimensional fashion via a suitable *element-wise* correction.

For all schemes presented in this paper, a cell entropy inequality and nonlinear stability in the energy norm can be proven for the semi-discrete case. In Section 6, numerical results are shown for a set of different test cases, ranging from the fluid to the solid limit of the GPR model. The conclusions are presented together with an outlook to future work in Section 7.

2. Governing partial differential equations

This paper is concerned with a new family of thermodynamically compatible schemes for the unified first order hyperbolic model of continuum mechanics of Godunov, Peshkov and Romenski (GPR model) see [3,9,16,17,63,64]. The governing PDE system, which in this paper has been regularized via appropriate thermodynamically compatible parabolic vanishing viscosity terms, reads as follows:

$$\frac{\partial \rho}{\partial t} + \frac{\partial (\rho v_k)}{\partial x_k} - \frac{\partial}{\partial x_m}\left(\epsilon \frac{\partial \rho}{\partial x_m} \right) = 0, \tag{1a}$$

$$\frac{\partial \rho v_i}{\partial t} + \frac{\partial (\rho v_i v_k + p\,\delta_{ik} + \sigma_{ik} + \omega_{ik})}{\partial x_k} - \frac{\partial}{\partial x_m}\left(\epsilon \frac{\partial \rho v_i}{\partial x_m} \right) = 0, \tag{1b}$$

$$\frac{\partial \rho S}{\partial t} + \frac{\partial (\rho S v_k + \beta_k)}{\partial x_k} - \frac{\partial}{\partial x_m}\left(\epsilon \frac{\partial \rho S}{\partial x_m} \right) = \Pi + \frac{\alpha_{ik}\alpha_{ik}}{\theta_1(\tau_1) T} + \frac{\beta_i \beta_i}{\theta_2(\tau_2) T} \geq 0, \tag{1c}$$

$$\frac{\partial A_{ik}}{\partial t} + \frac{\partial (A_{im} v_m)}{\partial x_k} + v_m \left(\frac{\partial A_{ik}}{\partial x_m} - \frac{\partial A_{im}}{\partial x_k} \right) - \frac{\partial}{\partial x_m}\left(\epsilon \frac{\partial A_{ik}}{\partial x_m} \right) = -\frac{\alpha_{ik}}{\theta_1(\tau_1)}, \tag{1d}$$

$$\frac{\partial J_k}{\partial t} + \frac{\partial (J_m v_m + T)}{\partial x_k} + v_m \left(\frac{\partial J_k}{\partial x_m} - \frac{\partial J_m}{\partial x_k} \right) - \frac{\partial}{\partial x_m}\left(\epsilon \frac{\partial J_k}{\partial x_m} \right) = -\frac{\beta_k}{\theta_2(\tau_2)}, \tag{1e}$$

$$\frac{\partial \mathcal{E}}{\partial t} + \frac{\partial (v_k(\mathcal{E}_1 + \mathcal{E}_2 + \mathcal{E}_3 + \mathcal{E}_4) + v_i\,(p\,\delta_{ik} + \sigma_{ik} + \omega_{ik}) + h_k)}{\partial x_k} - \frac{\partial}{\partial x_m}\left(\epsilon \frac{\partial \mathcal{E}}{\partial x_m} \right) = 0. \tag{1f}$$

with the state vector $\mathbf{q} = \{q_i\} = (\rho, \rho v_i, \rho S, A_{ik}, J_k)^T$ and the total energy density $\mathcal{E} = \rho E = \mathcal{E}_1 + \mathcal{E}_2 + \mathcal{E}_3 + \mathcal{E}_4$ with $\mathcal{E}_i = \rho E_i$. Throughout this paper the tensor indices i, k and m run from 1 to 3, i.e. we always consider the full equations written for

the three-dimensional case, independently of the actual number of space dimensions considered in the numerical scheme. The system above belongs to the class of overdetermined hyperbolic systems. The vanishing viscosity parameter is denoted by $\epsilon > 0$ and the entropy production term associated with the vanishing viscosity regularization reads

$$\Pi = \frac{\epsilon}{T}\, \partial_{x_m} q_i \; \partial^2_{q_i q_j} \mathcal{E}\, \partial_{x_m} q_j \geq 0, \tag{2}$$

where the nonnegativity is obtained by assuming $\epsilon > 0$, $T > 0$ and that the Hessian of the total energy potential is at least positive semi-definite, i.e. $\mathcal{H}_{ij} := \partial^2_{q_i q_j} \mathcal{E} \geq 0$. In the following, we will make use of the notations $\partial_p = \partial / \partial p$ and $\partial^2_{pq} = \partial^2 / (\partial p \partial q)$ for the first and second partial derivatives with respect to the quantities p and q. We will also assume the Einstein summation convention over repeated indices and we will make use bold symbols for vectors and matrix, for example $\mathbf{q} = \{q_i\}$ and $\mathbf{A} = \{A_{ik}\}$. In this paper, we write the total energy density as a sum of four contributions given by

$$\mathcal{E}_1 = \frac{\rho^\gamma}{\gamma - 1} e^{S/c_v}, \quad \mathcal{E}_2 = \frac{1}{2}\rho v_i v_i, \quad \mathcal{E}_3 = \frac{1}{4}\rho c_s^2 \mathring{G}_{ij} \mathring{G}_{ij}, \quad \mathcal{E}_4 = \frac{1}{2} c_h^2 \rho J_i J_i, \tag{3}$$

where $\mathbf{G}$ is a metric tensor defined as $G_{ik} = A_{ji} A_{jk}$. Its trace-free part, or deviator, is denoted by $\mathring{\mathbf{G}}$ and reads $\mathring{G}_{ik} = G_{ik} - \frac{1}{3} G_{mm} \delta_{ik}$. The main field or so-called thermodynamic dual variables are denoted by $\mathbf{p} = \partial_{\mathbf{q}} \mathcal{E} = \{p_i\} = (r, v_i, T, \alpha_{ik}, \beta_k)^T$ and are defined as

$$r = \partial_\rho \mathcal{E}, \qquad v_i = \partial_{\rho v_i} \mathcal{E}, \qquad T = \partial_{\rho S} \mathcal{E}, \qquad \alpha_{ik} = \partial_{A_{ik}} \mathcal{E}, \qquad \beta_k = \partial_{J_k} \mathcal{E}. \tag{4}$$

The hydrodynamic pressure p is given by $p = \rho\, \partial_\rho \mathcal{E} + \rho v_i\, \partial_{\rho v_i} \mathcal{E} + \rho S\, \partial_{\rho S} \mathcal{E} - \mathcal{E} = \rho^2 \partial_\rho E$, while the shear stress tensor and the thermal stress tensor read

$$\sigma_{ik} = A_{ji} \partial_{A_{jk}} \mathcal{E} = A_{ji} \alpha_{jk} = \rho c_s^2 G_{ij} \mathring{G}_{jk}, \qquad \omega_{ik} = J_i \partial_{J_k} \mathcal{E} = J_i \beta_k = \rho c_h^2 J_i J_k, \tag{5}$$

respectively. In the above model the heat flux is defined as

$$h_k = \partial_{\rho S} \mathcal{E}\, \partial_{J_k} \mathcal{E} = T \beta_k = \rho c_h^2 T J_k. \tag{6}$$

The total energy flux F_k in (1f) is the sum of two fluxes, $F_k = F_k^{12} + F_k^{34}$, where F_k^{12} is related to the Euler subsystem and F_k^{34} contains the work of the stress tensors σ_{ik} and ω_{ik} as well as the heat flux h_k, i.e.

$$F_k^{12} = v_k (\mathcal{E}_1 + \mathcal{E}_2) + v_i \delta_{ik} p, \qquad F_k^{34} = v_k (\mathcal{E}_3 + \mathcal{E}_4) + v_i (\sigma_{ik} + \omega_{ik}) + h_k. \tag{7}$$

Furthermore, $\theta_1(\tau_1) > 0$ and $\theta_2(\tau_2) > 0$ are functions that depend on $\mathbf{q}$ and on the relaxation times $\tau_1 > 0$ and $\tau_2 > 0$ as follows:

$$\theta_1 = \frac{1}{3} \rho z_1 \tau_1 c_s^2 \, |\mathbf{A}|^{-\frac{5}{3}}, \qquad \theta_2 = \rho z_2 \tau_2 c_h^2, \qquad z_1 = \frac{\rho_0}{\rho}, \qquad z_2 = \frac{\rho_0 T_0}{\rho T}. \tag{8}$$

Here, ρ_0 and T_0 are a reference density and a reference temperature, respectively. After some calculations one can verify that (1f) is a consequence of (1a)–(1e) since the following identity holds:

$$(1f) = r \cdot (1a) + v_i \cdot (1b) + T \cdot (1c) + \alpha_{ik} \cdot (1d) + \beta_k \cdot (1e). \tag{9}$$

The above relation is directly related to the Gibbs identity

$$1 \cdot d\mathcal{E} = r \cdot d\rho + v_i \cdot d(\rho v_i) + T \cdot d(\rho S) + \alpha_{ik} \cdot dA_{ik} + \beta_k \cdot dJ_k = \mathbf{p} \cdot d\mathbf{q}. \tag{10}$$

Note that in the above identity the factor in front of the total energy differential is simply *unity*. This not only highlights the privileged role that the total energy potential has in SHTC systems, but it also substantially eases the calculations when the PDE for $\mathcal{E}$ is taken as the consequence of all other equations, instead of the PDE for the entropy density. The factor T in front of the entropy differential can become rather complex for general EOS or for more complicated PDE systems. Instead, the factor of unity in front of the total energy differential is always trivial and is independent of the equation of state and even of the mechanical system under consideration. For other HTC systems with the same property, the reader is referred to Romenski et al. [11], Romenski [16], Favrie and Gavrilyuk [18], Dhaouadi et al. [19], Busto et al. [59], Busto and Dumbser [60], Dhaouadi and Dumbser [65].

A formal asymptotic analysis of the model (1) was presented in [64]. It is shown that for small relaxation times, τ_1 and τ_2, the Navier–Stokes–Fourier limit is obtained, i.e. the stress tensor σ_{ik} and the heat flux h_k tend to

$$\sigma_{ik} = -\frac{1}{6} \rho_0 c_s^2 \tau_1 \left(\partial_k v_i + \partial_i v_k - \frac{2}{3} (\partial_m v_m) \delta_{ik} \right), \qquad h_k = -\rho_0 T_0 c_h^2 \tau_2 \partial_k T. \tag{11}$$

In this case one can relate the viscosity coefficient to the relaxation time τ_1 and the shear sound speed c_s as $\mu = \frac{1}{6} \rho_0 c_s^2 \tau_1$, while the thermal conductivity coefficient is related to the relaxation time τ_2 and the heat wave speed c_h by $\kappa = \rho_0 T_0 c_h^2 \tau_2$.

In this paper, we will also make use of the following more compact formulation of the above PDE system, casting it into the general form

$$\partial_t \mathbf{q} + \partial_k \mathbf{f}_k(\mathbf{q}) + \partial_k \mathbf{h}_k(\mathbf{q}) + \mathbf{B}_k(\mathbf{q}) \partial_k \mathbf{q} - \partial_m (\epsilon \partial_m \mathbf{q}) = \mathbf{P} + \mathbf{S}(\mathbf{q}) \tag{12}$$

with the extra conservation law for the total energy density

$$\frac{\partial \mathcal{E}}{\partial t} + \partial_k F_k(\mathbf{q}) - \partial_m(\epsilon \partial_m \mathcal{E}) = 0. \tag{13}$$

Here, the flux $\mathbf{f}_k(\mathbf{q})$ is associated with the inviscid Euler subsystem (black terms), the flux $\mathbf{h}_k(\mathbf{q})$ and the non-conservative product $\mathbf{B}_k(\mathbf{q})\partial_k\mathbf{q}$ include the terms related to the distorsion field and the thermal impulse (red terms), the parabolic dissipation terms are $\partial_m(\epsilon\partial_m\mathbf{q})$ with the associated entropy production $\mathbf{P}$ (blue terms) and the algebraic relaxation source terms, which are potentially stiff, are denoted by $\mathbf{S}(\mathbf{q})$ (green). In the extra conservation law (13) the total energy flux is given by $F_k(\mathbf{q})$. Since $\mathbf{p} = \partial_{\mathbf{q}}\mathcal{E}$ and therefore $\mathbf{p}\cdot\partial_t\mathbf{q} = \partial_{\mathbf{q}}\mathcal{E}\cdot\partial_t\mathbf{q} = \partial_t\mathcal{E}$, for thermodynamic compatibility of system (12) with the extra conservation law (13) the following identities must be satisfied, in particular the compatibility of the conservative flux terms and of the non-conservative products with the total energy flux,

$$\mathbf{p}\cdot(\,\partial_k\mathbf{f}_k(\mathbf{q}) + \partial_k\mathbf{h}_k(\mathbf{q}) + \mathbf{B}_k(\mathbf{q})\partial_k\mathbf{q}\,) = \partial_k F_k. \tag{14}$$

More specifically, the flux of the Euler subsystem $\mathbf{f}_k$ must be compatible with the energy flux F_k^{12}

$$\mathbf{p}\cdot\partial_k\mathbf{f}_k(\mathbf{q}) = \partial_k F_k^{12} \tag{15}$$

and the remaining terms must be compatible with the energy flux F_k^{34}, i.e.

$$\mathbf{p}\cdot(\,\partial_k\mathbf{h}_k(\mathbf{q}) + \mathbf{B}_k(\mathbf{q})\partial_k\mathbf{q}\,) = \partial_k F_k^{34}. \tag{16}$$

Furthermore, one has the compatibility of the entropy production term with the parabolic dissipation terms

$$\mathbf{p}\cdot\mathbf{P} + \mathbf{p}\cdot\partial_m(\epsilon\partial_m\mathbf{q}) = \partial_m(\epsilon\partial_m\mathcal{E}), \tag{17}$$

and the compatibility of the algebraic relaxation source terms

$$\mathbf{p}\cdot\mathbf{S}(\mathbf{q}) = 0. \tag{18}$$

As already stated previously, the main peculiarity of the new algorithms presented in this manuscript is that the *entropy inequality* is solved as a primary evolution equation instead of the total energy conservation law, unlike in most traditional schemes for hyperbolic systems of conservation laws. Instead, in our framework, the total energy conservation is obtained as a *consequence* of the proposed thermodynamically compatible discretization.

3. Thermodynamically compatible finite volume schemes on collocated meshes

In favor of clarity and in order to ease the reading, we start presenting the construction of our thermodynamically compatible schemes step by step in one space dimension only, using the different colours in (1) as guidance. We start with the discretization of the inviscid Euler subsystem (black terms), then including the viscous terms (blue) and finally adding the distortion field and the specific thermal impulse (red terms). Throughout this paper, we use lower case subscripts, i, j, k, for tensor indices, while lower case superscript, ℓ, refer to the spatial discretization index. We denote the spatial control volumes in 1D by $\Omega^\ell = [x^{\ell-\frac{1}{2}}, x^{\ell+\frac{1}{2}}]$ and $\Delta x = x^{\ell+\frac{1}{2}} - x^{\ell-\frac{1}{2}}$ is the uniform mesh spacing.

3.1. Compatible discretization of the Euler subsystem in 1D

The inviscid Euler subsystem with the related extra conservation law for the total energy density reads

$$\partial_t\mathbf{q} + \partial_x\mathbf{f}_1(\mathbf{q}) = 0, \tag{19}$$

$$\partial_t\mathcal{E}^{12} + \partial_x F_1^{12} = 0. \tag{20}$$

A semi-discrete finite volume scheme for (19) is thus given by

$$\frac{d}{dt}\mathbf{q}^\ell = -\frac{\mathcal{F}^{\ell+\frac{1}{2}} - \mathcal{F}^{\ell-\frac{1}{2}}}{\Delta x} = -\frac{\left(\mathcal{F}^{\ell+\frac{1}{2}} - \mathbf{f}^\ell\right) - \left(\mathcal{F}^{\ell-\frac{1}{2}} - \mathbf{f}^\ell\right)}{\Delta x} = -\frac{\mathcal{D}_-^{\ell+\frac{1}{2}} + \mathcal{D}_+^{\ell-\frac{1}{2}}}{\Delta x}, \tag{21}$$

with $\mathbf{f}^\ell = \mathbf{f}_1(\mathbf{q}^\ell)$ to ease notation, $\mathbf{f}_1(\mathbf{q}) = (\rho v_1, \rho v_i v_1 + p\delta_{i1}, \rho S v_1, \mathbf{0}, \mathbf{0})^T$ the fluxes of the Euler subsystem and the associated total energy flux of the Euler subsystem $F_1^{12} = v_1(\mathcal{E}_1 + \mathcal{E}_2 + p)$ and the numerical flux $\mathcal{F}^{\ell+\frac{1}{2}}$. The fluctuations $\mathcal{D}_-^{\ell+\frac{1}{2}}$ and $\mathcal{D}_+^{\ell-\frac{1}{2}}$ are related to the numerical fluxes via the relations

$$\mathcal{D}_-^{\ell+\frac{1}{2}} = \mathcal{F}^{\ell+\frac{1}{2}} - \mathbf{f}^\ell, \qquad \mathcal{D}_+^{\ell-\frac{1}{2}} = \mathbf{f}^\ell - \mathcal{F}^{\ell-\frac{1}{2}}. \tag{22}$$

To obtain a discrete total energy conservation law as a consequence of the discretization of (19), see (9), we compute the dot product of the discrete dual variables, $\mathbf{p}^\ell = \partial_{\mathbf{q}}\mathcal{E}(\mathbf{q}^\ell)$, with the semi-discrete scheme (21),

$$\mathbf{p}^\ell\cdot\frac{d}{dt}\mathbf{q}^\ell = \frac{d}{dt}\mathcal{E}^\ell = -\mathbf{p}^\ell\cdot\frac{\left(\mathcal{F}^{\ell+\frac{1}{2}} - \mathbf{f}^\ell\right) + \left(\mathbf{f}^\ell - \mathcal{F}^{\ell-\frac{1}{2}}\right)}{\Delta x} = -\frac{D_{\mathcal{E},-}^{\ell+\frac{1}{2}} + D_{\mathcal{E},+}^{\ell-\frac{1}{2}}}{\Delta x} = -\frac{F_1^{12,\ell+\frac{1}{2}} - F_1^{12,\ell-\frac{1}{2}}}{\Delta x}. \tag{23}$$

We now look for a suitable numerical flux $\mathcal{F}^{\ell+\frac{1}{2}}$ that achieves thermodynamic compatibility of the finite volume scheme (21) with the discrete form of the total energy conservation law (23). For that purpose we define the right and left energy fluctuations as

$$D^{\ell+\frac{1}{2}}_{\mathcal{E},-} = \mathbf{p}^{\ell} \cdot \mathcal{D}^{\ell+\frac{1}{2}}_{-} = \mathbf{p}^{\ell} \cdot (\mathcal{F}^{\ell+\frac{1}{2}} - \mathbf{f}^{\ell}), \qquad D^{\ell-\frac{1}{2}}_{\mathcal{E},+} = \mathbf{p}^{\ell} \cdot \mathcal{D}^{\ell-\frac{1}{2}}_{+} = \mathbf{p}^{\ell} \cdot (\mathbf{f}^{\ell} - \mathcal{F}^{\ell-\frac{1}{2}}), \tag{24}$$

which must satisfy the consistency property

$$D^{\ell+\frac{1}{2}}_{\mathcal{E},-} + D^{\ell+\frac{1}{2}}_{\mathcal{E},+} = \mathbf{p}^{\ell} \cdot \mathcal{D}^{\ell+\frac{1}{2}}_{-} + \mathbf{p}^{\ell+1} \cdot \mathcal{D}^{\ell+\frac{1}{2}}_{+} = \mathbf{p}^{\ell} \cdot (\mathcal{F}^{\ell+\frac{1}{2}} - \mathbf{f}^{\ell}) + \mathbf{p}^{\ell+1} \cdot (\mathbf{f}^{\ell+1} - \mathcal{F}^{\ell+\frac{1}{2}}) = F_1^{12,\ell+1} - F_1^{12,\ell} \tag{25}$$

in order to obtain a conservative discretization of the extra conservation law (20). The numerical total energy fluxes $F_1^{12,\ell\pm\frac{1}{2}}$ appearing in (23) are related to the energy fluctuations via

$$D^{\ell+\frac{1}{2}}_{\mathcal{E},-} = F_1^{12,\ell+\frac{1}{2}} - F_1^{12,\ell}, \qquad D^{\ell-\frac{1}{2}}_{\mathcal{E},+} = F_1^{12,\ell} - F_1^{12,\ell-\frac{1}{2}}, \tag{26}$$

with $F_1^{12,\ell} = F_1^{12}(\mathbf{q}^{\ell})$ the discrete total energy flux related to the Euler subsystem evaluated in cell Ω^{ℓ}. Following the ideas outlined in the general framework [1], in the following we *assume* the thermodynamically compatible numerical flux $\mathcal{F}^{\ell+\frac{1}{2}}$ to have the rather general form

$$\mathcal{F}^{\ell+\frac{1}{2}} = \widetilde{\mathcal{F}}^{\ell+\frac{1}{2}} - \alpha^{\ell+\frac{1}{2}} \left(\mathbf{p}^{\ell+1} - \mathbf{p}^{\ell}\right) = \left(\mathcal{F}_{\rho}^{\ell+\frac{1}{2}}, \mathcal{F}_{\rho v_i}^{\ell+\frac{1}{2}}, \mathcal{F}_{\rho S}^{\ell+\frac{1}{2}}, \mathbf{0}, \mathbf{0}\right)^T, \tag{27}$$

where $\widetilde{\mathcal{F}}^{\ell+\frac{1}{2}}$ could be in principle any central numerical flux that does *not* necessarily guarantee discrete thermodynamic compatibility of the system of conservation laws (19) with the extra conservation law (20) and which is then *corrected* via a suitable scalar parameter $\alpha^{\ell+\frac{1}{2}}$ in order to achieve discrete thermodynamic compatibility. Imposing the condition (25) on the flux (27) we obtain

$$\mathbf{p}^{\ell} \cdot (\widetilde{\mathcal{F}}^{\ell+\frac{1}{2}} - \mathbf{f}^{\ell}) + \mathbf{p}^{\ell+1} \cdot (\mathbf{f}^{\ell+1} - \widetilde{\mathcal{F}}^{\ell+\frac{1}{2}}) - \alpha^{\ell+\frac{1}{2}}\, \mathbf{p}^{\ell} \cdot \left(\mathbf{p}^{\ell+1} - \mathbf{p}^{\ell}\right) + \alpha^{\ell+\frac{1}{2}}\, \mathbf{p}^{\ell+1} \cdot \left(\mathbf{p}^{\ell+1} - \mathbf{p}^{\ell}\right) = F_1^{12,\ell+1} - F_1^{12,\ell}. \tag{28}$$

Rearranging terms in the above equation yields

$$-\widetilde{\mathcal{F}}^{\ell+\frac{1}{2}} \cdot \left(\mathbf{p}^{\ell+1} - \mathbf{p}^{\ell}\right) + \mathbf{p}^{\ell+1} \cdot \mathbf{f}^{\ell+1} - \mathbf{p}^{\ell} \cdot \mathbf{f}^{\ell} + \alpha^{\ell+\frac{1}{2}} \left(\mathbf{p}^{\ell+1} - \mathbf{p}^{\ell}\right)^2 = F_1^{12,\ell+1} - F_1^{12,\ell}, \tag{29}$$

from which we can obtain the scalar correction factor $\alpha^{\ell+\frac{1}{2}}$

$$\alpha^{\ell+\frac{1}{2}} = \frac{F_1^{12,\ell+1} - F_1^{12,\ell} + \widetilde{\mathcal{F}}^{\ell+\frac{1}{2}} \cdot \left(\mathbf{p}^{\ell+1} - \mathbf{p}^{\ell}\right) - \left(\mathbf{p}^{\ell+1} \cdot \mathbf{f}^{\ell+1} - \mathbf{p}^{\ell} \cdot \mathbf{f}^{\ell}\right)}{\left(\mathbf{p}^{\ell+1} - \mathbf{p}^{\ell}\right)^2} \tag{30}$$

that guarantees the discrete thermodynamic compatibility of the scheme (21) with the discrete extra conservation law (23). In the case of a vanishing denominator, $\left(\mathbf{p}^{\ell+1} - \mathbf{p}^{\ell}\right)^2 = 0$, we set $\alpha^{\ell+\frac{1}{2}} = 0$. Throughout this paper we simply choose the dissipationless *central flux* as underlying numerical flux $\widetilde{\mathcal{F}}^{\ell+\frac{1}{2}}$, i.e.

$$\widetilde{\mathcal{F}}^{\ell+\frac{1}{2}} = \frac{1}{2}\left(\mathbf{f}^{\ell} + \mathbf{f}^{\ell+1}\right), \tag{31}$$

since suitable numerical dissipation terms that are compatible with the first and second law of thermodynamics will be provided in the next section. We stress that the numerical flux (27) with (30) does *not* need the Godunov parametrization of the flux $\mathbf{f}_1 = \partial_{\mathbf{p}}(v_1 L)$ in terms of a generating potential L, unlike the HTC finite volume schemes presented in [59–61]. Note that this part of the scheme is only related to the reversible (inviscid) terms of the governing equations, hence it is sufficient to consider the simple central flux (31) in (27). A proper thermodynamically compatible discretization of the viscous terms, which mimics the parabolic vanishing viscosity regularization of the governing PDE system, including the non-negative entropy production term, is done separately and will be presented later in the next section.

3.2. Thermodynamically compatible discretization of the viscous terms in 1D

In the end we are interested in constructing a *dissipative* scheme for (1) that is thermodynamically compatible. For this purpose, and since the compatible numerical flux (27) with (31) and (30) developed in the previous section is dissipationless, we now still need to add a thermodynamically compatible numerical viscosity in order to get a dissipative scheme that also works in the presence of shock waves and other discontinuities. Hence, the flux (27) is extended by a dissipative contribution and a corresponding non-negative entropy production term, which mimic the vanishing viscosity regularization introduced in the governing PDE system (1) at the discrete level:

$$\frac{d}{dt}\mathbf{q}^{\ell} + \frac{\mathcal{F}^{\ell+\frac{1}{2}} - \mathcal{F}^{\ell-\frac{1}{2}}}{\Delta x} = \frac{\mathcal{G}^{\ell+\frac{1}{2}} - \mathcal{G}^{\ell-\frac{1}{2}}}{\Delta x} + \mathbf{P}^{\ell}. \tag{32}$$

The dissipative numerical flux is chosen as

$$\mathcal{G}^{\ell+\frac{1}{2}} = \epsilon^{\ell+\frac{1}{2}} \frac{\Delta \mathbf{q}^{\ell+\frac{1}{2}}}{\Delta x}, \qquad \Delta \mathbf{q}^{\ell+\frac{1}{2}} = \mathbf{q}^{\ell+1} - \mathbf{q}^{\ell}, \tag{33}$$

with a scalar numerical viscosity coefficient that can be either chosen to be constant, i.e. $\epsilon^{\ell+\frac{1}{2}} = \epsilon$, or which is chosen as follows,

$$\epsilon^{\ell+\frac{1}{2}} = \frac{1}{2}\left(1 - \phi^{\ell+\frac{1}{2}}\right) \Delta x \, s_{\max}^{\ell+\frac{1}{2}} \geq 0, \tag{34}$$

where $s_{\max}^{\ell+\frac{1}{2}}$ according to the Rusanov or local Lax-Friedrichs flux is chosen as the maximum signal speed arising at the cell interface and $\phi^{\ell+\frac{1}{2}}$ is a flux limiter allowing to reduce the numerical viscosity regions where the numerical solution is smooth. In the following, and if not stated otherwise, we will employ the minbee flux limiter given by

$$\phi^{\ell+\frac{1}{2}} = \min\left(\phi_-^{\ell+\frac{1}{2}}, \phi_+^{\ell+\frac{1}{2}}\right), \quad \text{with} \quad \phi_\pm^{\ell+\frac{1}{2}} = \max\left(0, \min\left(1, h_\pm^{\ell+\frac{1}{2}}\right)\right), \tag{35}$$

where the ratios of total energy slopes, similar to the SLIC scheme of Toro [66], read

$$h_-^{\ell+\frac{1}{2}} = \frac{\mathcal{E}^{\ell} - \mathcal{E}^{\ell-1}}{\mathcal{E}^{\ell+1} - \rho^{\ell}}, \qquad \text{and} \qquad h_+^{\ell+\frac{1}{2}} = \frac{\mathcal{E}^{\ell+2} - \mathcal{E}^{\ell+1}}{\mathcal{E}^{\ell+1} - \rho^{\ell}}. \tag{36}$$

The final thermodynamically compatible dissipative Rusanov flux, which includes both the convective and the diffusive terms, is given by

$$\mathcal{F}^{\ell+\frac{1}{2}} + \mathcal{G}^{\ell+\frac{1}{2}} = \frac{1}{2}\left(\mathbf{f}^{\ell+1} + \mathbf{f}^{\ell}\right) - \alpha^{\ell+\frac{1}{2}}\left(\mathbf{p}^{\ell+1} - \mathbf{p}^{\ell}\right) - \frac{\epsilon^{\ell+\frac{1}{2}}}{\Delta x}\left(\mathbf{q}^{\ell+1} - \mathbf{q}^{\ell}\right), \tag{37}$$

where we have used our choice (31) and where $\alpha^{\ell+\frac{1}{2}}$ is given by (30). Unlike in [59,61] the flux (37) does *not* require the evaluation of path integrals in phase space and is therefore computationally much more efficient, as shown later by numerical experiments.

Taking the dot product of Eq. (32) with the dual variables $\mathbf{p}^{\ell}$ yields

$$\frac{d\mathcal{E}^{\ell}}{dt} + \frac{1}{\Delta x}\left(F_1^{12,\ell+\frac{1}{2}} - F_1^{12,\ell-\frac{1}{2}}\right) = \frac{1}{\Delta x}\mathbf{p}^{\ell} \cdot \left(\mathcal{G}^{\ell+\frac{1}{2}} - \mathcal{G}^{\ell-\frac{1}{2}}\right) + \mathbf{p}^{\ell} \cdot \mathbf{P}^{\ell}. \tag{38}$$

The thermodynamic compatibility of the inviscid part on the left hand side of (38) is obvious since it was already shown in the previous section. Therefore, we can now simply focus on the terms appearing on the right hand side of (38). After some calculations we obtain

$$\begin{aligned}
&\mathbf{p}^{\ell} \cdot \mathbf{P}^{\ell} + \mathbf{p}^{\ell} \cdot \frac{\mathcal{G}^{\ell+\frac{1}{2}} - \mathcal{G}^{\ell-\frac{1}{2}}}{\Delta x} \\
&= \mathbf{p}^{\ell} \cdot \mathbf{P}^{\ell} + \frac{1}{\Delta x}\left(\frac{1}{2}\mathbf{p}^{\ell} \cdot \mathcal{G}^{\ell+\frac{1}{2}} + \frac{1}{2}\mathbf{p}^{\ell+1} \cdot \mathcal{G}^{\ell+\frac{1}{2}} + \frac{1}{2}\mathbf{p}^{\ell} \cdot \mathcal{G}^{\ell+\frac{1}{2}} - \frac{1}{2}\mathbf{p}^{\ell+1} \cdot \mathcal{G}^{\ell+\frac{1}{2}}\right) \\
&\quad - \frac{1}{\Delta x}\left(\frac{1}{2}\mathbf{p}^{\ell} \cdot \mathcal{G}^{\ell-\frac{1}{2}} + \frac{1}{2}\mathbf{p}^{\ell-1} \cdot \mathcal{G}^{\ell-\frac{1}{2}} + \frac{1}{2}\mathbf{p}^{\ell} \cdot \mathcal{G}^{\ell-\frac{1}{2}} - \frac{1}{2}\mathbf{p}^{\ell-1} \cdot \mathcal{G}^{\ell-\frac{1}{2}}\right) \\
&= \mathbf{p}^{\ell} \cdot \mathbf{P}^{\ell} + \frac{1}{2}\frac{\mathbf{p}^{\ell+1} + \mathbf{p}^{\ell}}{\Delta x} \cdot \epsilon^{\ell+\frac{1}{2}} \frac{\Delta \mathbf{q}^{\ell+\frac{1}{2}}}{\Delta x} - \frac{1}{2}\frac{\mathbf{p}^{\ell} + \mathbf{p}^{\ell-1}}{\Delta x} \cdot \epsilon^{\ell-\frac{1}{2}} \frac{\Delta \mathbf{q}^{\ell-\frac{1}{2}}}{\Delta x} \\
&\quad - \frac{1}{2}\frac{\mathbf{p}^{\ell+1} - \mathbf{p}^{\ell}}{\Delta x} \cdot \epsilon^{\ell+\frac{1}{2}} \frac{\Delta \mathbf{q}^{\ell+\frac{1}{2}}}{\Delta x} - \frac{1}{2}\frac{\mathbf{p}^{\ell} - \mathbf{p}^{\ell-1}}{\Delta x} \cdot \epsilon^{\ell-\frac{1}{2}} \frac{\Delta \mathbf{q}^{\ell-\frac{1}{2}}}{\Delta x}.
\end{aligned} \tag{39}$$

Because of the relation

$$\int_{\mathbf{q}^{\ell}}^{\mathbf{q}^{\ell+1}} \mathbf{p} \cdot d\mathbf{q} = \int_{\mathbf{q}^{\ell}}^{\mathbf{q}^{\ell+1}} \partial_{\mathbf{q}} \mathcal{E} \cdot d\mathbf{q} = \mathcal{E}^{\ell+1} - \mathcal{E}^{\ell} = \Delta \mathcal{E}^{\ell+\frac{1}{2}}, \tag{40}$$

one may interpret the term $\frac{1}{2}(\mathbf{p}^{\ell+1} + \mathbf{p}^{\ell}) \cdot \Delta \mathbf{q}^{\ell+\frac{1}{2}}$ as an *approximation* of the total energy density difference $\Delta \mathcal{E}^{\ell+\frac{1}{2}}$, with an approximation of the path integral via the simple trapezoidal rule. Due to (39) and (40), the energy flux including convective and diffusive terms is

$$F_d^{\ell+\frac{1}{2}} = F_1^{12,\ell+\frac{1}{2}} - \frac{1}{2}(\mathbf{p}^{\ell+1} + \mathbf{p}^{\ell}) \cdot \epsilon^{\ell+\frac{1}{2}} \frac{\Delta \mathbf{q}^{\ell+\frac{1}{2}}}{\Delta x} \approx F_1^{12,\ell+\frac{1}{2}} - \epsilon^{\ell+\frac{1}{2}} \frac{\Delta \mathcal{E}^{\ell+\frac{1}{2}}}{\Delta x}. \tag{41}$$

In order to control the sign of the entropy production, we now rewrite the jump terms in the dual $\mathbf{p}$ variables as jumps in the conservative $\mathbf{q}$ variables. To this end, we make use of a Roe-type matrix $\partial^2_{\mathbf{qq}} \tilde{\mathcal{E}}^{\ell+\frac{1}{2}}$ that verifies the Roe property

$$\partial^2_{\mathbf{qq}} \tilde{\mathcal{E}}^{\ell+\frac{1}{2}} \cdot (\mathbf{q}^{\ell+1} - \mathbf{q}^{\ell}) = \mathbf{p}^{\ell+1} - \mathbf{p}^{\ell}. \tag{42}$$

The simple segment path $\tilde{\boldsymbol{\psi}}$ in the conservative $\mathbf{q}$ variables,

$$\tilde{\boldsymbol{\psi}}(s) = \mathbf{q}^{\ell} + s\left(\mathbf{q}^{\ell+1} - \mathbf{q}^{\ell}\right), \qquad 0 \le s \le 1, \tag{43}$$

allows us to construct the Roe matrix that we are looking for:

$$\partial^2_{\mathbf{qq}}\tilde{\mathcal{E}}^{\ell+\frac{1}{2}} = \int_0^1 \partial^2_{\mathbf{qq}}\mathcal{E}\left(\tilde{\boldsymbol{\psi}}(s)\right) ds =: \left(\partial^2_{\mathbf{pp}}\tilde{L}^{\ell+\frac{1}{2}}\right)^{-1}, \tag{44}$$

which satisfies (42) and allows to rewrite (38), after substitution of (39), as

$$\frac{d}{dt}\mathcal{E}^{\ell} + \frac{F_d^{\ell+\frac{1}{2}} - F_d^{\ell-\frac{1}{2}}}{\Delta x} = \mathbf{p}^{\ell}\cdot\mathbf{P}^{\ell} - \frac{1}{2}\epsilon^{\ell+\frac{1}{2}}\frac{\mathbf{q}^{\ell+1}-\mathbf{q}^{\ell}}{\Delta x}\cdot\partial^2_{\mathbf{qq}}\tilde{\mathcal{E}}^{\ell+\frac{1}{2}}\frac{\mathbf{q}^{\ell+1}-\mathbf{q}^{\ell}}{\Delta x} - \frac{1}{2}\epsilon^{\ell-\frac{1}{2}}\frac{\mathbf{q}^{\ell}-\mathbf{q}^{\ell-1}}{\Delta x}\cdot\partial^2_{\mathbf{qq}}\tilde{\mathcal{E}}^{\ell-\frac{1}{2}}\frac{\mathbf{q}^{\ell}-\mathbf{q}^{\ell-1}}{\Delta x}. \tag{45}$$

The only equation in the governing PDE system (1) that admits the addition of a non-negative production term on the right hand side is obviously the entropy inequality given by (1c). Hence, in order to obtain discrete total energy conservation (1f) as a consequence of all other equations, we need to balance all contributions due to the discretization of the dissipative terms by defining the production term $\mathbf{P}^{\ell} = (0, \mathbf{0}, \Pi^{\ell}, \mathbf{0}, \mathbf{0})^T$ as

$$\mathbf{p}^{\ell}\cdot\mathbf{P}^{\ell} = T^{\ell}\Pi^{\ell} = \frac{1}{2}\epsilon^{\ell+\frac{1}{2}}\frac{\Delta\mathbf{q}^{\ell+\frac{1}{2}}}{\Delta x}\cdot\partial^2_{\mathbf{qq}}\tilde{\mathcal{E}}^{\ell+\frac{1}{2}}\frac{\Delta\mathbf{q}^{\ell+\frac{1}{2}}}{\Delta x} + \frac{1}{2}\epsilon^{\ell-\frac{1}{2}}\frac{\Delta\mathbf{q}^{\ell-\frac{1}{2}}}{\Delta x}\cdot\partial^2_{\mathbf{qq}}\tilde{\mathcal{E}}^{\ell-\frac{1}{2}}\frac{\Delta\mathbf{q}^{\ell-\frac{1}{2}}}{\Delta x}. \tag{46}$$

This choice leads to the sought semi-discrete total energy conservation law

$$\frac{d}{dt}\mathcal{E}^{\ell} + \frac{F_d^{\ell+\frac{1}{2}} - F_d^{\ell-\frac{1}{2}}}{\Delta x} = 0. \tag{47}$$

3.3. Thermodynamically compatible discretization of the remaining terms in 1D

We now take into account also the remaining terms of the governing PDE system (1), i.e. the red and green terms. The thermodynamically compatible finite volume scheme in 1D reads

$$\frac{d}{dt}\mathbf{q}^{\ell} + \frac{\mathcal{F}^{\ell+\frac{1}{2}} - \mathcal{F}^{\ell-\frac{1}{2}}}{\Delta x} + \frac{\mathcal{R}_-^{\ell+\frac{1}{2}} + \mathcal{R}_+^{\ell-\frac{1}{2}}}{\Delta x} = \frac{\mathcal{G}^{\ell+\frac{1}{2}} - \mathcal{G}^{\ell-\frac{1}{2}}}{\Delta x} + \mathbf{P}^{\ell} + \mathbf{S}\left(\mathbf{q}^{\ell}\right). \tag{48}$$

According to the detailed derivation provided in Busto et al. [61], the thermodynamically compatible discretization of the fluctuations $\mathcal{R}_-^{\ell+\frac{1}{2}}$ and $\mathcal{R}_+^{\ell+\frac{1}{2}}$ in 1D is

$$\mathcal{R}_-^{\ell+\frac{1}{2}} = \begin{pmatrix} 0 \\ \sigma_{i1}^{\ell+\frac{1}{2}} - \sigma_{i1}^{\ell} + \omega_{i1}^{\ell+\frac{1}{2}} - \omega_{i1}^{\ell} \\ \frac{1}{2}\left(\beta_1^{\ell+1} - \beta_1^{\ell}\right) \\ \frac{1}{2}A_{im}^{\ell+\frac{1}{2}}\left(v_m^{\ell+1} - v_m^{\ell}\right)n_k + \frac{1}{2}\tilde{u}_A^{\ell+\frac{1}{2}}\left(A_{ik}^{\ell+1} - A_{ik}^{\ell}\right) \\ \frac{1}{2}J_m^{\ell+\frac{1}{2}}\left(v_m^{\ell+1} - v_m^{\ell}\right)n_k + \frac{1}{2}\tilde{u}_J^{\ell+\frac{1}{2}}\left(J_k^{\ell+1} - J_k^{\ell}\right) + \frac{1}{2}\left(T^{\ell+1} - T^{\ell}\right)n_k \end{pmatrix}, \tag{49}$$

and

$$\mathcal{R}_+^{\ell+\frac{1}{2}} = \begin{pmatrix} 0 \\ \sigma_{i1}^{\ell+1} - \sigma_{i1}^{\ell+\frac{1}{2}} + \omega_{i1}^{\ell+1} - \omega_{i1}^{\ell+\frac{1}{2}} \\ \frac{1}{2}\left(\beta_1^{\ell+1} - \beta_1^{\ell}\right) \\ \frac{1}{2}A_{im}^{\ell+\frac{1}{2}}\left(v_m^{\ell+1} - v_m^{\ell}\right)n_k + \frac{1}{2}\tilde{u}_A^{\ell+\frac{1}{2}}\left(A_{ik}^{\ell+1} - A_{ik}^{\ell}\right) \\ \frac{1}{2}J_m^{\ell+\frac{1}{2}}\left(v_m^{\ell+1} - v_m^{\ell}\right)n_k + \frac{1}{2}\tilde{u}_J^{\ell+\frac{1}{2}}\left(J_k^{\ell+1} - J_k^{\ell}\right) + \frac{1}{2}\left(T^{\ell+1} - T^{\ell}\right)n_k \end{pmatrix}, \tag{50}$$

with the normal $\mathbf{n} = (1, 0, 0)$ for this one-dimensional case, the compatible discretization of the stress tensors

$$\sigma_{ik}^{\ell+\frac{1}{2}} = \frac{1}{2}\left(A_{mi}^{\ell+1} + A_{mi}^{\ell}\right)\frac{1}{2}\left(\alpha_{mk}^{\ell+1} + \alpha_{mk}^{\ell}\right), \quad \omega_{ik}^{\ell+\frac{1}{2}} = \frac{1}{2}\left(J_i^{\ell+1} + J_i^{\ell}\right)\frac{1}{2}\left(\beta_k^{\ell+1} + \beta_k^{\ell}\right) \tag{51}$$

and

$$A_{im}^{\ell+\frac{1}{2}} = \frac{1}{2}\left(A_{im}^{\ell+1} + A_{im}^{\ell}\right), \qquad \tilde{u}_A^{\ell_z} = \frac{\mathcal{F}_{\rho}^{\ell+\frac{1}{2}}\left(E_3^{\ell+1} - E_3^{\ell}\right)}{\frac{1}{2}\left(\alpha_{ik}^{\ell+1} + \alpha_{ik}^{\ell}\right)\left(A_{ik}^{\ell+1} - A_{ik}^{\ell}\right)}, \tag{52}$$

$$J_i^{\ell+\frac{1}{2}} = \frac{1}{2}\left(J_i^{\ell} + J_i^{\ell+1}\right), \qquad \tilde{u}_J^{\ell+\frac{1}{2}} = \frac{\mathcal{F}_{\rho}^{\ell+\frac{1}{2}}\left(E_4^{\ell+1} - E_4^{\ell}\right)}{\frac{1}{2}\left(\beta_k^{\ell+1} + \beta_k^{\ell}\right)\left(J_k^{\ell+1} - J_k^{\ell}\right)}, \tag{53}$$

while the discrete algebraic source term simply reads

$$\mathbf{S}\left(\mathbf{q}^{\ell}\right)=\begin{pmatrix}0\\ \mathbf{0}\\ \dfrac{\alpha_{ik}^{\ell}\alpha_{ik}^{\ell}}{\theta_1^{\ell}(\tau_1)T^{\ell}}+\dfrac{\beta_k^{\ell}\beta_k^{\ell}}{\theta_2^{\ell}(\tau_2)T^{\ell}}\\ -\dfrac{\alpha_{ik}^{\ell}}{\theta_1^{\ell}(\tau_1)}\\ -\dfrac{\beta_i^{\ell}}{\theta_2^{\ell}(\tau_2)}\end{pmatrix}. \tag{54}$$

Following [61] one can check that the fluctuations satisfy the compatibility relation with the total energy flux related to the red terms in (1):

$$\mathbf{p}^{\ell}\cdot\mathcal{R}_{-}^{\ell+\frac{1}{2}}+\mathbf{p}^{\ell+1}\cdot\mathcal{R}_{+}^{\ell+\frac{1}{2}}=F_1^{34,\ell+1}-F_1^{34,\ell}. \tag{55}$$

The thermodynamic compatibility of the algebraic source term,

$$\mathbf{p}^{\ell}\cdot\mathbf{S}\left(\mathbf{q}^{\ell}\right)=0, \tag{56}$$

is obvious, since it is clearly the pointwise discrete analogue of (18).

3.4. Thermodynamically compatible finite volume scheme in multiple space dimensions

In multiple space dimensions the construction of the thermodynamically compatible semi-discrete cell centered finite volume scheme is completely analogous to the one shown for the one-dimensional case illustrated in the previous section, making use of fluxes and fluctuations in the normal direction across the cell boundaries. In what follows, we will provide the precise expressions of the final scheme and prove the cell entropy inequality and the marginal nonlinear stability in the energy norm, which is a consequence of the discrete thermodynamic compatibility. We consider the spatial control volume Ω^{ℓ} with circumcenter $\mathbf{x}^{\ell}$, one of its neighbors Ω^{τ} and the common edge $\partial\Omega^{\ell\tau}$, $\mathbf{n}^{\ell\tau}=(n_1^{\ell\tau},n_2^{\ell\tau},n_3^{\ell\tau})^T$ being the outward unit normal vector to the face $\partial\Omega^{\ell\tau}$ pointing from element Ω^{ℓ} to Ω^{τ}, with the property $n_k^{\tau\ell}=-n_k^{\ell\tau}$ and N_{ℓ} being the set of neighbors of cell Ω^{ℓ}. Note that in two space dimensions $n_3^{\ell\tau}=0$. The mesh spacing in direction k is denoted by Δx_k. The semi-discrete finite volume scheme in multiple space dimensions reads

$$\frac{\partial\mathbf{q}^{\ell}}{\partial t}=-\frac{1}{|\Omega^{\ell}|}\sum_{\tau\in N_{\ell}}\left|\partial\Omega^{\ell\tau}\right|\left(\mathcal{F}\left(\mathbf{q}^{\ell},\mathbf{q}^{\tau}\right)\cdot\mathbf{n}^{\ell\tau}+\mathcal{R}\left(\mathbf{q}^{\ell},\mathbf{q}^{\tau}\right)\cdot\mathbf{n}^{\ell\tau}-\mathcal{G}\left(\mathbf{q}^{\ell},\mathbf{q}^{\tau}\right)\cdot\mathbf{n}^{\ell\tau}-\mathbf{P}\left(\mathbf{q}^{\ell},\mathbf{q}^{\tau}\right)\right)+\mathbf{S}(\mathbf{q}^{\ell}) \tag{57}$$

with the thermodynamically compatible flux in normal direction

$$\mathcal{F}^{\ell\tau}=\mathcal{F}\left(\mathbf{q}^{\ell},\mathbf{q}^{\tau}\right)\cdot\mathbf{n}^{\ell\tau}=\widetilde{\mathcal{F}}^{\ell\tau}-\alpha^{\ell\tau}\left(\mathbf{p}^{\tau}-\mathbf{p}^{\ell}\right)=\left(\mathcal{F}_{\rho}^{\ell\tau},\mathcal{F}_{\rho v_i}^{\ell\tau},\mathcal{F}_{\rho S}^{\ell\tau},\mathbf{0},\mathbf{0}\right)^T,\quad \widetilde{\mathcal{F}}^{\ell\tau}=\frac{1}{2}\left(\mathbf{f}_k^{\ell}+\mathbf{f}_k^{\tau}\right)n_k^{\ell\tau}, \tag{58}$$

$$\alpha^{\ell\tau}=\frac{F_k^{12,\tau}-F_k^{12,\ell}+\frac{1}{2}\left(\mathbf{f}_k^{\ell}+\mathbf{f}_k^{\tau}\right)\cdot\left(\mathbf{p}^{\tau}-\mathbf{p}^{\ell}\right)-\left(\mathbf{p}^{\tau}\cdot\mathbf{f}_k^{\tau}-\mathbf{p}^{\ell}\cdot\mathbf{f}_k^{\ell}\right)}{\left(\mathbf{p}^{\tau}-\mathbf{p}^{\ell}\right)^2}\cdot n_k^{\ell\tau}, \tag{59}$$

the numerical flux for the viscous terms

$$\mathcal{G}\left(\mathbf{q}^{\ell},\mathbf{q}^{\tau}\right)=\epsilon^{\ell\tau}\frac{\mathbf{q}^{\tau}-\mathbf{q}^{\ell}}{\delta^{\ell\tau}}=\epsilon^{\ell\tau}\frac{\Delta\mathbf{q}^{\ell\tau}}{\delta^{\ell\tau}},\quad \delta^{\ell\tau}=\left\|\mathbf{x}^{\tau}-\mathbf{x}^{\ell}\right\|=\Delta x_k n_k^{\ell\tau}, \tag{60}$$

and the fluctuations and entropy production term related to the viscosity

$$\mathcal{R}\left(\mathbf{q}^{\ell},\mathbf{q}^{\tau}\right)\cdot\mathbf{n}^{\ell\tau}=\begin{pmatrix}0\\ \left(\sigma_{ik}^{\ell\tau}-\sigma_{ik}^{\ell}\right)\cdot n_k^{\ell\tau}+\left(\omega_{ik}^{\ell\tau}-\omega_{ik}^{\ell}\right)\cdot n_k^{\ell\tau}\\ \frac{1}{2}\left(\beta_k^{\tau}-\beta_k^{\ell}\right)\cdot n_k^{\ell\tau}\\ \frac{1}{2}A_{im}^{\ell\tau}\left(v_m^{\tau}-v_m^{\ell}\right)n_k^{\ell\tau}+\frac{1}{2}\tilde{u}_A^{\ell\tau}\left(A_{ik}^{\tau}-A_{ik}^{\ell}\right)\\ \frac{1}{2}J_m^{\ell\tau}\left(v_m^{\tau}-v_m^{\ell}\right)n_k^{\ell\tau}+\frac{1}{2}\tilde{u}_j^{\ell\tau}\left(J_k^{\tau}-J_k^{\ell}\right)+\frac{1}{2}\left(T^{\tau}-T^{\ell}\right)n_k^{\ell\tau}\end{pmatrix},\quad \mathbf{P}\left(\mathbf{q}^{\ell},\mathbf{q}^{\tau}\right)=\begin{pmatrix}0\\ \mathbf{0}\\ \Pi^{\ell\tau}\\ \mathbf{0}\\ \mathbf{0}\end{pmatrix}, \tag{61}$$

where

$$\sigma_{jk}^{\ell\tau}=\frac{1}{2}\left(A_{ij}^{\ell}+A_{ij}^{\tau}\right)\frac{1}{2}\left(\alpha_{ik}^{\ell}+\alpha_{ik}^{\tau}\right),\quad \omega_{ik}^{\ell\tau}=\frac{1}{2}\left(J_i^{\ell}+J_i^{\tau}\right)\frac{1}{2}\left(\beta_k^{\ell}+\beta_k^{\tau}\right), \tag{62}$$

$$A_{im}^{\ell\tau}=\frac{1}{2}\left(A_{im}^{\ell}+A_{im}^{\tau}\right),\qquad \tilde{u}_A^{\ell\tau}=\frac{\mathcal{F}_{\rho}^{\ell\tau}\left(E_3^{\tau}-E_3^{\ell}\right)}{\frac{1}{2}\left(\alpha_{ik}^{\ell}+\alpha_{ik}^{\tau}\right)\left(A_{ik}^{\tau}-A_{ik}^{\ell}\right)}, \tag{63}$$

$$J_i^{\ell\imath} = \frac{1}{2}\left(J_i^\ell + J_i^\imath\right), \qquad \tilde{u}_J^{\ell\imath} = \frac{\mathcal{F}_\rho^{\ell\imath}\left(E_4^\imath - E_4^\ell\right)}{\frac{1}{2}\left(\beta_k^\ell + \beta_k^\imath\right)\left(J_k^\imath - J_k^\ell\right)}, \tag{64}$$

$$\Pi^{\ell\imath} = \frac{1}{2}\epsilon^{\ell\imath}\frac{\Delta\mathbf{q}^{\ell\imath}}{T^\ell}\cdot\partial^2_{\mathbf{qq}}\tilde{\mathcal{E}}^{\ell\imath}\frac{\Delta\mathbf{q}^{\ell\imath}}{\delta^{\ell\imath}}, \qquad T^\ell = \frac{\left(\rho^\ell\right)^{\gamma-1}}{(\gamma-1)c_v}e^{\frac{S^\ell}{c_v}}. \tag{65}$$

The Roe matrix of the Hessian of the energy potential reads

$$\partial^2_{\mathbf{qq}}\tilde{\mathcal{E}}^{\ell\imath} = \int_0^1 \partial^2_{\mathbf{qq}}\mathcal{E}\left(\tilde{\boldsymbol{\psi}}(s)\right)ds =: \left(\partial^2_{\mathbf{pp}}\tilde{L}^{\ell\imath}\right)^{-1}, \tag{66}$$

and is based on the simple straight line segment path in $\mathbf{q}$ variables

$$\tilde{\boldsymbol{\psi}}(s) = \mathbf{q}^\ell + s\left(\mathbf{q}^\imath - \mathbf{q}^\ell\right), \qquad 0 \le s \le 1. \tag{67}$$

By construction, the Roe matrix $\partial^2_{\mathbf{qq}}\tilde{\mathcal{E}}^{\ell\imath}$ satisfies the Roe property

$$\partial^2_{\mathbf{qq}}\tilde{\mathcal{E}}^{\ell\imath}\cdot\left(\mathbf{q}^\imath - \mathbf{q}^\ell\right) = \left(\mathbf{p}^\imath - \mathbf{p}^\ell\right), \tag{68}$$

which allows to convert jumps in the conservative variables into jumps of the thermodynamic dual variables, i.e. into jumps in the main field. Throughout this paper the path integral in (66) is calculated *numerically* with a Gauss-Legendre quadrature formula using three quadrature points. However, we stress that in the theoretical analysis of the schemes presented later, we assume that the quadrature is *exact*. For a detailed analysis on the influence of the quadrature error the reader is referred to [61]. Finally, the algebraic source terms are defined according to (54). It is easy to check that, by construction, the numerical flux, the fluctuations and the source terms verify the compatibility conditions:

$$\mathbf{p}^\ell\cdot\left(\mathcal{F}^{\ell\imath} - \mathbf{f}_k^\ell n_k^{\ell\imath}\right) + \mathbf{p}^\imath\cdot\left(\mathbf{f}_k^\imath n_k^{\ell\imath} - \mathcal{F}^{\ell\imath}\right) = \left(F_k^{12,\imath} - F_k^{12,\ell}\right)n_k^{\ell\imath}; \tag{69}$$

$$\mathbf{p}^\ell\cdot\mathcal{R}\left(\mathbf{q}^\ell,\mathbf{q}^\imath\right)\cdot\mathbf{n}^{\ell\imath} + \mathbf{p}^\imath\cdot\mathcal{R}\left(\mathbf{q}^\imath,\mathbf{q}^\ell\right)\cdot\mathbf{n}^{\imath\ell} = \left(F_k^{34,\imath} - F_k^{34,\ell}\right)n_k^{\ell\imath}; \tag{70}$$

$$\mathbf{p}^\ell\cdot\mathbf{S}\left(\mathbf{q}^\ell\right) = 0. \tag{71}$$

It is also obvious that the following identity holds,

$$\sum_{\imath\in N_\ell}\left|\partial\Omega^{\ell\imath}\right|\mathbf{n}^{\ell\imath} = 0, \tag{72}$$

since the integral of the normal vector over a closed surface vanishes.

Theorem 3.1 (Cell entropy inequality)**.** *The HTC FV scheme (57) satisfies the following cell entropy inequality:*

$$\frac{\partial\rho S^\ell}{\partial t} + \frac{1}{|\Omega^\ell|}\sum_{\imath\in N_\ell}\left|\Omega^{\ell\imath}\right|\left(\mathcal{F}_{\rho S}\left(\mathbf{q}^\ell,\mathbf{q}^\imath\right)\mathbf{n}^{\ell\imath} + \frac{1}{2}\left(\beta_k^\imath + \beta_k^\ell\right)\cdot n_k^{\ell\imath} - \mathcal{G}_{\rho S}\left(\mathbf{q}^\ell,\mathbf{q}^\imath\right)\cdot\mathbf{n}^{\ell\imath}\right) \ge 0. \tag{73}$$

Proof. Taking the discrete equation for the entropy density from (57), substituting (61), (65) and (54), and using the fact that the integral of the normal vector over a closed surface vanishes

$$\sum_{\imath\in N_\ell}\left|\partial\Omega^{\ell\imath}\right|n_k^{\ell\imath} = 0$$

multiplied by β_k^ℓ, we obtain

$$\begin{aligned}&\frac{\partial(\rho S)^\ell}{\partial t} + \frac{1}{|\Omega^\ell|}\sum_{\imath\in N_\ell}\left|\partial\Omega^{\ell\imath}\right|\left(\mathcal{F}_{\rho S}\left(\mathbf{q}^\ell,\mathbf{q}^\imath\right)\cdot\mathbf{n}^{\ell\imath} + \frac{1}{2}\left(\beta_k^\imath + \beta_k^\ell\right)\cdot n_k^{\ell\imath} - \mathcal{G}_{\rho S}\left(\mathbf{q}^\ell,\mathbf{q}^\imath\right)\cdot\mathbf{n}^{\ell\imath}\right)\\ &= \frac{1}{|\Omega^\ell|}\sum_{\imath\in N_\ell}\left|\partial\Omega^{\ell\imath}\right|\frac{1}{2}\epsilon^{\ell\imath}\frac{\Delta\mathbf{q}^{\ell\imath}}{T^\ell}\cdot\partial^2_{\mathbf{qq}}\tilde{\mathcal{E}}^{\ell\imath}\frac{\Delta\mathbf{q}^{\ell\imath}}{\delta^{\ell\imath}} + \frac{\alpha_{ik}^\ell\alpha_{ik}^\ell}{\theta_1^\ell(\tau_1)T^\ell} + \frac{\beta_k^\ell\beta_k^\ell}{\theta_2^\ell(\tau_2)T^\ell} \ge 0,\end{aligned}$$

where the positivity of the right hand side is obtained thanks to θ_1^ℓ, θ_2^ℓ and T^ℓ being positive and due to the positive semi-definiteness of the Hessian $\partial^2_{\mathbf{qq}}\mathcal{E}$. □

Theorem 3.2 (Nonlinear stability in the energy norm)**.** *The scheme (57) with the numerical flux, the viscous and source terms defined in (58)–(65) is nonlinearly stable in the energy norm in the sense that, for vanishing boundary fluxes, we have*

$$\int_{\Omega} \frac{\partial \mathcal{E}}{\partial t} d\mathbf{x} = 0. \tag{74}$$

Proof. To demonstrate non-linear stability in the energy norm, we first compute the semi-discrete energy conservation law resulting from the dot product of the thermodynamically dual variables $\mathbf{p}^\ell$ with the semi-discrete scheme (57):

$$\begin{aligned}
\mathbf{p}^\ell \cdot \frac{\partial \mathbf{q}^\ell}{\partial t} = &-\frac{1}{|\Omega^\ell|} \sum_{\tau \in N_\ell} \left|\partial\Omega^{\ell\tau}\right| \left(\mathbf{p}^\ell \cdot \mathcal{F}\left(\mathbf{q}^\ell, \mathbf{q}^\tau\right) \cdot \mathbf{n}^{\ell\tau} + \mathbf{p}^\ell \cdot \mathcal{R}\left(\mathbf{q}^\ell, \mathbf{q}^\tau\right) \cdot \mathbf{n}^{\ell\tau}\right) \\
&+\frac{1}{|\Omega^\ell|} \sum_{\tau \in N_\ell} \left|\partial\Omega^{\ell\tau}\right| \left(\mathbf{p}^\ell \cdot \mathcal{G}\left(\mathbf{q}^\ell, \mathbf{q}^\tau\right) \cdot \mathbf{n}^{\ell\tau} + \mathbf{p}^\ell \cdot \mathbf{P}\left(\mathbf{q}^\ell, \mathbf{q}^\tau\right)\right) + \mathbf{p}^\ell \cdot \mathbf{S}(\mathbf{q}^\ell).
\end{aligned}$$

From (71) the source terms in the former equation cancel. Moreover, adding and subtracting the terms corresponding to $\frac{1}{2}\mathbf{p}^\tau \cdot \mathcal{R}\left(\mathbf{q}^\tau, \mathbf{q}^\ell\right) \cdot \mathbf{n}^{\tau\ell}$, $\frac{1}{2}\mathbf{p}^\tau \cdot \mathcal{F}^{\ell\tau}$ and $\frac{1}{2}\mathbf{p}^\tau \cdot \mathcal{G}\left(\mathbf{q}^\ell, \mathbf{q}^\tau\right) \cdot \mathbf{n}^{\ell\tau}$, we get

$$\begin{aligned}
\frac{\partial \mathcal{E}^\ell}{\partial t} = &-\frac{1}{|\Omega^\ell|} \sum_{\tau \in N_\ell} \left|\partial\Omega^{\ell\tau}\right| \left(\frac{1}{2}\left(\mathbf{p}^\ell + \mathbf{p}^\tau\right) \cdot \mathcal{F}^{\ell\tau}\right) - \frac{1}{|\Omega^\ell|} \sum_{\tau \in N_\ell} \left|\partial\Omega^{\ell\tau}\right| \left(\frac{1}{2}\left(\mathbf{p}^\ell - \mathbf{p}^\tau\right) \cdot \mathcal{F}^{\ell\tau}\right) \\
&-\frac{1}{|\Omega^\ell|} \sum_{\tau \in N_\ell} \left|\partial\Omega^{\ell\tau}\right| \left(\frac{1}{2}\mathbf{p}^\ell \cdot \mathcal{R}\left(\mathbf{q}^\ell, \mathbf{q}^\tau\right) \cdot \mathbf{n}^{\ell\tau} + \frac{1}{2}\mathbf{p}^\tau \cdot \mathcal{R}\left(\mathbf{q}^\tau, \mathbf{q}^\ell\right) \cdot \mathbf{n}^{\tau\ell}\right) \\
&-\frac{1}{|\Omega^\ell|} \sum_{\tau \in N_\ell} \left|\partial\Omega^{\ell\tau}\right| \left(\frac{1}{2}\mathbf{p}^\ell \cdot \mathcal{R}\left(\mathbf{q}^\ell, \mathbf{q}^\tau\right) \cdot \mathbf{n}^{\ell\tau} - \frac{1}{2}\mathbf{p}^\tau \cdot \mathcal{R}\left(\mathbf{q}^\tau, \mathbf{q}^\ell\right) \cdot \mathbf{n}^{\tau\ell}\right) \\
&+\frac{1}{|\Omega^\ell|} \sum_{\tau \in N_\ell} \left|\partial\Omega^{\ell\tau}\right| \left(\frac{1}{2}\left(\mathbf{p}^\ell + \mathbf{p}^\tau\right) \cdot \mathcal{G}\left(\mathbf{q}^\ell, \mathbf{q}^\tau\right) \cdot \mathbf{n}^{\ell\tau} + \frac{1}{2}\left(\mathbf{p}^\ell - \mathbf{p}^\tau\right) \cdot \mathcal{G}\left(\mathbf{q}^\ell, \mathbf{q}^\tau\right) \cdot \mathbf{n}^{\ell\tau} + \mathbf{p}^\ell \cdot \mathbf{P}\left(\mathbf{q}^\ell, \mathbf{q}^\tau\right)\right).
\end{aligned}$$

The compatibility conditions (69) and (70) and $\mathbf{n}^{\tau\ell} = -\mathbf{n}^{\ell\tau}$ yield

$$\begin{aligned}
\frac{\partial \mathcal{E}^\ell}{\partial t} = &-\frac{1}{2|\Omega^\ell|} \sum_{\tau \in N_\ell} \left|\partial\Omega^{\ell\tau}\right| \left(F_k^{12,\tau} - F_k^{12,\ell}\right) n_k^{\ell\tau} \\
&-\frac{1}{2|\Omega^\ell|} \sum_{\tau \in N_\ell} \left|\partial\Omega^{\ell\tau}\right| \left(\mathbf{p}^\ell \cdot \mathbf{f}_k^\ell - \mathbf{p}^\tau \cdot \mathbf{f}_k^\tau\right) n_k^{\ell\tau} - \frac{1}{2|\Omega^\ell|} \sum_{\tau \in N_\ell} \left|\partial\Omega^{\ell\tau}\right| \left(\mathbf{p}^\ell + \mathbf{p}^\tau\right) \cdot \mathcal{F}^{\ell\tau} \\
&-\frac{1}{2|\Omega^\ell|} \sum_{\tau \in N_\ell} \left|\partial\Omega^{\ell\tau}\right| \left(F_k^{34,\tau} - F_k^{34,\ell}\right) n_k^{\ell\tau} - \frac{1}{2|\Omega^\ell|} \sum_{\tau \in N_\ell} \left|\partial\Omega^{\ell\tau}\right| \left(\mathbf{p}^\ell \cdot \mathcal{R}\left(\mathbf{q}^\ell, \mathbf{q}^\tau\right) + \mathbf{p}^\tau \cdot \mathcal{R}\left(\mathbf{q}^\tau, \mathbf{q}^\ell\right)\right) \cdot \mathbf{n}^{\ell\tau} \\
&+\frac{1}{|\Omega^\ell|} \sum_{\tau \in N_\ell} \left|\partial\Omega^{\ell\tau}\right| \left(\frac{1}{2}\left(\mathbf{p}^\ell + \mathbf{p}^\tau\right) \cdot \mathcal{G}\left(\mathbf{q}^\ell, \mathbf{q}^\tau\right) \cdot \mathbf{n}^{\ell\tau} + \frac{1}{2}\left(\mathbf{p}^\ell - \mathbf{p}^\tau\right) \cdot \mathcal{G}\left(\mathbf{q}^\ell, \mathbf{q}^\tau\right) \cdot \mathbf{n}^{\ell\tau} + \mathbf{p}^\ell \cdot \mathbf{P}\left(\mathbf{q}^\ell, \mathbf{q}^\tau\right)\right).
\end{aligned}$$

Adding $\mathbf{p}^\ell \cdot \mathbf{f}_k^\ell$ multiplied by (72) and using (60) and (65), we get

$$\begin{aligned}
\frac{\partial \mathcal{E}^\ell}{\partial t} = &-\frac{1}{2|\Omega^\ell|} \sum_{\tau \in N_\ell} \left|\partial\Omega^{\ell\tau}\right| \left(F_k^\tau + F_k^\ell\right) n_k^{\ell\tau} + \frac{1}{2|\Omega^\ell|} \sum_{\tau \in N_\ell} \left|\partial\Omega^{\ell\tau}\right| \left(\mathbf{p}^\tau \cdot \mathbf{f}_k^\tau + \mathbf{p}^\ell \cdot \mathbf{f}_k^\ell\right) n_k^{\ell\tau} \\
&-\frac{1}{2|\Omega^\ell|} \sum_{\tau \in N_\ell} \left|\partial\Omega^{\ell\tau}\right| \left(\mathbf{p}^\ell + \mathbf{p}^\tau\right) \cdot \mathcal{F}^{\ell\tau} - \frac{1}{2|\Omega^\ell|} \sum_{\tau \in N_\ell} \left|\partial\Omega^{\ell\tau}\right| \left(\mathbf{p}^\ell \cdot \mathcal{R}\left(\mathbf{q}^\ell, \mathbf{q}^\tau\right) + \mathbf{p}^\tau \cdot \mathcal{R}\left(\mathbf{q}^\tau, \mathbf{q}^\ell\right)\right) \cdot \mathbf{n}^{\ell\tau} \\
&+\frac{1}{|\Omega^\ell|} \sum_{\tau \in N_\ell} \left|\partial\Omega^{\ell\tau}\right| \left(\frac{1}{2}\left(\mathbf{p}^\ell + \mathbf{p}^\tau\right) \cdot \mathcal{G}\left(\mathbf{q}^\ell, \mathbf{q}^\tau\right) \cdot \mathbf{n}^{\ell\tau} + \frac{1}{2}\left(\mathbf{p}^\ell - \mathbf{p}^\tau\right) \cdot \epsilon^{\ell\tau} \frac{\Delta \mathbf{q}^{\ell\tau}}{\delta^{\ell\tau}} + \frac{1}{2}\epsilon^{\ell\tau} \Delta \mathbf{q}^{\ell\tau} \cdot \partial^2_{\mathbf{qq}} \tilde{\mathcal{E}}^{\ell\tau} \frac{\Delta \mathbf{q}^{\ell\tau}}{\delta^{\ell\tau}}\right).
\end{aligned}$$

Since the last two terms cancel due to the Roe property (68) of the Roe matrix of the Hessian of the total energy potential, we finally obtain the discrete energy conservation law in terms of a sum of numerical total energy fluxes as

$$\begin{aligned}
\frac{\partial \mathcal{E}^\ell}{\partial t} = &-\frac{1}{2|\Omega^\ell|} \sum_{\tau \in N_\ell} \left|\partial\Omega^{\ell\tau}\right| \left(F_k^\tau + F_k^\ell\right) n_k^{\ell\tau} + \frac{1}{2|\Omega^\ell|} \sum_{\tau \in N_\ell} \left|\partial\Omega^{\ell\tau}\right| \left(\mathbf{p}^\tau \cdot \mathbf{f}_k^\tau + \mathbf{p}^\ell \cdot \mathbf{f}_k^\ell\right) n_k^{\ell\tau} \\
&-\frac{1}{2|\Omega^\ell|} \sum_{\tau \in N_\ell} \left|\partial\Omega^{\ell\tau}\right| \left(\mathbf{p}^\ell + \mathbf{p}^\tau\right) \cdot \left(\mathcal{F}^{\ell\tau} - \mathcal{G}\left(\mathbf{q}^\ell, \mathbf{q}^\tau\right) \cdot \mathbf{n}^{\ell\tau}\right) \\
&-\frac{1}{2|\Omega^\ell|} \sum_{\tau \in N_\ell} \left|\partial\Omega^{\ell\tau}\right| \left(\mathbf{p}^\ell \cdot \mathcal{R}\left(\mathbf{q}^\ell, \mathbf{q}^\tau\right) + \mathbf{p}^\tau \cdot \mathcal{R}\left(\mathbf{q}^\tau, \mathbf{q}^\ell\right)\right) \cdot \mathbf{n}^{\ell\tau}.
\end{aligned}$$

As a consequence we obtain the sought nonlinear stability in the energy norm

$$\int_\Omega \frac{\partial \mathcal{E}}{\partial t} d\mathbf{x} = \sum_\ell \frac{\partial \mathcal{E}^\ell}{\partial t} = 0$$

by assuming the fluxes to be zero at the boundary and after applying the telescopic sum of the fluxes at the interfaces. □

4. Thermodynamically compatible discontinuous Galerkin finite element schemes of type I

The first kind of HTC DG schemes proposed in this manuscript is built by simply using the numerical HTC flux for the inviscid part developed for the HTC finite volume scheme described previously. Like in the FV case, we will first detail the derivation of such DG type I scheme in 1D and we will then move to the multi-dimensional case.

4.1. One dimensional case

To introduce a first HTC DG scheme for the discretization of (1), called HTC DG scheme of type I in the following, we start defining a one dimensional cell as $T^\ell = [x^{\ell-\frac{1}{2}}, x^{\ell+\frac{1}{2}}]$. We also introduce a DG approximation space with spatial basis functions, $\varphi_m(x)$, given by the Lagrange interpolation polynomials of degree N passing through the $N+1$ Gauss-Legendre quadrature points in each element and which are allowed to jump at the element boundaries. Thus, we assume that the solution $\mathbf{q}(x,t)$ can be expressed as a linear combination of a set of spatial basis functions as

$$\mathbf{q}_h(x,t) = \sum_{m=0}^{N} \varphi_m(x) \hat{\mathbf{q}}_m^\ell(t), \tag{75}$$

where $\hat{\mathbf{q}}_m^\ell(t)$ are the time dependent degrees of freedom and N denotes the polynomial approximation degree. Accordingly, one could also write the thermodynamic dual variables, $\mathbf{p}$, as a linear combination of basis functions as

$$\mathbf{p}_h(x,t) = \sum_{m=0}^{N} \varphi_m(x) \hat{\mathbf{p}}_m^\ell(t), \qquad \hat{\mathbf{p}}_m^\ell(t) = \mathbf{p}\left(\hat{\mathbf{q}}_m^\ell(t)\right), \tag{76}$$

as well as the total energy, $\mathcal{E}$,

$$\mathcal{E}_h(x,t) = \sum_{m=0}^{N} \varphi_m(x) \hat{\mathcal{E}}_m^\ell(t), \qquad \hat{\mathcal{E}}_m^\ell(t) = \mathcal{E}\left(\hat{\mathbf{q}}_m^\ell(t)\right). \tag{77}$$

Besides, in the following, we will denote

$$\varphi_k^{\ell-\frac{1}{2}} = \varphi_k\left(x_+^{\ell-\frac{1}{2}}\right), \quad \varphi_k^{\ell+\frac{1}{2}} = \varphi_k\left(x_-^{\ell+\frac{1}{2}}\right), \quad \partial_x\varphi_k^{\ell-\frac{1}{2}} = \partial_x\varphi_k\left(x_+^{\ell-\frac{1}{2}}\right), \quad \partial_x\varphi_k^{\ell+\frac{1}{2}} = \partial_x\varphi_k\left(x_-^{\ell+\frac{1}{2}}\right).$$

We now substitute (75) in (1a)–(1e) multiply by a test function φ_k, integrate on a cell T^ℓ and apply integration by parts to the convective and viscous terms obtaining

$$\begin{aligned}
&\int_{x^{\ell-\frac{1}{2}}}^{x^{\ell+\frac{1}{2}}} \varphi_k \partial_t \mathbf{q}_h dx + \varphi_k^{\ell+\frac{1}{2}} \mathcal{F}^{\ell+\frac{1}{2}} - \varphi_k^{\ell-\frac{1}{2}} \mathcal{F}^{\ell-\frac{1}{2}} - \int_{x_+^{\ell-\frac{1}{2}}}^{x_-^{\ell+\frac{1}{2}}} \partial_x\varphi_k \mathbf{f}_1(\mathbf{q}_h) dx \\
&+\varphi_k^{\ell+\frac{1}{2}} \mathcal{R}_-^{\ell+\frac{1}{2}} + \varphi_k^{\ell-\frac{1}{2}} \mathcal{R}_+^{\ell-\frac{1}{2}} + \int_{x_+^{\ell-\frac{1}{2}}}^{x_-^{\ell+\frac{1}{2}}} \varphi_k(\partial_x \mathbf{h}_1(\mathbf{q}_h) + \mathbf{B}_1(\mathbf{q}_h)\partial_x\mathbf{q}_h) dx = \int_{x^{\ell-\frac{1}{2}}}^{x^{\ell+\frac{1}{2}}} \varphi_k \mathbf{S}(\mathbf{q}_h) dx \\
&+\varphi_k^{\ell+\frac{1}{2}} \mathcal{G}^{\ell+\frac{1}{2}} - \varphi_k^{\ell-\frac{1}{2}} \mathcal{G}^{\ell-\frac{1}{2}} + \partial_x\varphi_k^{\ell+\frac{1}{2}} \mathcal{V}^{\ell+\frac{1}{2}} + \partial_x\varphi_k^{\ell-\frac{1}{2}} \mathcal{V}^{\ell-\frac{1}{2}} - \int_{x_+^{\ell-\frac{1}{2}}}^{x_-^{\ell+\frac{1}{2}}} \partial_x\varphi_k \epsilon \partial_x\mathbf{q}_h dx + \mathbf{P}_k.
\end{aligned} \tag{78}$$

In the former equation, the thermodynamically compatible flux is chosen exactly as in the finite volume case (27) and therefore reads

$$\mathcal{F}^{\ell+\frac{1}{2}} = \mathcal{F}\left(\mathbf{q}_-^{\ell+\frac{1}{2}}, \mathbf{q}_+^{\ell+\frac{1}{2}}\right) = \widetilde{\mathcal{F}}^{\ell+\frac{1}{2}} - \alpha^{\ell+\frac{1}{2}}\left(\mathbf{p}_-^{\ell+1} - \mathbf{p}_+^{\ell}\right) = \left(\mathcal{F}_\rho^{\ell+\frac{1}{2}}, \mathcal{F}_{\rho v_i}^{\ell+\frac{1}{2}}, \mathcal{F}_{\rho S}^{\ell+\frac{1}{2}}, \mathbf{0}, \mathbf{0}\right), \tag{79}$$

with the central flux, which is in general not compatible,

$$\widetilde{\mathcal{F}}^{\ell+\frac{1}{2}} = \frac{1}{2}\left(\mathbf{f}_1\left(\mathbf{q}_-^{\ell+\frac{1}{2}}\right) + \mathbf{f}_1\left(\mathbf{q}_+^{\ell+\frac{1}{2}}\right)\right), \tag{80}$$

and the scalar correction factor

$$\alpha^{\ell+\frac{1}{2}} = \frac{F_1^{12}\left(\mathbf{q}_-^{\ell+\frac{1}{2}}\right) - F_1^{12}\left(\mathbf{q}_+^{\ell+\frac{1}{2}}\right) + \widetilde{\mathcal{F}}^{\ell+\frac{1}{2}} \cdot \left(\mathbf{p}_+^{\ell+\frac{1}{2}} - \mathbf{p}_-^{\ell+\frac{1}{2}}\right) - \left(\mathbf{p}_+^{\ell+\frac{1}{2}} \cdot \mathbf{f}_+^{\ell+\frac{1}{2}} - \mathbf{p}_-^{\ell+\frac{1}{2}} \cdot \mathbf{f}_-^{\ell+\frac{1}{2}}\right)}{\left(\mathbf{p}_+^{\ell+\frac{1}{2}} - \mathbf{p}_-^{\ell+\frac{1}{2}}\right)^2}. \tag{81}$$

In the case of vanishing denominator, the correction factor is set to zero. The numerical flux can be rewritten in terms of fluctuations as follows,

$$\mathcal{D}_-^{\ell+\frac{1}{2}} = \mathcal{F}^{\ell+\frac{1}{2}} - \mathbf{f}\left(\mathbf{q}_-^{\ell+\frac{1}{2}}\right) \qquad \text{and} \qquad \mathcal{D}_+^{\ell+\frac{1}{2}} = \mathbf{f}\left(\mathbf{q}_+^{\ell+\frac{1}{2}}\right) - \mathcal{F}^{\ell+\frac{1}{2}}. \tag{82}$$

Thanks to the particular construction of the numerical flux, the fluctuations satisfy the following compatibility relation, corresponding to (15) on the discrete level:

$$\mathbf{p}_-^{\ell+\frac{1}{2}} \cdot \mathcal{D}_-^{\ell+\frac{1}{2}} + \mathbf{p}_+^{\ell+\frac{1}{2}} \cdot \mathcal{D}_+^{\ell+\frac{1}{2}} = F_1^{12}\left(\mathbf{q}_+^{\ell+\frac{1}{2}}\right) - F_1^{12}\left(\mathbf{q}_-^{\ell+\frac{1}{2}}\right), \tag{83}$$

similar to the compatibility relation (25) of the finite volume scheme presented previously. We stress again that our thermodynamically compatible numerical flux does *not* rely on an underlying Godunov parametrization of the physical flux as $\mathbf{f}_k = \partial_{\mathbf{p}}(v_k L)$ in terms of a generating potential L, unlike the schemes presented in Busto et al. [59–62]. Moreover, we have the viscous numerical flux $\mathcal{G}^{\ell+\frac{1}{2}} = \left(\mathcal{G}_\rho^{\ell+\frac{1}{2}}, \mathcal{G}_{\rho v_i}^{\ell+\frac{1}{2}}, \mathcal{G}_{\rho S}^{\ell+\frac{1}{2}}, \mathcal{G}_{A_{ik}}^{\ell+\frac{1}{2}}, \mathcal{G}_{J_k}^{\ell+\frac{1}{2}}\right)$ given by

$$\mathcal{G}^{\ell+\frac{1}{2}} = \frac{1}{2}\epsilon\, \partial^2_{\mathbf{pp}} \tilde{L}^{\ell+\frac{1}{2}} \left(\partial_x \mathbf{p}_-^{\ell+\frac{1}{2}} + \partial_x \mathbf{p}_+^{\ell+\frac{1}{2}}\right) + \eta^{\ell+\frac{1}{2}} \left(\mathbf{q}_+^{\ell+\frac{1}{2}} - \mathbf{q}_-^{\ell+\frac{1}{2}}\right), \qquad \eta^{\ell+\frac{1}{2}} = \frac{1}{2} s_{\max}^{\ell+\frac{1}{2}} + \frac{2N+1}{\Delta x}\epsilon \tag{84}$$

following the seminal ideas of Gassner et al. [67]. The jump terms related to the viscous terms read

$$\mathcal{V}^{\ell+\frac{1}{2}} = \frac{1}{2}\epsilon\left(\mathbf{q}_+^{\ell+\frac{1}{2}} - \mathbf{q}_-^{\ell+\frac{1}{2}}\right), \tag{85}$$

and the discrete entropy production term related to the viscous terms $\mathbf{P}_k = (0, \mathbf{0}, \Pi_k, \mathbf{0}, \mathbf{0})^T$ with

$$\begin{aligned}\Pi_k = &\int_{x^{\ell-\frac{1}{2}}}^{x^{\ell+\frac{1}{2}}} \varphi_k \frac{\epsilon}{T} \partial_x \mathbf{q}_h \cdot \partial^2_{\mathbf{qq}} \mathcal{E}\, \partial_x \mathbf{q}_h dx + \varphi_k^{\ell-\frac{1}{2}} \frac{\eta^{\ell-\frac{1}{2}}}{2\, T_+^{\ell-\frac{1}{2}}} \left(\mathbf{q}_+^{\ell-\frac{1}{2}} - \mathbf{q}_-^{\ell-\frac{1}{2}}\right) \cdot \partial^2_{\mathbf{qq}} \tilde{\mathcal{E}}^{\ell-\frac{1}{2}} \left(\mathbf{q}_+^{\ell-\frac{1}{2}} - \mathbf{q}_-^{\ell-\frac{1}{2}}\right) \\ &+ \varphi_k^{\ell+\frac{1}{2}} \frac{\eta^{\ell+\frac{1}{2}}}{2\, T_-^{\ell+\frac{1}{2}}} \left(\mathbf{q}_+^{\ell+\frac{1}{2}} - \mathbf{q}_-^{\ell+\frac{1}{2}}\right) \cdot \partial^2_{\mathbf{qq}} \tilde{\mathcal{E}}^{\ell+\frac{1}{2}} \left(\mathbf{q}_+^{\ell+\frac{1}{2}} - \mathbf{q}_-^{\ell+\frac{1}{2}}\right).\end{aligned} \tag{86}$$

Alternatively, to ease calculations in the proofs shown later, we can also use a one sided production term, i.e.,

$$\Pi_k^{\ell+\frac{1}{2}} = \int_{x^{\ell-\frac{1}{2}}}^{x^{\ell+\frac{1}{2}}} \varphi_k \frac{\epsilon}{T} \partial_x \mathbf{q}_h \cdot \partial^2_{\mathbf{qq}} \mathcal{E}\, \partial_x \mathbf{q}_h dx + \varphi_k^{\ell+\frac{1}{2}} \frac{\eta^{\ell+\frac{1}{2}}}{T_-^{\ell+\frac{1}{2}}} \left(\mathbf{q}_+^{\ell+\frac{1}{2}} - \mathbf{q}_-^{\ell+\frac{1}{2}}\right) \cdot \partial^2_{\mathbf{qq}} \tilde{\mathcal{E}}_{i+\frac{1}{2}} \left(\mathbf{q}_+^{\ell+\frac{1}{2}} - \mathbf{q}_-^{\ell+\frac{1}{2}}\right). \tag{87}$$

Finally, the fluctuations $\mathcal{R}_\pm^{\ell+\frac{1}{2}} = \left(\mathcal{R}_\rho^{\ell+\frac{1}{2}}, \mathcal{R}_{\rho v_i,\pm}^{\ell+\frac{1}{2}}, \mathcal{R}_{\rho S}^{\ell+\frac{1}{2}}, \mathcal{R}_{A_{ik}}^{\ell+\frac{1}{2}}, \mathcal{R}_{J_k}^{\ell+\frac{1}{2}}\right)$ are given by

$$\mathcal{R}_-^{\ell+\frac{1}{2}} = \begin{pmatrix} 0 \\ \sigma_{i1}^{\ell+\frac{1}{2}} - \sigma_{i1}^{\ell+\frac{1}{2},-} + \omega_{i1}^{\ell+\frac{1}{2}} - \omega_{i1}^{\ell+\frac{1}{2},-} \\ \frac{1}{2}\left(\beta_1^{\ell+\frac{1}{2},+} - \beta_1^{\ell+\frac{1}{2},-}\right) \\ \frac{1}{2} A_{im}^{\ell+\frac{1}{2}} \left(v_m^{\ell+\frac{1}{2},+} - v_m^{\ell+\frac{1}{2},-}\right) n_k + \frac{1}{2}\tilde{u}_A^{\ell+\frac{1}{2}} \left(A_{ik}^{\ell+\frac{1}{2},+} - A_{ik}^{\ell+\frac{1}{2},-}\right) \\ \frac{1}{2} J_m^{\ell+\frac{1}{2}} \left(v_m^{\ell+\frac{1}{2},+} - v_m^{\ell+\frac{1}{2},-}\right) n_k + \frac{1}{2}\tilde{u}_J^{\ell+\frac{1}{2}} \left(J_k^{\ell+\frac{1}{2},+} - J_k^{\ell+\frac{1}{2},-}\right) + \frac{1}{2}\left(T^{\ell+\frac{1}{2},+} - T^{\ell+\frac{1}{2},-}\right) n_k \end{pmatrix} \tag{88}$$

and

$$\mathcal{R}_+^{\ell+\frac{1}{2}} = \begin{pmatrix} 0 \\ \sigma_{i1}^{\ell+\frac{1}{2},+} - \sigma_{i1}^{\ell+\frac{1}{2}} + \omega_{i1}^{\ell+\frac{1}{2},+} - \omega_{i1}^{\ell+\frac{1}{2}} \\ \frac{1}{2}\left(\beta_1^{\ell+\frac{1}{2},+} - \beta_1^{\ell+\frac{1}{2},-}\right) \\ \frac{1}{2} A_{im}^{\ell+\frac{1}{2}} \left(v_m^{\ell+\frac{1}{2},+} - v_m^{\ell+\frac{1}{2},-}\right) n_k + \frac{1}{2}\tilde{u}_A^{\ell+\frac{1}{2}} \left(A_{ik}^{\ell+\frac{1}{2},+} - A_{ik}^{\ell+\frac{1}{2},-}\right) \\ \frac{1}{2} J_m^{\ell+\frac{1}{2}} \left(v_m^{\ell+\frac{1}{2},+} - v_m^{\ell+\frac{1}{2},-}\right) n_k + \frac{1}{2}\tilde{u}_J^{\ell+\frac{1}{2}} \left(J_k^{\ell+\frac{1}{2},+} - J_k^{\ell+\frac{1}{2},-}\right) + \frac{1}{2}\left(T^{\ell+\frac{1}{2},+} - T^{\ell+\frac{1}{2},-}\right) n_k \end{pmatrix} \tag{89}$$

with the compatible discretization of the stress tensors

$$\sigma_{ik}^{\ell+\frac{1}{2}} = \frac{1}{2}\left(A_{mi}^{\ell+\frac{1}{2},+} + A_{mi}^{\ell+\frac{1}{2},-}\right)\frac{1}{2}\left(\alpha_{mk}^{\ell+\frac{1}{2},+} + \alpha_{mk}^{\ell+\frac{1}{2},-}\right),\ \ \omega_{ik}^{\ell+\frac{1}{2}} = \frac{1}{2}\left(J_{i}^{\ell+\frac{1}{2},+} + J_{i}^{\ell+\frac{1}{2},-}\right)\frac{1}{2}\left(\beta_{k}^{\ell+\frac{1}{2},+} + \beta_{k}^{\ell+\frac{1}{2},-}\right), \tag{90}$$

where

$$A_{im}^{\ell+\frac{1}{2}} = \frac{1}{2}\left(A_{im}^{\ell+\frac{1}{2},+} + A_{im}^{\ell+\frac{1}{2},-}\right), \qquad \tilde{u}_{A}^{\ell+\frac{1}{2}} = \frac{\mathcal{F}_{\rho}^{\ell+\frac{1}{2}}\left(E_{3}^{\ell+\frac{1}{2},+} - E_{3}^{\ell+\frac{1}{2},-}\right)}{\frac{1}{2}\left(\alpha_{ik}^{\ell+\frac{1}{2},+} + \alpha_{ik}^{\ell+\frac{1}{2},-}\right)\left(A_{ik}^{\ell+\frac{1}{2},+} - A_{ik}^{\ell+\frac{1}{2},-}\right)}, \tag{91}$$

$$J_{i}^{\ell+\frac{1}{2}} = \frac{1}{2}\left(J_{i}^{\ell+\frac{1}{2},+} + J_{i}^{\ell+\frac{1}{2},-}\right), \qquad \tilde{u}_{J}^{\ell+\frac{1}{2}} = \frac{\mathcal{F}_{\rho}^{\ell+\frac{1}{2}}\left(E_{4}^{\ell+\frac{1}{2},+} - E_{4}^{\ell+\frac{1}{2},-}\right)}{\frac{1}{2}\left(\beta_{k}^{\ell+\frac{1}{2},+} + \beta_{k}^{\ell+\frac{1}{2},-}\right)\left(J_{k}^{\ell+\frac{1}{2},+} - J_{k}^{\ell+\frac{1}{2},-}\right)}, \tag{92}$$

and $\mathbf{n} = (1, 0, 0)$ in the 1D case. As for the finite volume scheme, the fluctuations satisfy the compatibility relation (16) at the discrete level:

$$\mathbf{p}_{-}^{\ell+\frac{1}{2}} \cdot \mathcal{R}_{-}^{\ell+\frac{1}{2}} + \mathbf{p}_{+}^{\ell+\frac{1}{2}} \cdot \mathcal{R}_{+}^{\ell+\frac{1}{2}} = F_{1}^{34}\left(\mathbf{q}_{+}^{\ell+\frac{1}{2}}\right) - F_{1}^{34}\left(\mathbf{q}_{-}^{\ell+\frac{1}{2}}\right). \tag{93}$$

Theorem 4.1 (Cell entropy inequality)**.** *The HTC DG scheme of type I (78) satisfies the following cell entropy inequality:*

$$\int_{x^{\ell-\frac{1}{2}}}^{x^{\ell+\frac{1}{2}}} \partial_t (\rho S)_h dx + \mathcal{F}_{\rho S}^{\ell+\frac{1}{2}} - \mathcal{F}_{\rho S}^{\ell-\frac{1}{2}} + \beta_1^{\ell+\frac{1}{2}} - \beta_2^{\ell-\frac{1}{2}} - \mathcal{G}_{\rho S}^{\ell+\frac{1}{2}} + \mathcal{G}_{\rho S}^{\ell-\frac{1}{2}} \geq 0. \tag{94}$$

Proof. Choosing as test function the constant function $\varphi_k = 1$ inside a cell, we obtain the evolution equation for the *cell average* of the entropy density ρS according to the HTC DG scheme of type I (78) as follows:

$$\int_{x^{\ell-\frac{1}{2}}}^{x^{\ell+\frac{1}{2}}} \partial_t (\rho S)_h dx + \mathcal{F}_{\rho S}^{\ell+\frac{1}{2}} - \mathcal{F}_{\rho S}^{\ell-\frac{1}{2}} + \mathcal{R}_{\rho S}^{\ell+\frac{1}{2}} + \mathcal{R}_{\rho S}^{\ell-\frac{1}{2}} + \int_{x_{+}^{\ell-\frac{1}{2}}}^{x_{-}^{\ell+\frac{1}{2}}} \partial_x \beta_1 \, dx = \int_{x^{\ell-\frac{1}{2}}}^{x^{\ell+\frac{1}{2}}} \pi \, dx$$

$$+\mathcal{G}_{\rho S}^{\ell+\frac{1}{2}} - \mathcal{G}_{\rho S}^{\ell-\frac{1}{2}} + \int_{x^{\ell-\frac{1}{2}}}^{x^{\ell+\frac{1}{2}}} \frac{\epsilon}{T} \partial_x \mathbf{q}_h \cdot \partial_{\mathbf{qq}}^2 \mathcal{E} \, \partial_x \mathbf{q}_h dx + \frac{\eta^{\ell+\frac{1}{2}}}{T_{-}^{\ell+\frac{1}{2}}} \left(\mathbf{q}_{+}^{\ell+\frac{1}{2}} - \mathbf{q}_{-}^{\ell+\frac{1}{2}}\right) \cdot \partial_{\mathbf{qq}}^2 \tilde{\mathcal{E}}_{i+\frac{1}{2}} \left(\mathbf{q}_{+}^{\ell+\frac{1}{2}} - \mathbf{q}_{-}^{\ell+\frac{1}{2}}\right), \tag{95}$$

where we have introduced the abbreviation

$$\pi = \frac{\alpha_{ik}\alpha_{ik}}{\theta_1(\tau_1)T} + \frac{\beta_i \beta_i}{\theta_2(\tau_2)T} \geq 0. \tag{96}$$

Since the red terms reduce to a flux difference

$$\mathcal{R}_{\rho S}^{\ell+\frac{1}{2}} + \mathcal{R}_{\rho S}^{\ell-\frac{1}{2}} + \int_{x_{+}^{\ell-\frac{1}{2}}}^{x_{-}^{\ell+\frac{1}{2}}} \partial_x \beta_1 \, dx = \frac{1}{2}\left(\beta_1^{\ell+\frac{1}{2},+} - \beta_1^{\ell+\frac{1}{2},-}\right) + \frac{1}{2}\left(\beta_1^{\ell-\frac{1}{2},+} - \beta_1^{\ell-\frac{1}{2},-}\right) + \beta_1^{\ell+\frac{1}{2},-} - \beta_1^{\ell-\frac{1}{2},+}$$

$$= \frac{1}{2}\left(\beta_1^{\ell+\frac{1}{2},+} + \beta_1^{\ell+\frac{1}{2},-}\right) - \frac{1}{2}\left(\beta_1^{\ell-\frac{1}{2},+} + \beta_1^{\ell-\frac{1}{2},-}\right) := \beta_1^{\ell+\frac{1}{2}} - \beta_1^{\ell-\frac{1}{2}}$$

we can rewrite (95) as

$$\int_{x^{\ell-\frac{1}{2}}}^{x^{\ell+\frac{1}{2}}} \partial_t (\rho S)_h dx + \mathcal{F}_{\rho S}^{\ell+\frac{1}{2}} - \mathcal{F}_{\rho S}^{\ell-\frac{1}{2}} + \beta_1^{\ell+\frac{1}{2}} - \beta_1^{\ell-\frac{1}{2}} - \mathcal{G}_{\rho S}^{\ell+\frac{1}{2}} + \mathcal{G}_{\rho S}^{\ell-\frac{1}{2}} = \int_{x^{\ell-\frac{1}{2}}}^{x^{\ell+\frac{1}{2}}} \pi \, dx +$$

$$+ \int_{x^{\ell-\frac{1}{2}}}^{x^{\ell+\frac{1}{2}}} \frac{\epsilon}{T} \partial_x \mathbf{q}_h \cdot \partial_{\mathbf{qq}}^2 \mathcal{E} \, \partial_x \mathbf{q}_h dx + \frac{\eta^{\ell+\frac{1}{2}}}{T_{-}^{\ell+\frac{1}{2}}} \left(\mathbf{q}_{+}^{\ell+\frac{1}{2}} - \mathbf{q}_{-}^{\ell+\frac{1}{2}}\right) \cdot \partial_{\mathbf{qq}}^2 \tilde{\mathcal{E}}_{i+\frac{1}{2}} \left(\mathbf{q}_{+}^{\ell+\frac{1}{2}} - \mathbf{q}_{-}^{\ell+\frac{1}{2}}\right) \geq 0, \tag{97}$$

which concludes the proof, since we are assuming the Hessian of the total energy potential to be at least positive semi-definite and all the terms on the right hand side of (97) are quadratic forms and are thus non-negative. □

Theorem 4.2 (Nonlinear stability in the energy norm)**.** *The scheme (78) with the numerical flux, the fluctuations, the viscous flux and the source terms defined in (79)–(89) is nonlinearly stable in the energy norm in the sense that, for vanishing boundary fluxes, we have*

$$\int_{\Omega} \frac{\partial \mathcal{E}}{\partial t} dx = 0. \tag{98}$$

Proof. To show that the proposed scheme is thermodynamically compatible, we take the dot product of $\mathbf{p}_h$ with (78), apply (77) and integrate by parts the volume integral of the physical flux, getting

$$\begin{aligned}
&\int_{x^{\ell-\frac{1}{2}}}^{x^{\ell+\frac{1}{2}}} \mathbf{p}_h \cdot \partial_t \mathbf{q}_h dx + \mathbf{p}_-^{\ell+\frac{1}{2}} \cdot \mathcal{F}^{\ell+\frac{1}{2}} - \mathbf{p}_+^{\ell-\frac{1}{2}} \cdot \mathcal{F}^{\ell-\frac{1}{2}} - \left(\mathbf{p}_-^{\ell+\frac{1}{2}} \cdot \mathbf{f}_-^{\ell+\frac{1}{2}} - \mathbf{p}_+^{\ell-\frac{1}{2}} \cdot \mathbf{f}_+^{\ell-\frac{1}{2}} \right) \\
&+\mathbf{p}_-^{\ell+\frac{1}{2}} \cdot \mathcal{R}_-^{\ell+\frac{1}{2}} + \mathbf{p}_+^{\ell-\frac{1}{2}} \cdot \mathcal{R}_+^{\ell-\frac{1}{2}} + \int_{x_+^{\ell-\frac{1}{2}}}^{x_-^{\ell+\frac{1}{2}}} \mathbf{p}_h \cdot (\partial_x \mathbf{f} + \partial_x \mathbf{h}_1(\mathbf{q}_h) + \mathbf{B}_1(\mathbf{q}_h) \partial_x \mathbf{q}_h) dx = \int_{x^{\ell-\frac{1}{2}}}^{x^{\ell+\frac{1}{2}}} \mathbf{p}_h \cdot \mathbf{S}(\mathbf{q}_h) dx \\
&+\mathbf{p}_-^{\ell+\frac{1}{2}} \cdot \mathcal{G}^{\ell+\frac{1}{2}} - \mathbf{p}_+^{\ell-\frac{1}{2}} \cdot \mathcal{G}^{\ell-\frac{1}{2}} + \partial_x \mathbf{p}_-^{\ell+\frac{1}{2}} \cdot \mathcal{V}^{\ell+\frac{1}{2}} + \partial_x \mathbf{p}_+^{\ell-\frac{1}{2}} \cdot \mathcal{V}^{\ell-\frac{1}{2}} - \int_{x_+^{\ell-\frac{1}{2}}}^{x_-^{\ell+\frac{1}{2}}} \partial_x \mathbf{p}_h \cdot \epsilon \partial_x \mathbf{q}_h dx + \mathbf{P}_k \cdot \hat{\mathbf{p}}_k^{\ell}.
\end{aligned} \tag{99}$$

Next, adding and subtracting $\mathbf{p}_+^{\ell+\frac{1}{2}} \cdot \mathcal{F}^{\ell+\frac{1}{2}}$, $\mathbf{p}_+^{\ell+\frac{1}{2}} \cdot \mathbf{f}_+^{\ell+\frac{1}{2}}$ and $\mathbf{p}_+^{\ell+\frac{1}{2}} \cdot \mathcal{R}_+^{\ell+\frac{1}{2}}$ and rearranging terms yields

$$\begin{aligned}
&\int_{x^{\ell-\frac{1}{2}}}^{x^{\ell+\frac{1}{2}}} \partial_t \mathcal{E}_h dx + \left(\mathbf{p}_+^{\ell+\frac{1}{2}} \cdot \left(\mathcal{F}^{\ell+\frac{1}{2}} - \mathbf{f}_+^{\ell+\frac{1}{2}} \right) - \mathbf{p}_+^{\ell-\frac{1}{2}} \cdot \left(\mathcal{F}^{\ell-\frac{1}{2}} - \mathbf{f}_+^{\ell-\frac{1}{2}} \right) \right) + \left(\mathbf{p}_+^{\ell-\frac{1}{2}} \cdot \mathcal{R}_+^{\ell-\frac{1}{2}} - \mathbf{p}_+^{\ell+\frac{1}{2}} \cdot \mathcal{R}_+^{\ell+\frac{1}{2}} \right) \\
&+\mathbf{p}_-^{\ell+\frac{1}{2}} \cdot \left(\mathcal{F}^{\ell+\frac{1}{2}} - \mathbf{f}_-^{\ell+\frac{1}{2}} \right) + \mathbf{p}_+^{\ell+\frac{1}{2}} \cdot \left(\mathbf{f}_+^{\ell+\frac{1}{2}} - \mathcal{F}^{\ell+\frac{1}{2}} \right) + \left(\mathbf{p}_-^{\ell+\frac{1}{2}} \cdot \mathcal{R}_-^{\ell+\frac{1}{2}} + \mathbf{p}_+^{\ell+\frac{1}{2}} \cdot \mathcal{R}_+^{\ell+\frac{1}{2}} \right) \\
&+ \int_{x_+^{\ell-\frac{1}{2}}}^{x_-^{\ell+\frac{1}{2}}} \mathbf{p}_h \cdot (\partial_x \mathbf{f} + \partial_x \mathbf{h}_1(\mathbf{q}_h) + \mathbf{B}_1(\mathbf{q}_h) \partial_x \mathbf{q}_h) dx \\
&= \mathbf{p}_-^{\ell+\frac{1}{2}} \cdot \mathcal{G}^{\ell+\frac{1}{2}} - \mathbf{p}_+^{\ell-\frac{1}{2}} \cdot \mathcal{G}^{\ell-\frac{1}{2}} + \partial_x \mathbf{p}_-^{\ell+\frac{1}{2}} \cdot \mathcal{V}^{\ell+\frac{1}{2}} + \partial_x \mathbf{p}_+^{\ell-\frac{1}{2}} \cdot \mathcal{V}^{\ell-\frac{1}{2}} \\
&- \int_{x_+^{\ell-\frac{1}{2}}}^{x_-^{\ell+\frac{1}{2}}} \partial_x \mathbf{p}_h \cdot \epsilon \partial_x \mathbf{q}_h dx + \mathbf{P}_k \cdot \hat{\mathbf{p}}_k^{\ell} + \int_{x^{\ell-\frac{1}{2}}}^{x^{\ell+\frac{1}{2}}} \mathbf{p}_h \cdot \mathbf{S}(\mathbf{q}_h) dx.
\end{aligned}$$

Applying the compatibility Eqs. (83) and (93) and using (14) leads to

$$\begin{aligned}
&\int_{x^{\ell-\frac{1}{2}}}^{x^{\ell+\frac{1}{2}}} \partial_t \mathcal{E}_h dx + \left(\mathbf{p}_+^{\ell+\frac{1}{2}} \cdot \left(\mathcal{F}^{\ell+\frac{1}{2}} - \mathbf{f}_+^{\ell+\frac{1}{2}} \right) - \mathbf{p}_+^{\ell-\frac{1}{2}} \cdot \left(\mathcal{F}^{\ell-\frac{1}{2}} - \mathbf{f}_+^{\ell-\frac{1}{2}} \right) \right) + \left(\mathbf{p}_+^{\ell-\frac{1}{2}} \cdot \mathcal{R}_+^{\ell-\frac{1}{2}} - \mathbf{p}_+^{\ell+\frac{1}{2}} \cdot \mathcal{R}_+^{\ell+\frac{1}{2}} \right) \\
&+F_1\left(\mathbf{q}_+^{\ell+\frac{1}{2}} \right) - F_1\left(\mathbf{q}_-^{\ell+\frac{1}{2}} \right) + F_1\left(\mathbf{q}_-^{\ell+\frac{1}{2}} \right) - F_1\left(\mathbf{q}_+^{\ell-\frac{1}{2}} \right) \\
&= \mathbf{p}_-^{\ell+\frac{1}{2}} \cdot \mathcal{G}^{\ell+\frac{1}{2}} - \mathbf{p}_+^{\ell-\frac{1}{2}} \cdot \mathcal{G}^{\ell-\frac{1}{2}} + \partial_x \mathbf{p}_-^{\ell+\frac{1}{2}} \cdot \mathcal{V}^{\ell+\frac{1}{2}} + \partial_x \mathbf{p}_+^{\ell-\frac{1}{2}} \cdot \mathcal{V}^{\ell-\frac{1}{2}} \\
&- \int_{x_+^{\ell-\frac{1}{2}}}^{x_-^{\ell+\frac{1}{2}}} \partial_x \mathbf{p}_h \cdot \epsilon \partial_x \mathbf{q}_h dx + \mathbf{P}_k \cdot \hat{\mathbf{p}}_k^{\ell} + \int_{x^{\ell-\frac{1}{2}}}^{x^{\ell+\frac{1}{2}}} \mathbf{p}_h \cdot \mathbf{S}(\mathbf{q}_h) dx
\end{aligned}$$

which, taking into account (18), is equivalent to

$$\int_{x^{\ell-\frac{1}{2}}}^{x^{\ell+\frac{1}{2}}} \partial_t \mathcal{E}_h dx + \left[F_1\left(\mathbf{q}_+^{\ell+\frac{1}{2}} \right) + \mathbf{p}_+^{\ell+\frac{1}{2}} \cdot \left(\mathcal{F}^{\ell+\frac{1}{2}} - \mathbf{f}_+^{\ell+\frac{1}{2}} - \mathcal{R}_+^{\ell+\frac{1}{2}} \right) - F_1\left(\mathbf{q}_+^{\ell-\frac{1}{2}} \right) - \mathbf{p}_+^{\ell-\frac{1}{2}} \cdot \left(\mathcal{F}^{\ell-\frac{1}{2}} - \mathbf{f}_+^{\ell-\frac{1}{2}} - \mathcal{R}_+^{\ell-\frac{1}{2}} \right) \right]$$

$$= \mathbf{p}_-^{\ell+\frac{1}{2}} \cdot \mathcal{G}^{\ell+\frac{1}{2}} - \mathbf{p}_+^{\ell-\frac{1}{2}} \cdot \mathcal{G}^{\ell-\frac{1}{2}} + \partial_x \mathbf{p}_-^{\ell+\frac{1}{2}} \cdot \mathcal{V}^{\ell+\frac{1}{2}} + \partial_x \mathbf{p}_+^{\ell-\frac{1}{2}} \cdot \mathcal{V}^{\ell-\frac{1}{2}} - \int_{x_+^{\ell-\frac{1}{2}}}^{x_-^{\ell+\frac{1}{2}}} \partial_x \mathbf{p}_h \cdot \epsilon \partial_x \mathbf{q}_h dx + \mathbf{P}_k \cdot \hat{\mathbf{p}}_k^{\ell}.$$

We now focus on the terms related to dissipation. Adding and subtracting $\mathbf{p}_+^{\ell+\frac{1}{2}} \mathcal{G}^{\ell+\frac{1}{2}}$ and $\partial \mathbf{p}_+^{\ell+\frac{1}{2}} \mathcal{V}^{\ell+\frac{1}{2}}$ we get

$$\begin{aligned}
\int_{x^{\ell-\frac{1}{2}}}^{x^{\ell+\frac{1}{2}}} \partial_t \mathcal{E}_h dx + \left[F_1\left(\mathbf{q}_+^{\ell+\frac{1}{2}}\right) + \mathbf{p}_+^{\ell+\frac{1}{2}} \cdot \left(\mathcal{F}^{\ell+\frac{1}{2}} - \mathbf{f}_+^{\ell+\frac{1}{2}} - \mathcal{R}_+^{\ell+\frac{1}{2}} \right) - F_1\left(\mathbf{q}_+^{\ell-\frac{1}{2}}\right) - \mathbf{p}_+^{\ell-\frac{1}{2}} \cdot \left(\mathcal{F}^{\ell-\frac{1}{2}} - \mathbf{f}_+^{\ell-\frac{1}{2}} - \mathcal{R}_+^{\ell-\frac{1}{2}} \right) \right] \\
= \mathbf{p}_+^{\ell+\frac{1}{2}} \cdot \mathcal{G}^{\ell+\frac{1}{2}} - \mathbf{p}_+^{\ell-\frac{1}{2}} \cdot \mathcal{G}^{\ell-\frac{1}{2}} + \partial_x \mathbf{p}_+^{\ell-\frac{1}{2}} \cdot \mathcal{V}^{\ell-\frac{1}{2}} - \partial_x \mathbf{p}_+^{\ell+\frac{1}{2}} \cdot \mathcal{V}^{\ell+\frac{1}{2}} \\
+ \left(\mathbf{p}_-^{\ell+\frac{1}{2}} - \mathbf{p}_+^{\ell+\frac{1}{2}} \right) \cdot \mathcal{G}^{\ell+\frac{1}{2}} + \left(\partial_x \mathbf{p}_-^{\ell+\frac{1}{2}} + \partial_x \mathbf{p}_+^{\ell+\frac{1}{2}} \right) \cdot \mathcal{V}^{\ell+\frac{1}{2}} - \int_{x_+^{\ell-\frac{1}{2}}}^{x_-^{\ell+\frac{1}{2}}} \partial_x \mathbf{p}_h \cdot \epsilon \partial_x \mathbf{q}_h dx + \mathbf{P}_k \cdot \hat{\mathbf{p}}_k^{\ell}.
\end{aligned}$$

The first four terms related to the viscosity are the sought viscous terms that lead to the numerical viscosity flux in the energy equation, while the remaining terms vanish:

$$\begin{aligned}
&\left(\mathbf{p}_-^{\ell+\frac{1}{2}} - \mathbf{p}_+^{\ell+\frac{1}{2}} \right) \cdot \mathcal{G}^{\ell+\frac{1}{2}} + \left(\partial_x \mathbf{p}_-^{\ell+\frac{1}{2}} + \partial_x \mathbf{p}_+^{\ell+\frac{1}{2}} \right) \cdot \mathcal{V}^{\ell+\frac{1}{2}} - \int_{x_+^{\ell-\frac{1}{2}}}^{x_-^{\ell+\frac{1}{2}}} \partial_x \mathbf{p}_h \cdot \epsilon \partial_x \mathbf{q}_h dx + \mathbf{P}_k \cdot \hat{\mathbf{p}}_k^{\ell} \\
&= -\left(\mathbf{p}_+^{\ell+\frac{1}{2}} - \mathbf{p}_-^{\ell+\frac{1}{2}} \right) \cdot \left(\frac{1}{2} \epsilon \, \partial^2_{\mathbf{pp}} \tilde{L}^{\ell+\frac{1}{2}} \left(\partial_x \mathbf{p}_-^{\ell+\frac{1}{2}} + \partial_x \mathbf{p}_+^{\ell+\frac{1}{2}} \right) + \eta^{\ell+\frac{1}{2}} \left(\mathbf{q}_+^{\ell+\frac{1}{2}} - \mathbf{q}_-^{\ell+\frac{1}{2}} \right) \right) \\
&+ \left(\partial_x \mathbf{p}_-^{\ell+\frac{1}{2}} + \partial_x \mathbf{p}_+^{\ell+\frac{1}{2}} \right) \cdot \left(\frac{1}{2} \epsilon \left(\mathbf{q}_+^{\ell+\frac{1}{2}} - \mathbf{q}_-^{\ell+\frac{1}{2}} \right) \right) - \int_{x_+^{\ell-\frac{1}{2}}}^{x_-^{\ell+\frac{1}{2}}} \partial_x \mathbf{p}_h \cdot \epsilon \partial_x \mathbf{q}_h dx + \mathbf{P}_k \cdot \hat{\mathbf{p}}_k^{\ell} = 0
\end{aligned}$$

since due to the Roe property of matrix $\partial^2_{\mathbf{pp}} \tilde{L}^{\ell+\frac{1}{2}}$ and by the definition of the production term, we have

$$\begin{aligned}
-\left(\mathbf{p}_+^{\ell+\frac{1}{2}} - \mathbf{p}_-^{\ell+\frac{1}{2}} \right) \cdot \eta^{\ell+\frac{1}{2}} \left(\mathbf{q}_+^{\ell+\frac{1}{2}} - \mathbf{q}_-^{\ell+\frac{1}{2}} \right) - \int_{x_+^{\ell-\frac{1}{2}}}^{x_-^{\ell+\frac{1}{2}}} \partial_x \mathbf{p}_h \cdot \epsilon \partial_x \mathbf{q}_h dx + \int_{x^{\ell-\frac{1}{2}}}^{x^{\ell+\frac{1}{2}}} \epsilon \partial_x \mathbf{q}_h \cdot \partial^2_{\mathbf{qq}} \mathcal{E} \, \partial_x \mathbf{q}_h dx \\
+ \eta^{\ell+\frac{1}{2}} \left(\mathbf{q}_+^{\ell+\frac{1}{2}} - \mathbf{q}_-^{\ell+\frac{1}{2}} \right) \cdot \partial^2_{\mathbf{qq}} \tilde{\mathcal{E}}_{i+\frac{1}{2}} \left(\mathbf{q}_+^{\ell+\frac{1}{2}} - \mathbf{q}_-^{\ell+\frac{1}{2}} \right) = 0.
\end{aligned}$$

Finally, we get the discrete total energy conservation law:

$$\begin{aligned}
\int_{x^{\ell-\frac{1}{2}}}^{x^{\ell+\frac{1}{2}}} \partial_t \mathcal{E}_h dx + \left[F_1\left(\mathbf{q}_+^{\ell+\frac{1}{2}}\right) + \mathbf{p}_+^{\ell+\frac{1}{2}} \cdot \left(\mathcal{F}^{\ell+\frac{1}{2}} - \mathbf{f}_+^{\ell+\frac{1}{2}} - \mathcal{R}_+^{\ell+\frac{1}{2}} \right) - F_1\left(\mathbf{q}_+^{\ell-\frac{1}{2}}\right) - \mathbf{p}_+^{\ell-\frac{1}{2}} \cdot \left(\mathcal{F}^{\ell-\frac{1}{2}} - \mathbf{f}_+^{\ell-\frac{1}{2}} - \mathcal{R}_+^{\ell-\frac{1}{2}} \right) \right] \\
= \mathbf{p}_+^{\ell+\frac{1}{2}} \cdot \mathcal{G}^{\ell+\frac{1}{2}} - \mathbf{p}_+^{\ell-\frac{1}{2}} \cdot \mathcal{G}^{\ell-\frac{1}{2}} + \partial_x \mathbf{p}_+^{\ell-\frac{1}{2}} \cdot \mathcal{V}^{\ell-\frac{1}{2}} - \partial_x \mathbf{p}_+^{\ell+\frac{1}{2}} \cdot \mathcal{V}^{\ell+\frac{1}{2}}.
\end{aligned}$$

Summing over all elements and assuming the boundary fluxes to vanish, we get the sought result

$$\int_{\Omega} \partial_t \mathcal{E}_h dx = \sum_{\ell} \int_{x^{\ell-\frac{1}{2}}}^{x^{\ell+\frac{1}{2}}} \partial_t \mathcal{E}_h dx = 0,$$

since the internal fluxes cancel. □

4.2. HTC DG scheme of type I in multiple space dimensions

For the 2D case we define a Cartesian cell as $T_i = [x_1^{i_1-\frac{1}{2}}, x_1^{i_1+\frac{1}{2}}] \times [x_2^{i_2-\frac{1}{2}}, x_2^{i_2+\frac{1}{2}}]$, while in 3D it reads $T_i = [x_1^{i_1-\frac{1}{2}}, x_1^{i_1+\frac{1}{2}}] \times [x_2^{i_2-\frac{1}{2}}, x_2^{i_2+\frac{1}{2}}] \times [x_3^{i_3-\frac{1}{2}}, x_3^{i_3+\frac{1}{2}}]$ with multi-index i and we assume that the solution $\mathbf{q}(\mathbf{x}, t)$ can be expressed as a linear com-

bination of a set of spatial basis functions φ_m as

$$\mathbf{q}_h(\mathbf{x},t) = \sum_{m=0}^{\mathcal{N}} \varphi_m(\mathbf{x})\hat{\mathbf{q}}_m^i(t),$$

where $\hat{\mathbf{q}}_m^i(t)$ are the time dependent degrees of freedom and $\mathcal{N} = (N+1)^d$ is the total number of degrees of freedom in d space dimensions, related to the polynomial approximation degree. Moreover, we consider nodal basis functions computed from the Lagrange interpolation polynomials passing through the Gauss-Legendre quadrature points. Like in the one-dimensional case, we now compute the product of (1a)–(1e) by a test function φ_k, we integrate on the spacial control volume T_i and we apply integration by parts obtaining

$$\begin{aligned}
&\int_{T_i} \varphi_k \partial_t \mathbf{q} d\mathbf{x} + \int_{\partial T_i} \varphi_k \mathcal{F}(\mathbf{q}_h^\ell, \mathbf{q}_h^\text{r}) \cdot \mathbf{n}\, dS - \int_{T_i^\circ} \partial_m \varphi_k \mathbf{f}_m(\mathbf{q}_h) d\mathbf{x} \\
&+ \int_{\partial T_i} \varphi_k \mathcal{R}(\mathbf{q}_h^\ell, \mathbf{q}_h^\text{r}) \cdot \mathbf{n}\, dS + \int_{T_i^\circ} \varphi_k (\partial_m \mathbf{h}_m(\mathbf{q}_h) + \mathbf{B}_m(\mathbf{q}_h)\partial_m \mathbf{q}_h) d\mathbf{x} \\
&= \int_{\partial T_i} \varphi_k \mathcal{G}(\mathbf{q}_h^\ell, \mathbf{q}_h^\text{r}) \cdot \mathbf{n}\, dS + \int_{\partial T_i} \partial_m \varphi_k \mathcal{V}(\mathbf{q}_h^\ell, \mathbf{q}_h^\text{r}) \cdot n_m\, dS - \int_{T_i^\circ} \partial_m \varphi_k (\epsilon \partial_m \mathbf{q}_h) d\mathbf{x} + \mathbf{P}_k + \int_{T_i} \varphi_k \mathbf{S}(\mathbf{q}_h) d\mathbf{x}.
\end{aligned} \tag{100}$$

Let us note that, within this section, $\mathbf{q}_h^\ell$, $\mathbf{q}_h^\text{r}$ denote the boundary extrapolated values of the discrete solution at the left and the right sides of the element boundary, respectively. Then, in the DG scheme of type I we can directly employ the edge/face-based numerical fluxes and fluctuations already introduced for the finite volume case (57)–(59) and (61)–(65). On the other hand, the viscous fluxes are computed according to

$$\mathcal{G}\left(\mathbf{q}^\ell, \mathbf{q}^\text{r}\right) \cdot \mathbf{n} = \frac{1}{2}\epsilon\, \partial_{\mathbf{pp}}^2 \tilde{L}^{\ell\text{r}}\left(\partial_k \mathbf{p}^\ell + \partial_k \mathbf{p}^\text{r}\right) n_k + \eta^{\ell\text{r}}\left(\mathbf{q}^\text{r} - \mathbf{q}^\ell\right), \qquad \eta^{\ell\text{r}} = \frac{1}{2} s_{\max}^{\ell\text{r}} + \frac{2N+1}{\delta^{\ell\text{r}}}\epsilon^{\ell\text{r}}, \tag{101}$$

the jump terms read

$$\mathcal{V}\left(\mathbf{q}^\ell, \mathbf{q}^\text{r}\right) = \frac{1}{2}\epsilon^{\ell\text{r}}\left(\mathbf{q}^\text{r} - \mathbf{q}^\ell\right), \tag{102}$$

and the discretization of the non-negative entropy production term, $\mathbf{P}_k = (0, \mathbf{0}, \Pi_k, \mathbf{0}, \mathbf{0})^T$, is

$$\Pi_k = \int_{T_i^\circ} \varphi_k \frac{\epsilon}{T} \partial_k \mathbf{q}_h \cdot \partial_{\mathbf{qq}}^2 \mathcal{E}\, \partial_k \mathbf{q}_h d\mathbf{x} + \int_{\partial T_i} \varphi_k \frac{\eta^{\ell\text{r}}}{2T^\ell}\left(\mathbf{q}^\text{r} - \mathbf{q}^\ell\right) \cdot \partial_{\mathbf{qq}}^2 \tilde{\mathcal{E}}^{\ell\text{r}}\left(\mathbf{q}^\text{r} - \mathbf{q}^\ell\right) dS. \tag{103}$$

Theorem 4.3 (Cell entropy inequality)**.** *The HTC DG scheme of type I (100) satisfies the following cell entropy inequality:*

$$\int_{T_i} \partial_t (\rho S)_h d\mathbf{x} + \int_{\partial T_i} \mathcal{F}_{\rho S}(\mathbf{q}_h^\ell, \mathbf{q}_h^\text{r}) \cdot \mathbf{n}\, dS + \int_{\partial T_i} \frac{1}{2}\left(\beta_m^\ell + \beta_m^\text{r}\right) \cdot n_m\, dS - \int_{\partial T_i} \mathcal{G}_{\rho S}(\mathbf{q}_h^\ell, \mathbf{q}_h^\text{r}) \cdot \mathbf{n}\, dS \geq 0. \tag{104}$$

Proof. Setting the test function $\varphi_k = 1$ in (100) and notation (96) together with (103), we have

$$\begin{aligned}
&\int_{T_i} \partial_t \rho S d\mathbf{x} + \int_{\partial T_i} \mathcal{F}_{\rho S}(\mathbf{q}_h^\ell, \mathbf{q}_h^\text{r}) \cdot \mathbf{n}\, dS + \int_{\partial T_i} \mathcal{R}_{\rho S}(\mathbf{q}_h^\ell, \mathbf{q}_h^\text{r}) \cdot \mathbf{n}\, dS \\
&+ \int_{T_i^\circ} (\partial_m \mathbf{h}_m(\mathbf{q}_h) + \mathbf{B}_m(\mathbf{q}_h)\partial_m \mathbf{q}_h) d\mathbf{x} - \int_{\partial T_i} \mathcal{G}_{\rho S}(\mathbf{q}_h^\ell, \mathbf{q}_h^\text{r}) \cdot \mathbf{n}\, dS = \int_{T_i} \pi\, d\mathbf{x} \\
&+ \int_{T_i^\circ} \frac{\epsilon}{T} \partial_k \mathbf{q}_h \cdot \partial_{\mathbf{qq}}^2 \mathcal{E}\, \partial_k \mathbf{q}_h d\mathbf{x} + \int_{\partial T_i} \frac{\eta^{\ell\text{r}}}{2T^\ell}\left(\mathbf{q}^\text{r} - \mathbf{q}^\ell\right) \cdot \partial_{\mathbf{qq}}^2 \tilde{\mathcal{E}}^{\ell\text{r}}\left(\mathbf{q}^\text{r} - \mathbf{q}^\ell\right) dS.
\end{aligned}$$

Using (61), we get

$$\int_{T_i} \partial_t \rho S d\mathbf{x} + \int_{\partial T_i} \mathcal{F}_{\rho S}(\mathbf{q}_h^\ell, \mathbf{q}_h^\text{r}) \cdot \mathbf{n}\, dS + \int_{\partial T_i} \frac{1}{2}\left(\beta_k^\text{r} - \beta_k^\ell\right) \cdot n_k\, dS + \int_{T_i^\circ} \partial_m \beta_m d\mathbf{x} - \int_{\partial T_i} \mathcal{G}_{\rho S}(\mathbf{q}_h^\ell, \mathbf{q}_h^\text{r}) \cdot \mathbf{n}\, dS$$
$$= \int_{T_i} \pi\, d\mathbf{x} + \int_{T_i^\circ} \frac{\epsilon}{T} \partial_k \mathbf{q}_h \cdot \partial^2_{\mathbf{qq}} \mathcal{E}\, \partial_k \mathbf{q}_h d\mathbf{x} + \int_{\partial T_i} \frac{\eta^{\ell\text{r}}}{2\,T^\ell} \left(\mathbf{q}^\text{r} - \mathbf{q}^\ell\right) \cdot \partial^2_{\mathbf{qq}} \tilde{\mathcal{E}}^{\ell\text{r}} \left(\mathbf{q}^\text{r} - \mathbf{q}^\ell\right) dS.$$

Finally, applying Gauss' theorem results in

$$\int_{T_i} \partial_t \rho S d\mathbf{x} + \int_{\partial T_i} \mathcal{F}_{\rho S}(\mathbf{q}_h^\ell, \mathbf{q}_h^\text{r}) \cdot \mathbf{n}\, dS + \int_{\partial T_i} \frac{1}{2}\left(\beta_k^\text{r} + \beta_k^\ell\right) \cdot n_k\, dS - \int_{\partial T_i} \mathcal{G}_{\rho S}(\mathbf{q}_h^\ell, \mathbf{q}_h^\text{r}) \cdot \mathbf{n}\, dS$$
$$= \int_{T_i} \pi\, d\mathbf{x} + \int_{T_i^\circ} \frac{\epsilon}{T} \partial_k \mathbf{q}_h \cdot \partial^2_{\mathbf{qq}} \mathcal{E}\, \partial_k \mathbf{q}_h d\mathbf{x} + \int_{\partial T_i} \frac{\eta^{\ell\text{r}}}{2\,T^\ell} \left(\mathbf{q}^\text{r} - \mathbf{q}^\ell\right) \cdot \partial^2_{\mathbf{qq}} \tilde{\mathcal{E}}^{\ell\text{r}} \left(\mathbf{q}^\text{r} - \mathbf{q}^\ell\right) dS \geq 0,$$

where the positivity of the right hand side comes from $\pi \geq 0$ and $\partial^2_{\mathbf{qq}} \mathcal{E} \geq 0$. So we have obtained the sought cell entropy inequality. □

Theorem 4.4 (Nonlinear stability in the energy norm)**.** *The scheme (100) with the flux, viscous and source terms defined in (57)–(59), (61)–(65) and (101)–(103) is nonlinearly stable in the energy norm in the sense that, for vanishing boundary fluxes, we have*

$$\int_\Omega \frac{\partial \mathcal{E}}{\partial t} d\mathbf{x} = 0. \tag{105}$$

Proof. Similarly to what has been done in the one dimensional case we multiply scheme (100) by $\hat{\mathbf{p}}_m^i$ and sum up all equations, leading to

$$\int_{T_i} \mathbf{p}_h \cdot \partial_t \mathbf{q}_h d\mathbf{x} + \int_{\partial T_i} \mathbf{p}_h^\ell \cdot \mathcal{F}(\mathbf{q}_h^\ell, \mathbf{q}_h^\text{r}) \cdot \mathbf{n}\, dS - \int_{T_i^\circ} \partial_m \mathbf{p}_h \cdot \mathbf{f}_m(\mathbf{q}_h) d\mathbf{x}$$
$$+ \int_{\partial T_i} \mathbf{p}_h^\ell \cdot \mathcal{R}(\mathbf{q}_h^\ell, \mathbf{q}_h^\text{r}) \cdot \mathbf{n}\, dS + \int_{T_i^\circ} \mathbf{p}_h \cdot (\partial_m \mathbf{h}_m(\mathbf{q}_h) + \mathbf{B}_m(\mathbf{q}_h) \partial_m \mathbf{q}_h) d\mathbf{x}$$
$$= \int_{\partial T_i} \mathbf{p}_h^\ell \cdot \mathcal{G}(\mathbf{q}_h^\ell, \mathbf{q}_h^\text{r}) \cdot \mathbf{n}\, dS + \int_{\partial T_i} \partial_m \mathbf{p}_h^\ell \cdot \mathcal{V}(\mathbf{q}_h^\ell, \mathbf{q}_h^\text{r}) \cdot n_m\, dS - \int_{T_i^\circ} \partial_m \mathbf{p}_h \cdot (\epsilon\, \partial_m \mathbf{q}_h) d\mathbf{x} + \mathbf{P}_k \cdot \hat{\mathbf{p}}_k^i + \int_{T_i} \mathbf{p}_h \cdot \mathbf{S}(\mathbf{q}_h) d\mathbf{x}.$$

Applying integration by parts, we get

$$\int_{T_i} \mathbf{p}_h \cdot \partial_t \mathbf{q}_h d\mathbf{x} + \int_{\partial T_i} \mathbf{p}_h^\ell \cdot \left(\mathcal{F}(\mathbf{q}_h^\ell, \mathbf{q}_h^\text{r}) \cdot \mathbf{n} - \mathbf{f}_m(\mathbf{q}_h^\ell) n_m\right) dS$$
$$+ \int_{\partial T_i} \mathbf{p}_h^\ell \cdot \mathcal{R}(\mathbf{q}_h^\ell, \mathbf{q}_h^\text{r}) \cdot \mathbf{n}\, dS + \int_{T_i^\circ} \mathbf{p}_h \cdot (\partial_m f_m(\mathbf{q}_h) + \partial_m \mathbf{h}_m(\mathbf{q}_h) + \mathbf{B}_m(\mathbf{q}_h) \partial_m \mathbf{q}_h) d\mathbf{x}$$
$$= \int_{\partial T_i} \mathbf{p}_h^\ell \cdot \mathcal{G}(\mathbf{q}_h^\ell, \mathbf{q}_h^\text{r}) \cdot \mathbf{n}\, dS + \int_{\partial T_i} \partial_m \mathbf{p}_h^\ell \cdot \mathcal{V}(\mathbf{q}_h^\ell, \mathbf{q}_h^\text{r}) \cdot n_m\, dS - \int_{T_i^\circ} \partial_m \mathbf{p}_h \cdot (\epsilon\, \partial_m \mathbf{q}_h) d\mathbf{x} + \mathbf{P}_k \cdot \hat{\mathbf{p}}_k^i.$$

Using (14), the notation $\mathcal{F}^{\ell\text{r}} = \mathcal{F}(\mathbf{q}_h^\ell, \mathbf{q}_h^\text{r}) \cdot \mathbf{n}$ and adding and subtracting $\frac{1}{2} \int_{\partial T_i} \mathbf{p}_h^\text{r} \cdot \mathbf{f}_m(\mathbf{q}_h^\text{r}) n_m dS$, we obtain

$$\int_{T_i} \partial_t \mathcal{E}_h d\mathbf{x} + \frac{1}{2} \int_{\partial T_i} \mathbf{p}_h^\ell \cdot \left(\mathcal{F}^{\ell\text{r}} - \mathbf{f}_m(\mathbf{q}_h^\ell) n_m\right) dS + \frac{1}{2} \int_{\partial T_i} \mathbf{p}_h^\ell \cdot \left(\mathcal{F}^{\ell\text{r}} - \mathbf{f}_m(\mathbf{q}_h^\ell) n_m\right) dS$$
$$+ \frac{1}{2} \int_{\partial T_i} \mathbf{p}_h^\text{r} \cdot \left(\mathbf{f}_m(\mathbf{q}_h^\text{r}) n_m - \mathcal{F}^{\ell\text{r}}\right) dS - \frac{1}{2} \int_{\partial T_i} \mathbf{p}_h^\text{r} \cdot \left(\mathbf{f}_m(\mathbf{q}_h^\text{r}) n_m - \mathcal{F}^{\ell\text{r}}\right) dS$$
$$+ \int_{\partial T_i} \mathbf{p}_h^\ell \cdot \mathcal{R}(\mathbf{q}_h^\ell, \mathbf{q}_h^\text{r}) \cdot \mathbf{n}\, dS + \int_{T_i^\circ} \partial_m F_m d\mathbf{x}$$
$$= \int_{\partial T_i} \mathbf{p}_h^\ell \cdot \mathcal{G}(\mathbf{q}_h^\ell, \mathbf{q}_h^\text{r}) \cdot \mathbf{n}\, dS + \int_{\partial T_i} \partial_m \mathbf{p}_h^\ell \cdot \mathcal{V}(\mathbf{q}_h^\ell, \mathbf{q}_h^\text{r}) \cdot n_m\, dS - \int_{T_i^\circ} \partial_m \mathbf{p}_h \cdot (\epsilon\, \partial_m \mathbf{q}_h) d\mathbf{x} + \mathbf{P}_k \cdot \hat{\mathbf{p}}_k^i.$$

Rearranging terms and adding and subtracting $\int_{\partial T_i} \frac{1}{2}\mathbf{p}_h^\tau \cdot \mathcal{R}(\mathbf{q}_h^\tau, \mathbf{q}_h^\ell) \cdot (-\mathbf{n})\, dS$, yields

$$\begin{aligned}
&\int_{T_i} \partial_t \mathcal{E}_h d\mathbf{x} + \frac{1}{2}\int_{\partial T_i} \left(\mathbf{p}_h^\ell + \mathbf{p}_h^\tau\right) \cdot \mathcal{F}^{\ell\tau} dS - \frac{1}{2}\int_{\partial T_i} \left(\mathbf{p}_h^\tau \cdot \mathbf{f}_m(\mathbf{q}_h^\tau) + \mathbf{p}_h^\ell \cdot \mathbf{f}_m(\mathbf{q}_h^\ell)\right) n_m dS \\
&\qquad + \int_{T_i^\circ} \partial_m F_m d\mathbf{x} + \frac{1}{2}\int_{\partial T_i} \left(F_m^{12,\tau} - F_m^{12,\ell}\right) n_m dS \\
&+ \int_{\partial T_i} \frac{1}{2}\left(\mathbf{p}_h^\ell \cdot \mathcal{R}(\mathbf{q}_h^\ell, \mathbf{q}_h^\tau) - \mathbf{p}_h^\tau \cdot \mathcal{R}(\mathbf{q}_h^\tau, \mathbf{q}_h^\ell)\right) \cdot \mathbf{n}\, dS + \int_{\partial T_i} \frac{1}{2}\left(\mathbf{p}_h^\ell \cdot \mathcal{R}(\mathbf{q}_h^\ell, \mathbf{q}_h^\tau) + \mathbf{p}_h^\tau \cdot \mathcal{R}(\mathbf{q}_h^\tau, \mathbf{q}_h^\ell)\right) \cdot \mathbf{n}\, dS \\
&\quad = \int_{\partial T_i} \mathbf{p}_h^\ell \cdot \mathcal{G}(\mathbf{q}_h^\ell, \mathbf{q}_h^\tau) \cdot \mathbf{n}\, dS + \int_{\partial T_i} \partial_m \mathbf{p}_h^\ell \cdot \mathcal{V}(\mathbf{q}_h^\ell, \mathbf{q}_h^\tau) \cdot n_m\, dS - \int_{T_i^\circ} \partial_m \mathbf{p}_h \cdot (\epsilon\, \partial_m \mathbf{q}_h) d\mathbf{x} + \mathbf{P}_k \cdot \hat{\mathbf{p}}_k^i.
\end{aligned}$$

Applying Gauss' theorem and taking into account (70) with $\mathbf{n}^{\tau\ell} = -\mathbf{n}^{\ell\tau}$, we have

$$\begin{aligned}
&\int_{T_i} \partial_t \mathcal{E}_h d\mathbf{x} + \frac{1}{2}\int_{\partial T_i} \left[\left(\mathbf{p}_h^\ell + \mathbf{p}_h^\tau\right) \cdot \mathcal{F}^{\ell\tau} - \left(\mathbf{p}_h^\tau \cdot \mathbf{f}_m(\mathbf{q}_h^\tau) + \mathbf{p}_h^\ell \cdot \mathbf{f}_m(\mathbf{q}_h^\ell)\right) n_m\right] dS + \int_{\partial T_i} F_m^\ell n_m dS \\
&+ \frac{1}{2}\int_{\partial T_i} \left(F_m^{12,\tau} - F_m^{12,\ell}\right) n_m dS + \frac{1}{2}\int_{\partial T_i} \left(F_m^{34,\tau} - F_m^{34,\ell}\right) n_m dS + \int_{\partial T_i} \frac{1}{2}\left(\mathbf{p}_h^\ell \cdot \mathcal{R}(\mathbf{q}_h^\ell, \mathbf{q}_h^\tau) + \mathbf{p}_h^\tau \cdot \mathcal{R}(\mathbf{q}_h^\tau, \mathbf{q}_h^\ell)\right) \cdot \mathbf{n}\, dS \\
&\quad = \int_{\partial T_i} \mathbf{p}_h^\ell \cdot \mathcal{G}(\mathbf{q}_h^\ell, \mathbf{q}_h^\tau) \cdot \mathbf{n}\, dS + \int_{\partial T_i} \partial_m \mathbf{p}_h^\ell \cdot \mathcal{V}(\mathbf{q}_h^\ell, \mathbf{q}_h^\tau) \cdot n_m\, dS - \int_{T_i^\circ} \partial_m \mathbf{p}_h \cdot (\epsilon\, \partial_m \mathbf{q}_h) d\mathbf{x} + \mathbf{P}_k \cdot \hat{\mathbf{p}}_k^i.
\end{aligned}$$

We now put together the contribution relations to the fluxes F:

$$\begin{aligned}
&\int_{T_i} \partial_t \mathcal{E}_h d\mathbf{x} + \frac{1}{2}\int_{\partial T_i} \left[\left(\mathbf{p}_h^\ell + \mathbf{p}_h^\tau\right) \cdot \mathcal{F}^{\ell\tau} - \left(\mathbf{p}_h^\tau \cdot \mathbf{f}_m(\mathbf{q}_h^\tau) + \mathbf{p}_h^\ell \cdot \mathbf{f}_m(\mathbf{q}_h^\ell)\right) n_m\right] dS + \frac{1}{2}\int_{\partial T_i} \left(F_m^\tau + F_m^\ell\right) n_m dS \\
&\qquad + \int_{\partial T_i} \frac{1}{2}\left(\mathbf{p}_h^\ell \cdot \mathcal{R}(\mathbf{q}_h^\ell, \mathbf{q}_h^\tau) + \mathbf{p}_h^\tau \cdot \mathcal{R}(\mathbf{q}_h^\tau, \mathbf{q}_h^\ell)\right) \cdot \mathbf{n}\, dS \\
&\quad = \int_{\partial T_i} \mathbf{p}_h^\ell \cdot \mathcal{G}(\mathbf{q}_h^\ell, \mathbf{q}_h^\tau) \cdot \mathbf{n}\, dS + \int_{\partial T_i} \partial_m \mathbf{p}_h^\ell \cdot \mathcal{V}(\mathbf{q}_h^\ell, \mathbf{q}_h^\tau) \cdot n_m\, dS - \int_{T_i^\circ} \partial_m \mathbf{p}_h \cdot (\epsilon\, \partial_m \mathbf{q}_h) d\mathbf{x} + \mathbf{P}_k \cdot \hat{\mathbf{p}}_k^i.
\end{aligned} \tag{106}$$

Finally, we analyse the terms related to dissipation. To this end, we add and subtract $\frac{1}{2}\int_{\partial T_i} \mathbf{p}_h^\tau \cdot \mathcal{G}(\mathbf{q}_h^\ell, \mathbf{q}_h^\tau) \cdot \mathbf{n}\, dS$ and $\frac{1}{2}\int_{\partial T_i} \partial_m \mathbf{p}_h^\tau \cdot \mathcal{V}(\mathbf{q}_h^\ell, \mathbf{q}_h^\tau) \cdot n_m\, dS$, obtaining

$$\begin{aligned}
&\int_{\partial T_i} \mathbf{p}_h^\ell \cdot \mathcal{G}(\mathbf{q}_h^\ell, \mathbf{q}_h^\tau) \cdot \mathbf{n}\, dS + \int_{\partial T_i} \partial_m \mathbf{p}_h^\ell \cdot \mathcal{V}(\mathbf{q}_h^\ell, \mathbf{q}_h^\tau) \cdot n_m\, dS - \int_{T_i^\circ} \partial_m \mathbf{p}_h \cdot (\epsilon\, \partial_m \mathbf{q}_h) d\mathbf{x} + \mathbf{P}_k \cdot \hat{\mathbf{p}}_k^i \\
&\qquad = \int_{\partial T_i} \frac{1}{2}\left(\mathbf{p}_h^\ell + \mathbf{p}_h^\tau\right) \cdot \mathcal{G}(\mathbf{q}_h^\ell, \mathbf{q}_h^\tau) \cdot \mathbf{n}\, dS + \int_{\partial T_i} \frac{1}{2}\left(\mathbf{p}_h^\ell - \mathbf{p}_h^\tau\right) \cdot \mathcal{G}(\mathbf{q}_h^\ell, \mathbf{q}_h^\tau) \cdot \mathbf{n}\, dS \\
&\quad + \int_{\partial T_i} \frac{1}{2}\left(\partial_m \mathbf{p}_h^\ell + \partial_m \mathbf{p}_h^\tau\right) \cdot \mathcal{V}(\mathbf{q}_h^\ell, \mathbf{q}_h^\tau) \cdot n_m\, dS + \int_{\partial T_i} \frac{1}{2}\left(\partial_m \mathbf{p}_h^\ell - \partial_m \mathbf{p}_h^\tau\right) \cdot \mathcal{V}(\mathbf{q}_h^\ell, \mathbf{q}_h^\tau) \cdot n_m\, dS \\
&\qquad - \int_{T_i^\circ} \partial_m \mathbf{p}_h \cdot (\epsilon\, \partial_m \mathbf{q}_h) d\mathbf{x} + \mathbf{P}_k \cdot \hat{\mathbf{p}}_k^i.
\end{aligned}$$

Taking into account the definition of the dissipative terms (101) and (102), yields

$$\begin{aligned}
&\int_{\partial T_i} \mathbf{p}_h^\ell \cdot \mathcal{G}(\mathbf{q}_h^\ell, \mathbf{q}_h^\tau) \cdot \mathbf{n}\, dS + \int_{\partial T_i} \partial_m \mathbf{p}_h^\ell \cdot \mathcal{V}(\mathbf{q}_h^\ell, \mathbf{q}_h^\tau) \cdot n_m\, dS - \int_{T_i^\circ} \partial_m \mathbf{p}_h \cdot (\epsilon\, \partial_m \mathbf{q}_h) d\mathbf{x} + \mathbf{P}_k \cdot \hat{\mathbf{p}}_k^i \\
&\qquad = \int_{\partial T_i} \frac{1}{2}\left(\mathbf{p}_h^\ell + \mathbf{p}_h^\tau\right) \cdot \mathcal{G}(\mathbf{q}_h^\ell, \mathbf{q}_h^\tau) \cdot \mathbf{n}\, dS
\end{aligned}$$

$$
\begin{aligned}
&- \int_{\partial T_i} \frac{1}{2}\left(\mathbf{p}_h^{\text{ɤ}} - \mathbf{p}_h^{\ell}\right) \cdot \left[\frac{1}{2}\epsilon^{\ell\text{ɤ}}\, \partial^2_{\mathbf{pp}} \tilde{L}^{\ell\text{ɤ}}\left(\partial_k \mathbf{p}_h^{\ell} + \partial_k \mathbf{p}_h^{\text{ɤ}}\right) n_k + \eta^{\ell\text{ɤ}}\left(\mathbf{q}_h^{\text{ɤ}} - \mathbf{q}_h^{\ell}\right)\right] dS \\
&+ \int_{\partial T_i} \frac{1}{2}\left(\partial_m \mathbf{p}_h^{\ell} + \partial_m \mathbf{p}_h^{\text{ɤ}}\right) \cdot \frac{1}{2}\epsilon^{\ell\text{ɤ}}\left(\mathbf{q}_h^{\text{ɤ}} - \mathbf{q}_h^{\ell}\right) \cdot n_m \, dS + \int_{\partial T_i} \frac{1}{2}\left(\partial_m \mathbf{p}_h^{\ell} - \partial_m \mathbf{p}_h^{\text{ɤ}}\right) \cdot \mathcal{V}(\mathbf{q}_h^{\ell}, \mathbf{q}_h^{\text{ɤ}}) \cdot n_m \, dS \\
&- \int_{T_i^{\circ}} \partial_m \mathbf{p}_h \cdot (\epsilon \partial_m \mathbf{q}_h) d\mathbf{x} + \mathbf{P}_k \cdot \hat{\mathbf{p}}_k^i.
\end{aligned}
$$

Introducing the production term, (103), and using the definition of Roe matrix of the Hessian and which makes the first term in the second integral and the third one cancel, we get

$$
\begin{aligned}
&\int_{\partial T_i} \mathbf{p}_h^{\ell} \cdot \mathcal{G}(\mathbf{q}_h^{\ell}, \mathbf{q}_h^{\text{ɤ}}) \cdot \mathbf{n} \, dS + \int_{\partial T_i} \partial_m \mathbf{p}_h^{\ell} \cdot \mathcal{V}(\mathbf{q}_h^{\ell}, \mathbf{q}_h^{\text{ɤ}}) \cdot n_m \, dS - \int_{T_i^{\circ}} \partial_m \mathbf{p}_h \cdot (\epsilon \partial_m \mathbf{q}_h) d\mathbf{x} + \mathbf{P}_k \cdot \hat{\mathbf{p}}_k^i \\
&= \int_{\partial T_i} \frac{1}{2}\left(\mathbf{p}_h^{\ell} + \mathbf{p}_h^{\text{ɤ}}\right) \cdot \mathcal{G}(\mathbf{q}_h^{\ell}, \mathbf{q}_h^{\text{ɤ}}) \cdot \mathbf{n} \, dS + \int_{\partial T_i} \frac{1}{2}\left(\partial_m \mathbf{p}_h^{\ell} - \partial_m \mathbf{p}_h^{\text{ɤ}}\right) \cdot \mathcal{V}(\mathbf{q}_h^{\ell}, \mathbf{q}_h^{\text{ɤ}}) \cdot n_m \, dS \\
&\quad - \int_{\partial T_i} \frac{1}{2}\left(\mathbf{p}_h^{\text{ɤ}} - \mathbf{p}_h^{\ell}\right) \cdot \left[\eta^{\ell\text{ɤ}}\left(\mathbf{q}_h^{\text{ɤ}} - \mathbf{q}_h^{\ell}\right)\right] dS - \int_{T_i^{\circ}} \partial_m \mathbf{p}_h \cdot (\epsilon \partial_m \mathbf{q}_h) d\mathbf{x} \\
&\quad + \int_{T_i^{\circ}} \epsilon \partial_k \mathbf{q}_h \cdot \partial^2_{\mathbf{qq}} \mathcal{E} \, \partial_k \mathbf{q}_h d\mathbf{x} + \int_{\partial T_i} \frac{1}{2} \eta^{\ell\text{ɤ}}\left(\mathbf{q}^{\text{ɤ}} - \mathbf{q}^{\ell}\right) \cdot \partial^2_{\mathbf{qq}} \tilde{\mathcal{E}}^{\ell\text{ɤ}}\left(\mathbf{q}^{\text{ɤ}} - \mathbf{q}^{\ell}\right) dS \\
&= \int_{\partial T_i} \frac{1}{2}\left(\mathbf{p}_h^{\ell} + \mathbf{p}_h^{\text{ɤ}}\right) \cdot \mathcal{G}(\mathbf{q}_h^{\ell}, \mathbf{q}_h^{\text{ɤ}}) \cdot \mathbf{n} \, dS + \int_{\partial T_i} \frac{1}{2}\left(\partial_m \mathbf{p}_h^{\ell} - \partial_m \mathbf{p}_h^{\text{ɤ}}\right) \cdot \mathcal{V}(\mathbf{q}_h^{\ell}, \mathbf{q}_h^{\text{ɤ}}) \cdot n_m \, dS.
\end{aligned}
$$

Substituting the fluxes obtained into (106) yields the discrete total energy conservation law

$$
\begin{aligned}
&\int_{T_i} \partial_t \mathcal{E}_h d\mathbf{x} + \int_{\partial T_i} \frac{1}{2}\left[\left(\mathbf{p}_h^{\ell} + \mathbf{p}_h^{\text{ɤ}}\right) \cdot \mathcal{F}^{\ell\text{ɤ}} - \left(\mathbf{p}_h^{\text{ɤ}} \cdot \mathbf{f}_m(\mathbf{q}_h^{\text{ɤ}}) + \mathbf{p}_h^{\ell} \cdot \mathbf{f}_m(\mathbf{q}_h^{\ell})\right) n_m\right] dS \\
&+ \int_{\partial T_i} \frac{1}{2}\left(F_m^{\text{ɤ}} + F_m^{\ell}\right) n_m dS + \int_{\partial T_i} \frac{1}{2}\left(\mathbf{p}_h^{\ell} \cdot \mathcal{R}(\mathbf{q}_h^{\ell}, \mathbf{q}_h^{\text{ɤ}}) + \mathbf{p}_h^{\text{ɤ}} \cdot \mathcal{R}(\mathbf{q}_h^{\text{ɤ}}, \mathbf{q}_h^{\ell})\right) \cdot \mathbf{n} \, dS \\
&= \int_{\partial T_i} \frac{1}{2}\left(\mathbf{p}_h^{\ell} + \mathbf{p}_h^{\text{ɤ}}\right) \cdot \mathcal{G}(\mathbf{q}_h^{\ell}, \mathbf{q}_h^{\text{ɤ}}) \cdot \mathbf{n} \, dS + \int_{\partial T_i} \frac{1}{2}\left(\partial_m \mathbf{p}_h^{\ell} - \partial_m \mathbf{p}_h^{\text{ɤ}}\right) \cdot \mathcal{V}(\mathbf{q}_h^{\ell}, \mathbf{q}_h^{\text{ɤ}}) \cdot n_m \, dS.
\end{aligned}
$$

Let us note that, when the states coincide then the second, fourth and sixth integrals above cancel remaining only the third and fifth integrals which correspond to the central part of the total energy flux.

Finally, integrating in the whole domain and assuming vanishing boundary fluxes, we obtain nonlinear stability in the energy norm:

$$
\int_{\Omega} \frac{\partial \mathcal{E}_h}{\partial t} d\mathbf{x} = \sum_{T_i} \int_{T_i} \partial_t \mathcal{E}_h d\mathbf{x} = 0,
$$

since the sum of all internal fluxes cancels. □

5. Thermodynamically compatible discontinuous Galerkin finite element schemes of type II

The second type of HTC DG schemes proposed in this paper ensures the HTC compatibility of the entire inviscid part of the GPR model (black and red terms) using a *element-wise* correction, thus making the approach genuinely multi-dimensional. As before, we start presenting the derivation of the HTC DG type II scheme in 1D and then we provide the numerical scheme for the 2D case together with the theoretical results proving the nonlinear stability of the scheme in the energy norm and the verification of a discrete cell entropy inequality.

5.1. One dimensional case

Here we use a genuinely multi-dimensional correction relying entirely on fluctuations, similar to the one developed in the framework of residual distribution (RD) schemes, Abgrall [1], Abgrall et al. [53]. Again, we assume the discrete solution

in cell $T^i = [x^{i-\frac{1}{2}}, x^{i+\frac{1}{2}}]$ to be defined as a sum of spatial basis functions $\varphi_l(x)$ and time dependent degrees of freedom $\hat{\mathbf{q}}_l^i(t)$

$$\mathbf{q}(x,t) = \sum_{l=0}^{N} \varphi_l(x)\hat{\mathbf{q}}_l^i(t), \tag{107}$$

with N the polynomial approximation degree and the nodal basis functions $\varphi_l(x)$ given by the Lagrange interpolation polynomials passing through the Gauss–Legendre quadrature points. Hence, by construction, the chosen basis functions $\varphi_l(x)$ satisfy the partition of unity property. The semi-discrete DG scheme applied to (12) can be derived by multiplication of (12) with a spatial test function $\varphi_k(x)$ by integrating the term including the divergence of the fluxes $\mathbf{f}$ and $\mathbf{h}$ by parts and by adding a boundary jump term related to the red terms contained in the non-conservative product,

$$\int_{x^{i-\frac{1}{2}}}^{x^{i+\frac{1}{2}}} \varphi_k \partial_t \mathbf{q}_h dx + \varphi_k^{i+\frac{1}{2}} \left(\widetilde{\mathcal{F}}^{i+\frac{1}{2}} + \mathcal{H}^{i+\frac{1}{2}} \right) - \varphi_k^{i-\frac{1}{2}} \left(\widetilde{\mathcal{F}}^{i-\frac{1}{2}} + \mathcal{H}^{i-\frac{1}{2}} \right) - \int_{x_+^{i-\frac{1}{2}}}^{x_-^{i+\frac{1}{2}}} \partial_x \varphi_k (\mathbf{f}_1(\mathbf{q}_h) + \mathbf{h}_1(\mathbf{q}_h)) dx$$

$$+\varphi_k^{i+\frac{1}{2}} \mathcal{D}^{i+\frac{1}{2}} + \varphi_k^{i-\frac{1}{2}} \mathcal{D}^{i-\frac{1}{2}} + \int_{x_+^{i-\frac{1}{2}}}^{x_-^{i+\frac{1}{2}}} \varphi_k (\mathbf{B}_1(\mathbf{q}_h) \partial_x \mathbf{q}_h) dx = \int_{x^{i-\frac{1}{2}}}^{x^{i+\frac{1}{2}}} \varphi_k \mathbf{S}(\mathbf{q}_h) dx + \int_{x_+^{i-\frac{1}{2}}}^{x_-^{i+\frac{1}{2}}} \varphi_k \partial_x (\epsilon \partial_x \mathbf{q}_h) dx + \mathbf{P}_k, \tag{108}$$

where

$$\widetilde{\mathcal{F}}^{i+\frac{1}{2}} = \widetilde{\mathcal{F}}^{i+\frac{1}{2}} \left(\mathbf{q}_-^{i+\frac{1}{2}}, \mathbf{q}_+^{i+\frac{1}{2}} \right) = \frac{1}{2} \left(\mathbf{f}_1 \left(\mathbf{q}_-^{i+\frac{1}{2}} \right) + \mathbf{f}_1 \left(\mathbf{q}_+^{i+\frac{1}{2}} \right) \right) \tag{109}$$

and

$$\mathcal{H}^{i+\frac{1}{2}} = \mathcal{H}^{i+\frac{1}{2}} \left(\mathbf{q}_-^{i+\frac{1}{2}}, \mathbf{q}_+^{i+\frac{1}{2}} \right) = \frac{1}{2} \left(\mathbf{h}_1 \left(\mathbf{q}_-^{i+\frac{1}{2}} \right) + \mathbf{h}_1 \left(\mathbf{q}_+^{i+\frac{1}{2}} \right) \right) \tag{110}$$

are two simple central numerical fluxes related to the conservative part of the system and

$$\mathcal{D}^{i+\frac{1}{2}} = \mathcal{D}^{i+\frac{1}{2}} \left(\mathbf{q}_-^{i+\frac{1}{2}}, \mathbf{q}_+^{i+\frac{1}{2}} \right) = \frac{1}{2} \mathbf{B}_1 \left(\bar{\mathbf{q}}^{i+\frac{1}{2}} \right) \left(\mathbf{q}_+^{i+\frac{1}{2}} - \mathbf{q}_-^{i+\frac{1}{2}} \right), \qquad \bar{\mathbf{q}}^{i+\frac{1}{2}} = \frac{1}{2} \left(\mathbf{q}_+^{i+\frac{1}{2}} + \mathbf{q}_-^{i+\frac{1}{2}} \right), \tag{111}$$

is a simple central approximation of the jump term related to the non-conservative product. The discretization of the viscous terms is identical to the one of HTC DG schemes of type I discussed before, hence

$$\int_{x^{i-\frac{1}{2}}}^{x^{i+\frac{1}{2}}} \varphi_k \, \partial_t \mathbf{q}_h dx + \varphi_k(x^{i+\frac{1}{2}}) \left(\widetilde{\mathcal{F}}^{i+\frac{1}{2}} + \mathcal{H}^{i+\frac{1}{2}} \right) - \varphi_k(x^{i-\frac{1}{2}}) \left(\widetilde{\mathcal{F}}^{i-\frac{1}{2}} + \mathcal{H}^{i-\frac{1}{2}} \right) +$$

$$+\varphi_k^{i+\frac{1}{2}} \mathcal{D}^{i+\frac{1}{2}} + \varphi_k^{i-\frac{1}{2}} \mathcal{D}^{i-\frac{1}{2}} - \int_{x_+^{i-\frac{1}{2}}}^{x_-^{i+\frac{1}{2}}} \partial_x \varphi_k (\mathbf{f}_1(\mathbf{q}_h) + \mathbf{h}_1(\mathbf{q}_h)) dx + \int_{x_+^{i-\frac{1}{2}}}^{x_-^{i+\frac{1}{2}}} \varphi_k (\mathbf{B}_1(\mathbf{q}_h) \partial_x \mathbf{q}_h) dx$$

$$= \varphi_k^{i+\frac{1}{2}} \mathcal{G}^{i+\frac{1}{2}} - \varphi_k^{i-\frac{1}{2}} \mathcal{G}^{i-\frac{1}{2}} + \partial_x \varphi_k^{i+\frac{1}{2}} \mathcal{V}^{i+\frac{1}{2}} + \partial_x \varphi_k^{i-\frac{1}{2}} \mathcal{V}^{i-\frac{1}{2}} - \int_{x^{i-\frac{1}{2}}}^{x^{i+\frac{1}{2}}} \partial_x \varphi_k \epsilon \partial_x \mathbf{q}_h dx$$

$$+\mathbf{P}_k + \int_{x^{i-\frac{1}{2}}}^{x^{i+\frac{1}{2}}} \varphi_k \mathbf{S}(\mathbf{q}_h) dx, \tag{112}$$

with the thermodynamically compatible numerical viscosity flux

$$\mathcal{G}^{i+\frac{1}{2}} = \frac{1}{2} \epsilon \, \partial^2_{\mathbf{pp}} \tilde{L}^{i+\frac{1}{2}} \left(\partial_x \mathbf{p}_-^{i+\frac{1}{2}} + \partial_x \mathbf{p}_+^{i+\frac{1}{2}} \right) - \eta^{i+\frac{1}{2}} \left(\mathbf{q}_+^{i+\frac{1}{2}} - \mathbf{q}_-^{i+\frac{1}{2}} \right), \qquad \eta^{i+\frac{1}{2}} = \frac{1}{2} s_{\max}^{i+\frac{1}{2}} + \frac{2N+1}{\Delta x} \epsilon, \tag{113}$$

the jump terms

$$\mathcal{V}^{i+\frac{1}{2}} = \frac{1}{2} \epsilon \left(\mathbf{q}_+^{i+\frac{1}{2}} - \mathbf{q}_-^{i+\frac{1}{2}} \right), \tag{114}$$

and the discrete entropy production term related to the viscous terms $\mathbf{P}_k = (0, \mathbf{0}, \Pi_k, \mathbf{0}, \mathbf{0})^T$ with

$$\Pi_k = \int_{x^{i-\frac{1}{2}}}^{x^{i+\frac{1}{2}}} \varphi_k \frac{\epsilon}{T} \partial_x \mathbf{q}_h \cdot \partial^2_{\mathbf{qq}} \mathcal{E} \, \partial_x \mathbf{q}_h dx + \varphi_k(x^{i-\frac{1}{2}}) \frac{\eta^{i-\frac{1}{2}}}{2 \, T_+^{i-\frac{1}{2}}} \left(\mathbf{q}_+^{i-\frac{1}{2}} - \mathbf{q}_-^{i-\frac{1}{2}} \right) \cdot \partial^2_{\mathbf{qq}} \tilde{\mathcal{E}}^{i-\frac{1}{2}} \left(\mathbf{q}_+^{i-\frac{1}{2}} - \mathbf{q}_-^{i-\frac{1}{2}} \right)$$

$$+\varphi_k(x^{i+\frac{1}{2}})\frac{\eta^{i+\frac{1}{2}}}{2\,T_-^{i+\frac{1}{2}}}\left(\mathbf{q}_+^{i+\frac{1}{2}}-\mathbf{q}_-^{i+\frac{1}{2}}\right)\cdot\partial^2_{\mathbf{qq}}\tilde{\mathcal{E}}^{i+\frac{1}{2}}\left(\mathbf{q}_+^{i+\frac{1}{2}}-\mathbf{q}_-^{i+\frac{1}{2}}\right). \tag{115}$$

Defining the total fluctuation of the DG discretization of the *inviscid part* of the PDE system (12) in cell $T^i=[x^{i-\frac{1}{2}},x^{i+\frac{1}{2}}]$ as

$$\tilde{\mathbf{\Phi}}_k^i=\varphi_k^{i+\frac{1}{2}}\left(\mathcal{F}^{i+\frac{1}{2}}+\mathcal{H}^{i+\frac{1}{2}}\right)-\varphi_k^{i-\frac{1}{2}}\left(\mathcal{F}^{i-\frac{1}{2}}+\mathcal{H}^{i-\frac{1}{2}}\right)+\varphi_k^{i+\frac{1}{2}}\,\mathcal{D}^{i+\frac{1}{2}}+\varphi_k^{i-\frac{1}{2}}\,\mathcal{D}^{i-\frac{1}{2}}$$
$$-\int_{x^{i-\frac{1}{2}}}^{x^{i+\frac{1}{2}}}\partial_x\varphi_k(\mathbf{f}_1(\mathbf{q})+\mathbf{h}_1(\mathbf{q}))dx+\int_{x_+^{i-\frac{1}{2}}}^{x_-^{i+\frac{1}{2}}}\varphi_k(\mathbf{B}_1(\mathbf{q})\partial_x\mathbf{q})dx, \tag{116}$$

and with the thermodynamically compatible discretization of the viscous terms from the DG scheme type I

$$\mathbf{\Psi}_k^i=\varphi_k^{i+\frac{1}{2}}\mathcal{G}^{i+\frac{1}{2}}-\varphi_k^{i-\frac{1}{2}}\mathcal{G}^{i-\frac{1}{2}}+\partial_x\varphi_k^{i+\frac{1}{2}}\,\mathcal{V}^{i+\frac{1}{2}}+\partial_x\varphi_k^{i-\frac{1}{2}}\,\mathcal{V}^{i-\frac{1}{2}}$$
$$-\int_{x^{i-\frac{1}{2}}}^{x^{i+\frac{1}{2}}}\partial_x\varphi_k\epsilon\,\partial_x\mathbf{q}_h dx+\mathbf{P}_k+\int_{x^{i-\frac{1}{2}}}^{x^{i+\frac{1}{2}}}\varphi_k\mathbf{S}(\mathbf{q}_h)dx, \tag{117}$$

the DG scheme (108) for cell T_i can be rewritten in a more compact way as

$$\left(\int_{x^{i-\frac{1}{2}}}^{x^{i+\frac{1}{2}}}\varphi_k\varphi_l dx\right)\frac{\partial\hat{\mathbf{q}}_l^i}{\partial t}+\tilde{\mathbf{\Phi}}_k^i=\tilde{\mathbf{\Psi}}_k^i. \tag{118}$$

The total fluctuations related to the inviscid terms $\tilde{\Phi}_k$ are not necessarily compatible with the extra conservation law (20), since no special care was taken in a proper compatible discretization of the numerical fluxes and of the jump terms, unlike in the previous DG schemes of type I. The total fluctuations are now *corrected* according to the following ansatz:

$$\mathbf{\Phi}_k^i=\tilde{\mathbf{\Phi}}_k^i+\alpha^i\left(\hat{\mathbf{p}}_k^i-\bar{\mathbf{p}}^i\right),\qquad \bar{\mathbf{p}}^i=\frac{1}{N+1}\sum_{l=0}^{N}\hat{\mathbf{p}}_l^i. \tag{119}$$

It is easy to check that the proposed correction is conservative, i.e. that

$$\sum_{k=0}^{N}\mathbf{\Phi}_k^i=\sum_{k=0}^{N}\tilde{\mathbf{\Phi}}_k^i \tag{120}$$

since obviously

$$\sum_{k=0}^{N}\left(\hat{\mathbf{p}}_k^i-\bar{\mathbf{p}}^i\right)=0. \tag{121}$$

The *scalar* correction factor α^i for each element T_i is now simply computed by *imposing* thermodynamic compatibility with the extra conservation law as follows:

$$\sum_{k=0}^{N}\hat{\mathbf{p}}_k^i\cdot\mathbf{\Phi}_k^i=\sum_{k=0}^{N}\left(\hat{\mathbf{p}}_k^i\cdot\tilde{\mathbf{\Phi}}_k^i+\alpha^i\,\hat{\mathbf{p}}_k^i\cdot\left(\hat{\mathbf{p}}_k^i-\bar{\mathbf{p}}^i\right)\right)=F_1^{i+\frac{1}{2}}-F_1^{i-\frac{1}{2}}. \tag{122}$$

It is easy to check that

$$\sum_{k=0}^{N}\hat{\mathbf{p}}_k^i\cdot\left(\hat{\mathbf{p}}_k^i-\bar{\mathbf{p}}^i\right)=\sum_{k=0}^{N}\left(\hat{\mathbf{p}}_k^i-\bar{\mathbf{p}}^i\right)^2\geq 0, \tag{123}$$

hence the discrete compatibility condition (122) allows to calculate the scalar correction factor α^i as

$$\alpha^i=\frac{F_1^{i+\frac{1}{2}}-F_1^{i-\frac{1}{2}}-\sum_{k=0}^{N}\hat{\mathbf{p}}_k^i\cdot\tilde{\mathbf{\Phi}}_k^i}{\sum_{k=0}^{N}\left(\hat{\mathbf{p}}_k^i-\bar{\mathbf{p}}^i\right)^2}. \tag{124}$$

In those cases where the denominator vanishes, we simply set $\alpha^i=0$. The thermodynamically compatible DG scheme of type II therefore becomes

$$\left(\int_{x^{i-\frac{1}{2}}}^{x^{i+\frac{1}{2}}}\varphi_k\varphi_l dx\right)\frac{\partial\hat{\mathbf{q}}_l^i}{\partial t}=-\tilde{\mathbf{\Phi}}_k^i-\alpha^i\left(\hat{\mathbf{p}}_k^i-\bar{\mathbf{p}}^i\right)+\mathbf{\Psi}_k^i, \tag{125}$$

with α^i given by (124). We stress that the proposed correction only applies to the inviscid part of the system. The parabolic viscous terms and the entropy production term must still be discretized in a thermodynamically compatible manner, exactly as in the case of the DG schemes of type I. Since the correction factor in DG schemes of type II is element-wise, the schemes are formally identical in one and multiple space dimensions. Also the proofs of entropy inequality and energy conservation are the same. For this reason, the proofs will be presented only in the multi-dimensional case in the next section.

5.2. Multi-dimensional case

The multi-dimensional extension of the DG schemes of type II is straightforward. The computational domain Ω is supposed to be divided into non-overlapping cells T_i and the discrete solution reads as

$$\mathbf{q}_h(\mathbf{x},t) = \sum_{l=1}^{\mathcal{N}} \varphi_l(\mathbf{x})\hat{\mathbf{q}}_l^i(t), \tag{126}$$

where N is again the polynomial approximation degree, the basis functions $\varphi_l(\mathbf{x})$ are assumed to be nodal basis functions that satisfy the partition of unity property $\sum_l \varphi_l(\mathbf{x}) = 1$ and $\mathcal{N}$ is the number of degrees of freedom per cell. Multiplying (12) with $\varphi_k(\mathbf{x})$, integration by parts of the flux divergence terms and introducing a numerical flux and jump terms on the boundary of T_i leads to

$$\begin{aligned}
&\int_{T_i} \varphi_k \partial_t \mathbf{q} d\mathbf{x} + \int_{\partial T_i} \varphi_k \Big(\mathcal{F}(\mathbf{q}_h^\ell, \mathbf{q}_h^\tau) + \mathcal{H}(\mathbf{q}_h^\ell, \mathbf{q}_h^\tau)\Big)\cdot \mathbf{n}\, dS + \int_{\partial T_i} \varphi_k \mathcal{D}(\mathbf{q}_h^\ell, \mathbf{q}_h^\tau)\cdot \mathbf{n}\, dS \\
&\qquad - \int_{T_i} \partial_m \varphi_k (\mathbf{f}_m(\mathbf{q}_h) + \mathbf{h}_m(\mathbf{q}_h)) d\mathbf{x} + \int_{T_i} \varphi_k \mathbf{B}_m(\mathbf{q}_h)\partial_m \mathbf{q}_h d\mathbf{x} \\
&= \int_{\partial T_i} \varphi_k \mathcal{G}(\mathbf{q}_h^\ell, \mathbf{q}_h^\tau)\cdot \mathbf{n}\, dS + \int_{\partial T_i} \partial_m \varphi_k \mathcal{V}(\mathbf{q}_h^\ell, \mathbf{q}_h^\tau)\cdot n_m\, dS - \int_{T_i} \partial_m \varphi_k (\epsilon \partial_m \mathbf{q}_h) d\mathbf{x} + \mathbf{P}_k + \int_{T_i} \varphi_k \mathbf{S}(\mathbf{q}_h) d\mathbf{x},
\end{aligned} \tag{127}$$

with the central fluxes in normal direction

$$\mathcal{F}(\mathbf{q}_h^\ell, \mathbf{q}_h^\tau)\cdot \mathbf{n} = \frac{1}{2}\Big(\mathbf{f}_m\big(\mathbf{q}_h^\ell\big) + \mathbf{f}_m\big(\mathbf{q}_h^\tau\big)\Big) n_m \tag{128}$$

and

$$\mathcal{H}(\mathbf{q}_h^\ell, \mathbf{q}_h^\tau)\cdot \mathbf{n} = \frac{1}{2}\Big(\mathbf{h}_m\big(\mathbf{q}_h^\ell\big) + \mathbf{h}_m\big(\mathbf{q}_h^\tau\big)\Big) n_m, \tag{129}$$

as in the one-dimensional case, the fluctuation

$$\mathcal{D}(\mathbf{q}_h^\ell, \mathbf{q}_h^\tau)\cdot \mathbf{n} = \frac{1}{2}(\mathbf{B}_m\, n_m)(\bar{\mathbf{q}})\big(\mathbf{q}_h^\tau - \mathbf{q}_h^\ell\big), \qquad \bar{\mathbf{q}} = \frac{1}{2}\big(\mathbf{q}_h^\ell + \mathbf{q}_h^\tau\big), \tag{130}$$

the viscous flux

$$\mathcal{G}(\mathbf{q}_h^\ell, \mathbf{q}_h^\tau)\cdot \mathbf{n} = \frac{1}{2}\epsilon\, \partial^2_{\mathbf{pp}} \tilde{L}\big(\partial_m \mathbf{p}_h^\ell + \partial_m \mathbf{p}_h^\tau\big) n_m - \eta\big(\mathbf{q}_h^\tau - \mathbf{q}_h^\ell\big), \qquad \eta = \frac{1}{2} s_{\max} + \frac{2N+1}{\delta^{\ell\tau}}\epsilon, \tag{131}$$

with $s_{\max} = \max(|\lambda_k(\mathbf{q}_h^\ell)|, |\lambda_k(\mathbf{q}_h^\tau)|)$ the maximum signal speed at the interface and the jump term

$$\mathcal{V}(\mathbf{q}_h^\ell, \mathbf{q}_h^\tau) = \frac{1}{2}\epsilon\big(\mathbf{q}_h^\tau - \mathbf{q}_h^\ell\big). \tag{132}$$

The non-negative entropy production term reads $\mathbf{P}_k = (0, \mathbf{0}, \Pi_k, \mathbf{0}, \mathbf{0})^T$ with

$$\Pi_k = \int_{T_i} \varphi_k \frac{\epsilon}{T} \partial_m \mathbf{q}_h \cdot \partial^2_{\mathbf{qq}} \mathcal{E}\, \partial_m \mathbf{q}_h dx + \int_{\partial T_i} \varphi_k \frac{\eta}{2\, T_h^\ell}\big(\mathbf{q}_h^\tau - \mathbf{q}_h^\ell\big)\cdot \partial^2_{\mathbf{qq}} \tilde{\mathcal{E}}^{\ell\tau}\big(\mathbf{q}_h^\tau - \mathbf{q}_h^\ell\big) dS \geq 0. \tag{133}$$

Also in the multi-dimensional case, we introduce the total fluctuation of the DG discretization related to the *inviscid part* in cell T_i as

$$\begin{aligned}
\tilde{\mathbf{\Phi}}_k^i &= \int_{\partial T_i} \varphi_k \Big(\mathcal{F}(\mathbf{q}_h^\ell, \mathbf{q}_h^\tau) + \mathcal{H}(\mathbf{q}_h^\ell, \mathbf{q}_h^\tau)\Big)\cdot \mathbf{n}\, dS + \int_{\partial T_i} \varphi_k \mathcal{D}(\mathbf{q}_h^\ell, \mathbf{q}_h^\tau)\cdot \mathbf{n}\, dS \\
&\quad - \int_{T_i} \partial_m \varphi_k \cdot (\mathbf{f}_m(\mathbf{q}) + \mathbf{h}_m(\mathbf{q})) d\mathbf{x} + \int_{T_i} \varphi_k (\mathbf{B}_m(\mathbf{q})\partial_m \mathbf{q}) d\mathbf{x}
\end{aligned} \tag{134}$$

and the thermodynamically compatible viscous fluctuations

$$\mathbf{\Psi}_k^i = \int_{\partial T_i} \varphi_k \mathcal{G}(\mathbf{q}_h^\ell, \mathbf{q}_h^\tau)\cdot \mathbf{n}\, dS + \int_{\partial T_i} \partial_m \varphi_k \mathcal{V}(\mathbf{q}_h^\ell, \mathbf{q}_h^\tau)\cdot n_m\, dS - \int_{T_i} \partial_m \varphi_k (\epsilon \partial_m \mathbf{q}_h) d\mathbf{x} + \mathbf{P}_k + \int_{T_i} \varphi_k \mathbf{S}(\mathbf{q}_h) d\mathbf{x}, \tag{135}$$

which allow to rewrite the previous DG scheme for cell T_i as

$$\left(\int_{T_i} \varphi_k \varphi_l dx\right) \frac{\partial \hat{\mathbf{q}}_l^i}{\partial t} + \tilde{\mathbf{\Phi}}_k^i = \mathbf{\Psi}_k^i. \tag{136}$$

Note that the inviscid part of scheme (136) is not thermodynamically compatible yet. The total fluctuations of the inviscid part are therefore *corrected*, as in the one-dimensional case, as

$$\mathbf{\Phi}_k^i = \tilde{\mathbf{\Phi}}_k^i + \alpha^i \left(\hat{\mathbf{p}}_k^i - \bar{\mathbf{p}}^i\right), \qquad \bar{\mathbf{p}}^i = \frac{1}{\mathcal{N}} \sum_{l=1}^{\mathcal{N}} \hat{\mathbf{p}}_l^i. \tag{137}$$

In multiple space dimensions the thermodynamic compatibility property with the extra conservation law reads

$$\sum_{k=0}^{N} \hat{\mathbf{p}}_k^i \cdot \mathbf{\Phi}_k^i = \sum_{k=0}^{N} \left(\hat{\mathbf{p}}_k^i \cdot \tilde{\mathbf{\Phi}}_k^i + \alpha^i \hat{\mathbf{p}}_k^i \cdot \left(\hat{\mathbf{p}}_k^i - \bar{\mathbf{p}}^i\right)\right) = \int_{\partial T_i} \frac{1}{2} \left(F_k^\ell + F_k^r\right) n_k \, dS, \tag{138}$$

which allows to compute the scalar correction factor α^i in multiple space dimensions in a way that is totally analogous to the 1D case:

$$\alpha^i = \frac{\displaystyle\int_{\partial T_i} \frac{1}{2} \left(F_k^\ell + F_k^r\right) n_k \, dS - \sum_{k=1}^{\mathcal{N}} \hat{\mathbf{p}}_k^i \cdot \tilde{\mathbf{\Phi}}_k^i}{\displaystyle\sum_{k=1}^{\mathcal{N}} \left(\hat{\mathbf{p}}_k^i - \bar{\mathbf{p}}^i\right)^2}. \tag{139}$$

We again set $\alpha^i = 0$ when the denominator vanishes. The final thermodynamically compatible DG scheme of type II in multiple space dimensions becomes

$$\left(\int_{T_i} \varphi_k \varphi_l d\mathbf{x}\right) \frac{\partial \hat{\mathbf{q}}_l^i}{\partial t} = -\tilde{\mathbf{\Phi}}_k^i - \alpha^i \left(\hat{\mathbf{p}}_k^i - \bar{\mathbf{p}}^i\right) + \mathbf{\Psi}_k^i, \tag{140}$$

with α^i computed according to (139). Note that the scalar correction factor is computed in a genuinely multi-dimensional manner, since it couples all degrees of freedom and all thermodynamically dual variables with each other in one single scalar.

Theorem 5.1 (Cell entropy inequality)**.** *The HTC DG scheme of type II (127) satisfies the following cell entropy inequality:*

$$\int_{T_i} \partial_t (\rho S)_h d\mathbf{x} + \int_{\partial T_i} \mathcal{F}_{\rho S}(\mathbf{q}_h^\ell, \mathbf{q}_h^r) \cdot \mathbf{n} \, dS + \int_{\partial T_i} \mathcal{H}_{\rho S}(\mathbf{q}_h^\ell, \mathbf{q}_h^r) \cdot \mathbf{n} \, dS - \int_{\partial T_i} \mathcal{G}_{\rho S}(\mathbf{q}_h^\ell, \mathbf{q}_h^r) \cdot \mathbf{n} \, dS \geq 0. \tag{141}$$

Proof. We start by summing up (140) over k. Since we use a nodal basis that must satisfy the partition of unity property,

$$\sum_{m=1}^{\mathcal{N}} \varphi_m(\mathbf{x}) = 1, \tag{142}$$

this corresponds to taking the test function $\varphi_k = 1$. We now consider only the discretization for the entropy density for which the non-conservative term $\mathbf{B}_m(\mathbf{q}_h)\partial_m \mathbf{q}_h$ disappears and consider the correction term given in (140) with (139). We then have

$$\int_{T_i} \partial_t (\rho S) d\mathbf{x} + \int_{\partial T_i} \left(\mathcal{F}_{\rho S}(\mathbf{q}_h^\ell, \mathbf{q}_h^r) + \mathcal{H}_{\rho S}(\mathbf{q}_h^\ell, \mathbf{q}_h^r)\right) \cdot \mathbf{n} \, dS + \int_{\partial T_i} \mathcal{D}_{\rho S}(\mathbf{q}_h^\ell, \mathbf{q}_h^r) \cdot \mathbf{n} \, dS = \int_{T_i} \pi \, d\mathbf{x}$$
$$+ \int_{\partial T_i} \mathcal{G}(\mathbf{q}_h^\ell, \mathbf{q}_h^r) \cdot \mathbf{n} \, dS + \int_{T_i^\circ} \frac{\epsilon}{T} \partial_k \mathbf{q}_h \cdot \partial^2_{\mathbf{qq}} \mathcal{E} \, \partial_k \mathbf{q}_h d\mathbf{x} + \int_{\partial T_i} \frac{\eta^{\ell r}}{2T^\ell} \left(\mathbf{q}^r - \mathbf{q}^\ell\right) \cdot \partial^2_{\mathbf{qq}} \tilde{\mathcal{E}}^{\ell r} \left(\mathbf{q}^r - \mathbf{q}^\ell\right) dS$$
$$- \sum_{k=1}^{\mathcal{N}} \alpha^i \left(\widehat{T}_k^i - \bar{T}^i\right).$$

Since $\mathcal{D}_{\rho S}(\mathbf{q}_h^\ell, \mathbf{q}_h^r) \cdot \mathbf{n} = 0$ and

$$\sum_{k=1}^{\mathcal{N}} \alpha^i \left(\widehat{T}_k^i - \bar{T}^i\right) = \alpha^i \sum_{k=1}^{\mathcal{N}} \widehat{T}_k^i - \alpha^i \sum_{k=1}^{\mathcal{N}} \bar{T}^i = \alpha^i \sum_{k=1}^{\mathcal{N}} \widehat{T}_k^i - \alpha^i \sum_{k=1}^{\mathcal{N}} \left(\frac{1}{\mathcal{N}} \sum_{l=1}^{\mathcal{N}} \hat{T}_l^i \right) = 0$$

we get the sought cell entropy inequality (141)

$$\int_{T_i} \partial_t(\rho S) d\mathbf{x} + \int_{\partial T_i} \Big(\mathcal{F}_{\rho S}(\mathbf{q}_h^\ell, \mathbf{q}_h^\tau) + \mathcal{H}_{\rho S}(\mathbf{q}_h^\ell, \mathbf{q}_h^\tau)\Big) \cdot \mathbf{n}\, dS - \int_{\partial T_i} \mathcal{G}(\mathbf{q}_h^\ell, \mathbf{q}_h^\tau) \cdot \mathbf{n}\, dS$$
$$= \int_{T_i} \pi\, d\mathbf{x} + \int_{T_i^\circ} \frac{\epsilon}{T} \partial_k \mathbf{q}_h \cdot \partial^2_{\mathbf{qq}} \mathcal{E}\, \partial_k \mathbf{q}_h d\mathbf{x} + \int_{\partial T_i} \frac{\eta^{\ell\tau}}{2\, T^\ell} \big(\mathbf{q}^\tau - \mathbf{q}^\ell\big) \cdot \partial^2_{\mathbf{qq}} \mathcal{E}^{\ell\tau} \big(\mathbf{q}^\tau - \mathbf{q}^\ell\big) dS \geq 0,$$

where the right hand side is positive due to $\pi \geq 0$ and because the Hessian of the energy potential is at least positive semi-definite. □

Theorem 5.2 (Nonlinear stability in the energy norm)**.** *The scheme (127) which takes the form (140) with the fluxes, fluctuations, jump, production and source terms given by (54), (128)–(133), is nonlinearly stable in the energy norm in the sense that, for vanishing boundary fluxes, we have*

$$\int_\Omega \frac{\partial \mathcal{E}}{\partial t} d\mathbf{x} = 0. \tag{143}$$

Proof. Multiplying (140) by $\hat{\mathbf{p}}_k^i$ and using (137) yields

$$\hat{\mathbf{p}}_k^i \cdot \left(\int_{T_i} \varphi_k \varphi_l d\mathbf{x} \right) \frac{\partial \hat{\mathbf{q}}_l^i}{\partial t} = -\hat{\mathbf{p}}_k^i \cdot \mathbf{\Phi}_k^i + \hat{\mathbf{p}}_k^i \cdot \mathbf{\Psi}_k^i,$$

Using the definition of the discrete solution and the property (138), we get

$$\int_{T_i} \mathbf{p}_h \cdot \frac{\partial \mathbf{q}_h}{\partial t} d\mathbf{x} + \int_{\partial T_i} \frac{1}{2} \big(F_k^\ell + F_k^\tau\big) n_k\, dS = \hat{\mathbf{p}}_k^i \cdot \mathbf{\Psi}_k^i. \tag{144}$$

Besides, from the DG schemes of type I, we have

$$\hat{\mathbf{p}}_k^i \cdot \mathbf{\Psi}_k^i = \int_{\partial T_i} \mathbf{p}_h^\ell \cdot \mathcal{G}(\mathbf{q}_h^\ell, \mathbf{q}_h^\tau) \cdot \mathbf{n}\, dS + \int_{\partial T_i} \partial_m \mathbf{p}_h^\ell \cdot \mathcal{V}(\mathbf{q}_h^\ell, \mathbf{q}_h^\tau) \cdot n_m\, dS - \int_{T_i^\circ} \partial_m \mathbf{p}_h \cdot (\epsilon\, \partial_m \mathbf{q}_h) d\mathbf{x} + \mathbf{P}_k \cdot \hat{\mathbf{p}}_k^i$$
$$- \int_{T_i} \mathbf{p}_h \cdot \mathbf{S}(\mathbf{q}_h) d\mathbf{x} = \int_{\partial T_i} \frac{1}{2} \big(\mathbf{p}_h^\ell + \mathbf{p}_h^\tau\big) \cdot \mathcal{G}(\mathbf{q}_h^\ell, \mathbf{q}_h^\tau) \cdot \mathbf{n}\, dS + \int_{\partial T_i} \frac{1}{2} \big(\partial_m \mathbf{p}_h^\ell - \partial_m \mathbf{p}_h^\tau\big) \cdot \mathcal{V}(\mathbf{q}_h^\ell, \mathbf{q}_h^\tau) \cdot n_m\, dS. \tag{145}$$

Gathering (144) and (145), we obtain

$$\int_{T_i} \partial_t \mathcal{E}_h d\mathbf{x} + \frac{1}{2} \int_{\partial T_i} \big(F_m^\tau + F_m^\ell\big) n_m dS$$
$$= \int_{\partial T_i} \frac{1}{2} \big(\mathbf{p}_h^\ell + \mathbf{p}_h^\tau\big) \cdot \mathcal{G}(\mathbf{q}_h^\ell, \mathbf{q}_h^\tau) \cdot \mathbf{n}\, dS + \int_{\partial T_i} \frac{1}{2} \big(\partial_m \mathbf{p}_h^\ell - \partial_m \mathbf{p}_h^\tau\big) \cdot \mathcal{V}(\mathbf{q}_h^\ell, \mathbf{q}_h^\tau) \cdot n_m\, dS.$$

Finally, integrating over the whole domain and assuming vanishing boundary fluxes, we obtain nonlinear stability in the energy norm also for the DG schemes of type II, (143). □

We would like to conclude this section with the following important remark. In all proofs above we have so far assumed the calculation of all integrals to be exact, see also [68]. However, a very important difference between DG schemes of type I and II is the following: in the DG schemes of type II, the numerical scheme is aware of the quadrature errors in the sense that all quadrature errors are automatically absorbed into the element-wise correction factor α^i, so that the thermodynamic compatibility condition (138) always holds, also in the presence of numerical quadrature errors.

6. Numerical results

If not specified otherwise, in all test cases for fluids the relaxation time τ_1 is computed from the dynamic viscosity μ and the shear sound speed c_s according to the relation $\mu = \frac{1}{6}\rho_0 c_s^2 \tau_1$. If not explicitly stated otherwise we set $\epsilon = 0$, $\gamma = 1.4$, $c_v = 1$ and $\rho_0 = 1$ for all test cases presented. The classical fourth order Runge–Kutta method is used as time integrator for all test problems, but also any other high order time integrator could be used, such as SSP Runge–Kutta schemes [69]. In all cases the time step size was chosen small enough to allow for an explicit discretization of the viscous terms and to allow the semi-discrete framework used in this paper to hold, with Courant numbers ranging from 0.1 to 0.5. For the numerical results presented in this section, we restrict ourselves to one and two space dimensions only. However, we always considers *all* variables of the PDE system for the general three-dimensional case, i.e. three components for the velocity v_i and the thermal impulse J_i and nine components of the distorsion field A_{ik}.

Table 1
Numerical convergence results at time $t = 0.25$ in L^2 norm for density ρ, momentum density ρv_1 and entropy density ρS using HTC cell centered FV and HTC DG schemes of type I applied to the Euler subsystem (black terms in (1)).

N_x	ρ	ρv_1	ρS	$\mathcal{O}(\rho)$	$\mathcal{O}(\rho v_1)$	$\mathcal{O}(\rho S)$
HTC CC FV						
64	5.1870E−03	1.8351E−03	3.1355E−04			
128	1.2747E−03	4.6020E−04	8.0154E−05	2.0	2.0	2.0
256	3.1726E−04	1.1516E−04	2.0144E−05	2.0	2.0	2.0
512	7.9226E−05	2.8847E−05	5.0427E−06	2.0	2.0	2.0
HTC DG type I - $N = 1$						
32	5.1870E−03	6.1093E−03	7.9857E−05			
64	1.2747E−03	1.4483E−03	1.1197E−05	2.0	2.1	2.8
128	3.1726E−04	3.5728E−04	1.4880E−06	2.0	2.0	2.9
256	7.9226E−05	8.9128E−05	1.9172E−07	2.0	2.0	3.0
HTC DG type I - $N = 2$						
16	2.9753E−03	4.7954E−03	1.6074E−05			
32	5.0543E−04	8.5266E−04	7.7748E−07	2.6	2.5	4.4
64	7.2395E−05	1.5411E−04	3.0162E−08	2.8	2.5	4.7
128	9.4557E−06	2.7237E−05	1.0471E−09	2.9	2.5	4.8
HTC DG type I - $N = 3$						
8	3.6067E−03	6.2320E−03	2.3026E−05			
16	2.4324E−04	6.9778E−04	4.6458E−07	3.9	3.2	5.6
32	1.2749E−05	2.7087E−05	2.7667E−09	4.3	4.7	7.4
48	2.3053E−06	6.7687E−06	1.4757E−10	4.2	3.4	7.2
HTC DG type I - $N = 4$						
8	6.8664E−04	1.8162E−03	3.9238E−06			
12	1.0909E−04	1.6206E−04	7.6967E−08	4.5	6.0	9.7
16	2.2145E−05	3.9053E−05	4.4581E−09	5.5	4.9	9.9
20	7.4773E−06	1.8647E−05	9.0447E−10	4.9	3.3	7.1
HTC DG type I - $N = 5$						
6	8.5757E−04	1.5182E−03	1.9402E−06			
8	1.3355E−04	3.0442E−04	1.3112E−07	6.5	5.6	9.4
12	1.6464E−05	6.1433E−05	3.7147E−09	5.2	3.9	8.8
16	2.6318E−06	1.5658E−05	1.9870E−10	6.4	4.8	10.2

6.1. Numerical convergence study

In order to verify the order of accuracy of the new HTC schemes proposed in this paper, we simulate the isentropic vortex problem, see [70], of the pure inviscid Euler equations, i.e. we apply the numerical schemes only to the black terms in (1). The model parameters are $\gamma = 1.4$, $c_s = 0$, $c_h = 0$ and the artificial viscosity is set to $\epsilon = 0$. The computational domain is the square $\Omega = [0, 10]^2$. All boundary conditions are periodic. The analytical expression of the initial condition in terms of primitive variables reads

$$(\rho, v_1, v_2, v_3, p) = (\delta\rho, \delta u, \delta v, 0, \delta p) \tag{146}$$

with the radius $r^2 = (x-5)^2 + (y-5)^2$, the vortex strength $\varepsilon = 5$, the entropy fluctuation $\delta S = 0$ and the velocity, temperature, density and pressure profiles given by

$$\begin{pmatrix} \delta u \\ \delta v \end{pmatrix} = \frac{\varepsilon}{2\pi} e^{\frac{1-r^2}{2}} \begin{pmatrix} 5-y \\ x-5 \end{pmatrix}, \quad \delta T = -\frac{(\gamma-1)\varepsilon^2}{8\gamma\pi^2} e^{1-r^2}, \quad \delta\rho = (1+\delta T)^{\frac{1}{\gamma-1}}, \quad \delta p = (1+\delta T)^{\frac{\gamma}{\gamma-1}}. \tag{147}$$

Since the vortex is stationary, the exact solution is the initial condition for all times. Simulations are run with all HTC schemes until time $t = 0.25$ using an equidistant Cartesian mesh composed of $N_x \times N_y$ elements. It is important to highlight that in this test case the artificial viscosity is set to $\epsilon = 0$. The L^2 errors together with the corresponding convergence rates obtained for the density ρ, the momentum density ρv_1 and the entropy density ρS are reported at the final time in Tables 1 and 2. One can observe that all proposed HTC schemes reach their nominal order of accuracy. More precisely, the HTC finite volume scheme is second order accurate in all variables, while the HTC DG schemes of type I and II in general reach their designed order of accuracy of $N+1$ in density, and momentum density, while the entropy density reaches orders between $2N+1$ and $2N+2$. This can be explained by the fact that the present test problem is *isentropic* and since for $\epsilon = 0$ the only entropy generation mechanism in both HTC DG schemes is the jump term $\frac{1}{2} s_{\max}(\mathbf{q}_h^{\epsilon} - \mathbf{q}_h^{\ell})$ in the numerical viscosity flux $\mathcal{G}$. But because the jumps tend to zero with order between $N+\frac{1}{2}$ to $N+1$ and the related entropy production term Π_k in the entropy inequality is *quadratic* in the jump, we indeed expect *twice* the convergence order for entropy in this test case. For isentropic flows this seems to be indeed a very interesting feature of our new HTC DG schemes that are based on the direct discretization of the entropy inequality in contrast to standard DG schemes which discretize the total energy conservation law. One remarkable difference between the HTC schemes proposed in this paper with respect to the original HTC schemes proposed in Busto et al. [61], Busto and Dumbser [62] is that we avoid the use of path integrals in

Table 2
Numerical convergence results at time $t = 0.25$ in L^2 norm for density ρ, momentum density ρv_1 and entropy density ρS using HTC cell centered FV and HTC DG schemes of type II applied to the Euler subsystem (black terms in (1)).

N_x	ρ	ρv_1	ρS	$\mathcal{O}(\rho)$	$\mathcal{O}(\rho v_1)$	$\mathcal{O}(\rho S)$
HTC CC FV						
64	5.1870E−03	1.8351E−03	3.1355E−04			
128	1.2747E−03	4.6020E−04	8.0154E−05	2.0	2.0	2.0
256	3.1726E−04	1.1516E−04	2.0144E−05	2.0	2.0	2.0
512	7.9226E−05	2.8847E−05	5.0427E−06	2.0	2.0	2.0
HTC DG type II - $N = 1$						
32	5.1979E−03	6.1038E−03	1.4077E−04			
64	1.2754E−03	1.4475E−03	2.0503E−05	2.0	2.1	2.8
128	3.1731E−04	3.5722E−04	2.7459E−06	2.0	2.0	2.9
256	7.9228E−05	8.9124E−05	3.5363E−07	2.0	2.0	3.0
HTC DG type II - $N = 2$						
16	2.9760E−03	4.8004E−03	1.9130E−05			
32	5.0550E−04	8.5273E−04	8.0526E−07	2.6	2.5	4.4
64	7.2396E−05	1.5411E−04	3.0200E−08	2.8	2.5	4.7
128	9.4557E−06	2.7238E−05	1.0519E−09	2.9	2.5	4.8
HTC DG type II - $N = 3$						
8	3.6075E−03	6.2317E−03	2.5859E−05			
16	2.4324E−04	6.9776E−04	5.2706E−07	3.9	3.2	5.6
32	1.2747E−05	2.7086E−05	7.7266E−09	4.3	4.7	6.1
48	2.3053E−06	6.7687E−06	6.4886E−10	4.2	3.4	6.1
HTC DG type II - $N = 4$						
8	6.8652E−04	1.8158E−03	5.6567E−06			
12	1.0909E−04	1.6204E−04	1.3708E−07	4.5	6.0	9.2
16	2.2144E−05	3.9052E−05	7.5439E−09	5.5	4.9	10.1
20	7.4773E−06	1.8647E−05	1.5860E−09	4.9	3.3	7.0
HTC DG type II - $N = 5$						
6	8.5757E−04	1.5181E−03	3.0778E−06			
8	1.3355E−04	3.0442E−04	1.4965E−07	6.5	5.6	10.5
12	1.6465E−05	6.1433E−05	3.9483E−09	5.2	3.9	9.0
16	2.6318E−06	1.5658E−05	2.0594E−10	6.4	4.8	10.3

Table 3
Computational time (s) employed to complete the isentropic vortex problem up to time $t = 0.25$ using the new HTC FV method proposed in this article (HTC CC FV) and the HTC FV method [61] based on path-integrals (HTC PI FV) applied to the Euler subsystem (black terms in (1)).

N_x	HTC CC FV	HTC PI FV	Ratio (t_{PI}/t_{CC})
16	0.00697	0.01264	1.81
32	0.02049	0.05664	2.77
64	0.09889	0.35564	3.60
128	0.68748	2.73660	3.98
256	5.33787	21.45535	4.02
512	41.71814	169.38102	4.06

the compatible numerical flux of the underlying Euler subsystem. As a consequence, the computational cost of the resulting algorithms is greatly reduced as it can be observed in Table 3, where both HTC FV schemes are analysed in terms of the CPU time needed to run the isentropic vortex test case up to $t = 0.25$ with four processes on an Intel® Core™ i9-10980XE.

6.2. Shear motion in solids and fluids

In the following, we consider the evolution of an isolated shear layer in the domain $\Omega = [-0.5, +0.5]$ in one space dimension. The initial conditions are set as $v_1 = v_3 = 0$, $\mathbf{J} = 0$, $\rho = 1$, $p = 1$, $\mathbf{A} = \mathbf{I}$ and $v_2 = -v_0$ for $x < 0$ and $v_2 = +v_0$ for $x \geq 0$ with $v_0 = 0.1$. We furthermore set $\gamma = 1.4$, $c_v = 1$, $\rho_0 = 1$, $c_s = 1$ and $c_h = 1$. The numerical simulations are run until $t = 0.4$ for different relaxation times using the new thermodynamically compatible HTC schemes developed in this paper, i.e. the compatible cell centered finite volume scheme as well as the thermodynamically compatible discontinuous Galerkin schemes of type I and II, for which we choose a polynomial approximation degree of $N = 5$. In order to obtain the same number of degrees of freedom we use 1024 elements for the DG schemes with $N = 5$ and 6144 control volumes in case of the finite volume method. For fluids we furthermore set $\kappa = \mu$. In the stiff relaxation limit of the GPR model, i.e. for $\tau_1 \ll 1$, the exact solution of the first problem of Stokes for the incompressible Navier–Stokes equations, see e.g. [64,71–73], can be

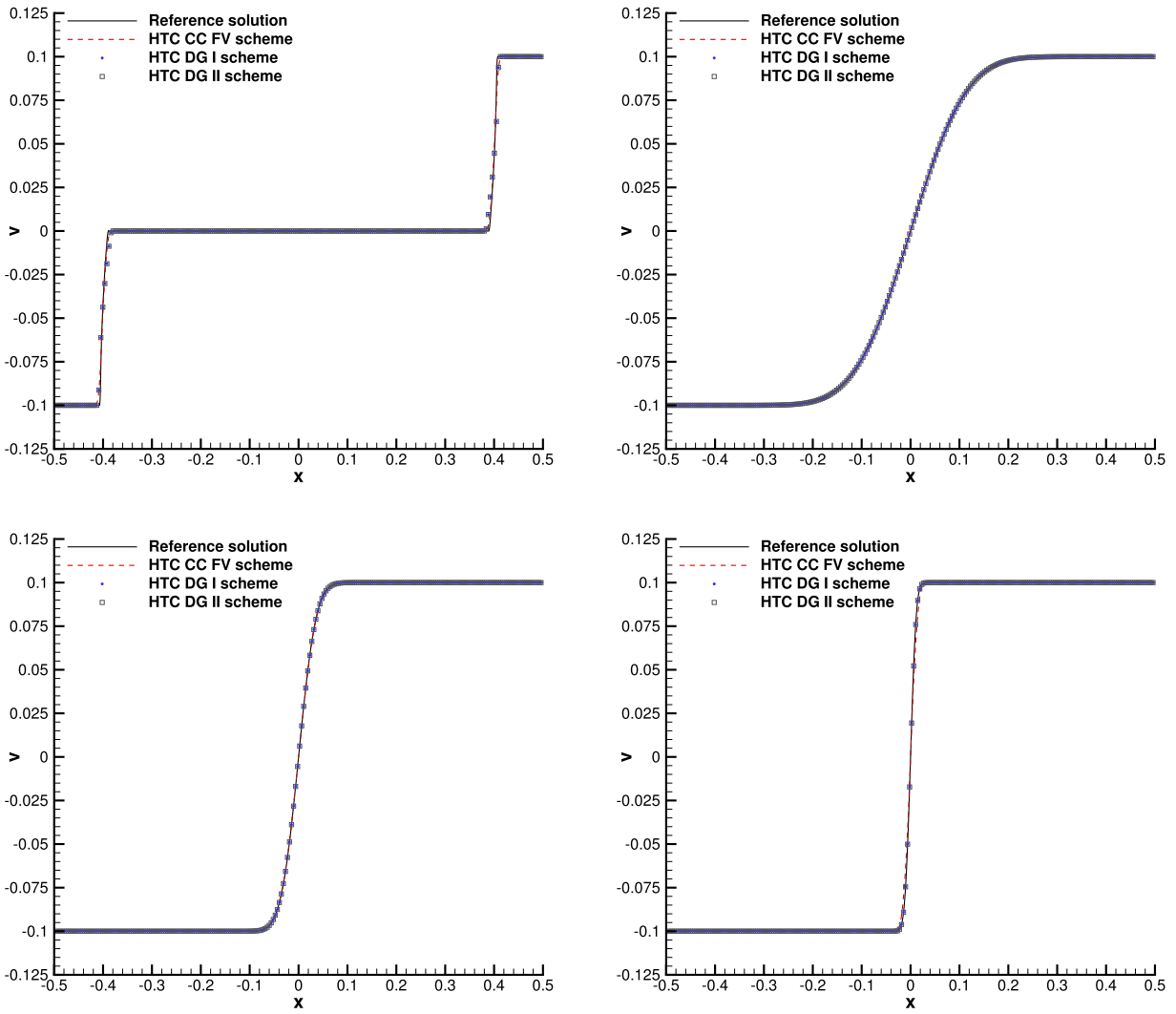

Fig. 1. Simple shear motion in an ideal elastic solid and in viscous fluids. Numerical solution of the GPR model at time $t = 0.4$ obtained with the new HTC finite volume scheme (6144 cells) and the new HTC DG schemes of type I and II (1024 elements, polynomial approximation degree $N = 5$). Top left: results for the solid setting $\tau_1 = \tau_2 = 10^{20}$. From top right to bottom right: results for fluids with viscosities: $\mu = 10^{-2}$, $\mu = 10^{-3}$ and $\mu = 10^{-4}$, respectively.

used as reference solution for v_2:

$$v_2(x,t) = v_0 \,\mathrm{erf}\left(\frac{1}{2}\frac{x}{\sqrt{\nu t}}\right), \tag{148}$$

with $\nu = \mu/\rho_0$. For the solid limit of the model, a reference solution is obtained by using a second order TVD finite volume scheme of the MUSCL-Hancock type, see [66], on 10,000 cells. In the solid limit of the GPR model the artificial viscosity is set to $\epsilon = 10^{-6}$. The obtained numerical results are depicted in Fig. 1, where an excellent agreement of all numerical solutions with the reference solutions can be observed.

6.3. Riemann problems

Next, we analyse a set of five Riemann problems with the left and right initial states and the location of the initial discontinuity x_c given in Table 4. The one-dimensional domain is $\Omega = [-0.5, +0.5]$. We consider the Euler subsystem (i.e. only the black terms in (1)), as well as the full GPR model (1). The exact solution of the Riemann problem for the Euler equations can be found in the textbook of Toro [66], while for the full GPR model a numerical reference solution is obtained by solving (1) at the aid of a second order MUSCL-Hancock method on a very fine mesh of 128,000 control volumes, solving the total energy Eq. (1f) instead of the entropy inequality (1c). The Riemann problems contain three test cases for the pure Euler equations, RP1, RP2, RP3, and two test problems for the fluid and solid limit of the GPR model, RP4 and RP5. For

Table 4
Left (L) and right (R) initial states for density, velocity, with $\mathbf{v} = (u, v, 0)$, and pressure p and location of the initial discontinuity x_c for five Riemann problems solved with the new HTC finite volume and discontinuous Galerkin schemes of type I and II proposed in this paper.

RP	ρ_L	u_L	v_L	p_L	ρ_R	u_R	v_R	p_R	x_c
RP1	1.0	0.0	0.0	1.0	0.125	0.0	0.0	0.1	0.0
RP2	5.99924	19.5975	0.0	460.894	5.99242	−6.19633	0.0	46.095	−0.2
RP3	1.0	−2.0	0.0	0.4	1.0	+2.0	0.0	0.4	0.0
RP4	1.0	0.0	−0.2	1.0	0.5	0.0	+0.2	0.5	0.0
RP5	1.0	0.0	−0.2	1.0	0.5	0.0	+0.2	0.5	0.0

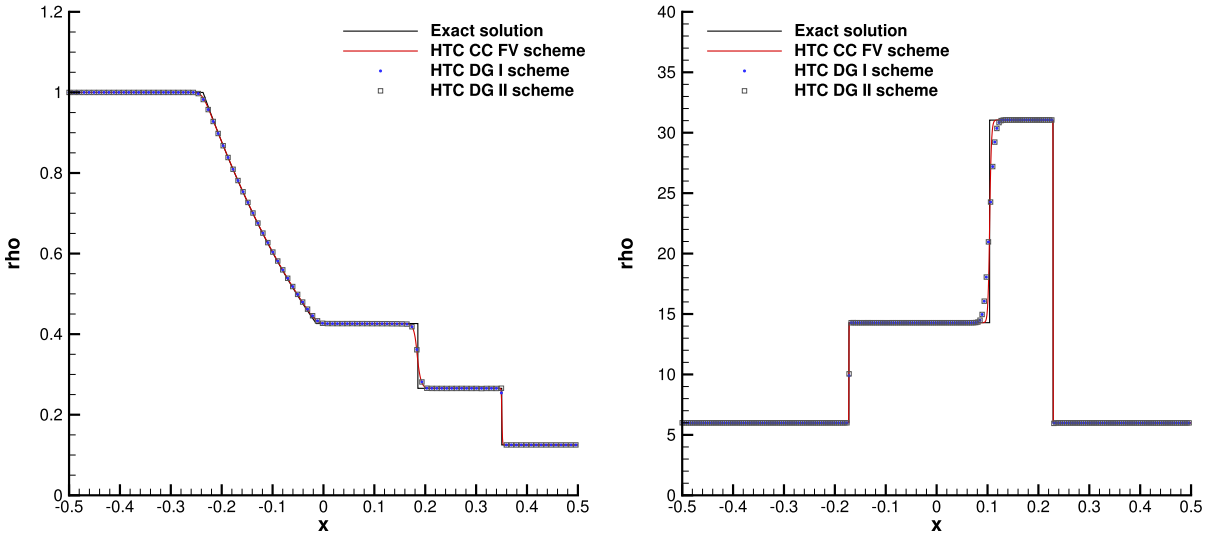

Fig. 2. Results of the density for Riemann problems RP1 (left) and RP2 (right) at times $t = 0.2$ and $t = 0.035$, respectively, obtained using the new thermodynamically compatible cell-centered HTC FV scheme (1536 cells for RP1, 6144 cells for RP2) and the HTC DG schemes of type I and II ($N = 5$, 256 elements for RP1, 1024 elements for RP2) applied to the compressible Euler equations. The exact solution, see [66], is represented with a black solid line.

RP4 and RP5 we set the initial conditions for $\mathbf{A}$ and $\mathbf{J}$ to $\mathbf{A} = \mathbf{I}$ and $\mathbf{J} = \mathbf{0}$. Furthermore, we choose $c_s = c_h = 1$ and $\gamma = 1.4$. For RP4 we choose the relaxation times so that $\mu = \kappa = 10^{-5}$ and for RP5 we set $\tau_1 = \tau_2 = 10^{20}$. In all cases the artificial viscosity is set to a constant value of $\epsilon = 10^{-5}$. The numerical results obtained with the new HTC schemes proposed in this paper are compared against the reference solution in Figs. 2–5. The employed mesh resolution is provided for each test case in the corresponding figure caption and the polynomial approximation degree for the HTC DG schemes of type I and II is set to $N = 5$. In all cases an excellent agreement between numerical solution and reference solution can be observed. In particular, we can observe that there is no spurious glitch in the temperature of the 123 problem (RP3) for both types of HTC DG schemes, unlike in the corresponding HTC FV method.

6.4. Viscous shock wave

The next test case is a stationary viscous shock with a characteristic shock Mach number of $M_s = 2$ and a Prandtl number in the fluid of Pr= 0.75, so that an exact solution of the compressible Navier–Stokes equations exists, see e.g. [74,75] and [64] for the details on the computation of the exact solution. The problem is solved in the one-dimensional domain $\Omega = [-0.5, +0.5]$ with the shock wave centered at $x = 0$ and the fluid moving into the shock from the left to the right. The data in front of the shock are $\rho_0 = 1$, $v_1^0 = 2$, $v_2^0 = v_3 = 0$ and $p^0 = 1/\gamma$, hence the sound speed in front of the shock is $c^0 = 1$. The Reynolds number based on the reference length $L = 1$ is $Re_s = \rho^0 c^0 M_s L \mu^{-1}$. The remaining parameters of the GPR model are chosen as $\gamma = 1.4$, $c_v = 2.5$, $c_h = c_s = 50$, $\mu = 2 \times 10^{-2}$ and $\kappa = 9\frac{1}{3} \times 10^{-2}$, hence the shock Reynolds number is $Re_s = 100$. The initial condition for $\mathbf{J}$ and $\mathbf{A}$ is $\mathbf{J} = \mathbf{0}$ and $\mathbf{A} = \sqrt[3]{\rho}\,\mathbf{I}$. The comparison of the solution obtained with the novel thermodynamically compatible HTC schemes applied to (1) and the exact solution obtained for the compressible Navier–Stokes equations is depicted in Fig. 6. For the HTC finite volume scheme we employ 1024 equidistant cells, while the HTC DG schemes of type I and II use 256 cells with polynomial approximation degree $N = 9$. For all quantities an excellent agreement is achieved.

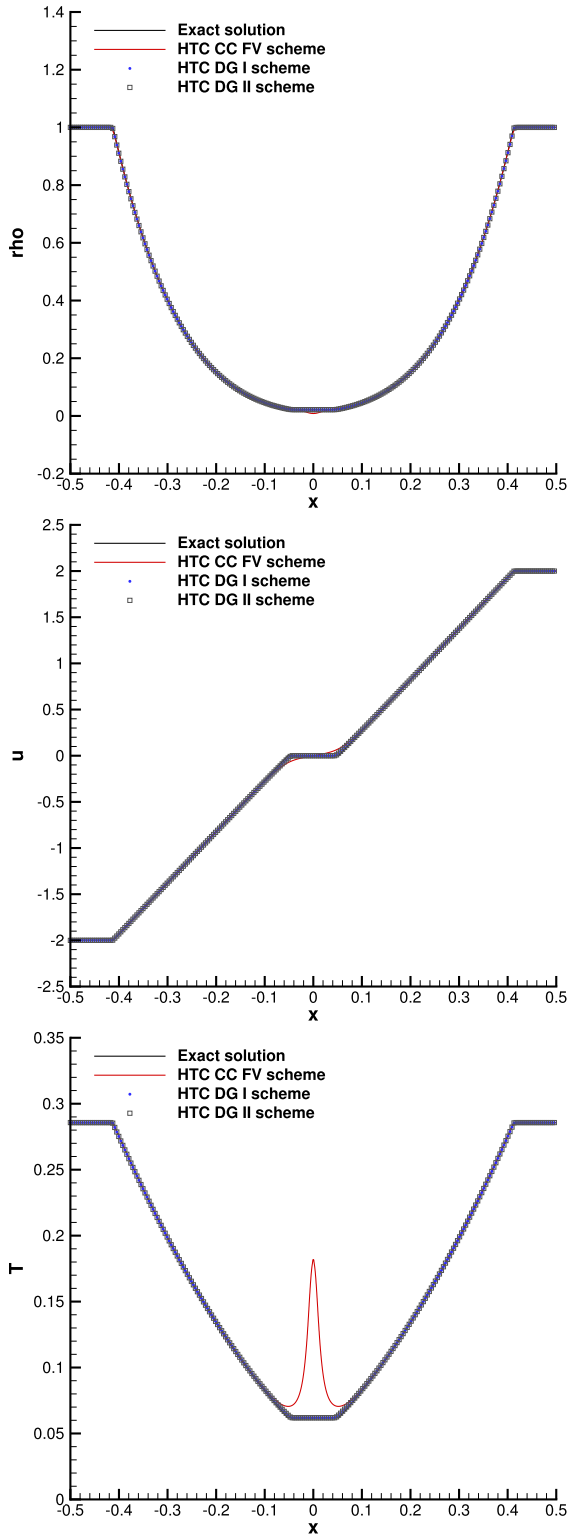

Fig. 3. Results for the 123 problem, RP3, at time $t = 0.15$, obtained using the new thermodynamically compatible cell-centered HTC FV scheme (6144 cells) and the HTC DG schemes of type I and II ($N = 5$, 1024 elements) applied to the compressible Euler equations. Density (top panel), velocity (central panel), temperature (bottom panel). The exact solution, see [66], is represented with a black solid line.

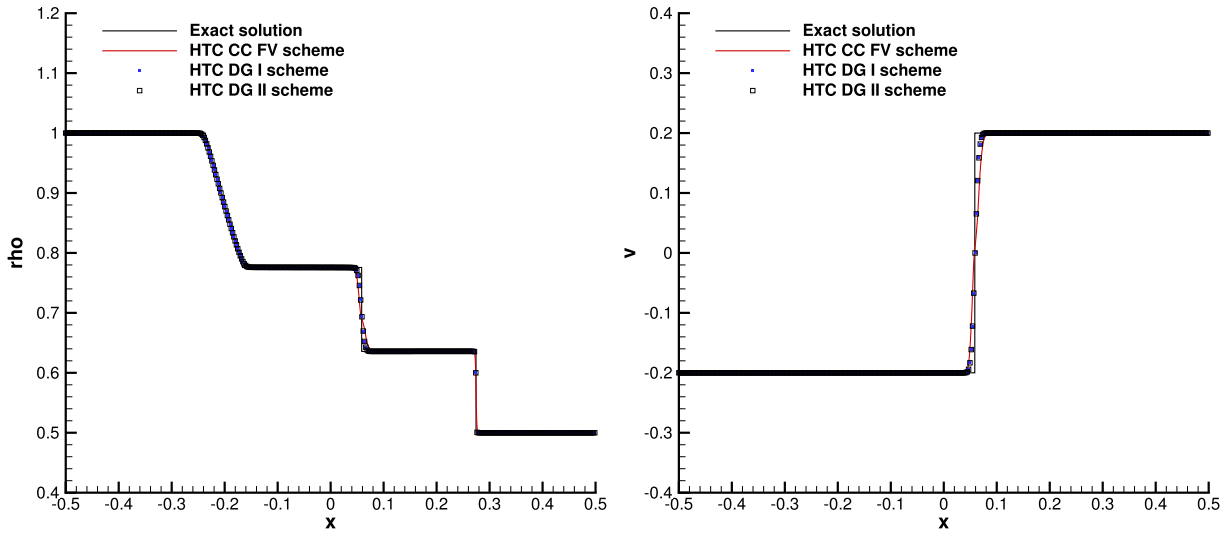

Fig. 4. Results for the density for Riemann problem RP4 at time $t = 0.2$, obtained using the new thermodynamically compatible cell-centered HTC FV scheme (6144 cells) and the HTC DG schemes of type I and II ($N = 5$, 1024 elements) applied to the GPR model in the stiff relaxation limit ($\mu = \kappa = 10^{-5}$). The exact solution of the compressible Euler equations, see [66], is represented with a black solid line as a reference solution.

6.5. Double shear layer

The double shear layer test was proposed in Bell et al. [76] and was subsequently used in Busto et al. [61], Dumbser et al. [64], Boscheri et al. [71], Bermúdez et al. [72], Busto et al. [73], Tavelli and Dumbser [77], 78] to assess the behaviour of compressible flow solvers in the weakly compressible regime, including applications to the GPR model (1). The two-dimensional domain is the unit square $\Omega = [0, 1]^2$ with periodic boundaries everywhere. The initial condition is given by

$$v_1 = \begin{cases} \tanh\left(\tilde{\rho}(y - \frac{1}{4})\right), & y \leq \frac{1}{2}, \\ \tanh\left(\tilde{\rho}(\frac{3}{4} - y)\right), & y > \frac{1}{2}, \end{cases} \qquad v_2 = \delta \sin(2\pi x),$$

$v_3 = 0$, $\rho = \rho_0 = 1$, $p = 10^2/\gamma$, $\mathbf{A} = \mathbf{I}$ and $\mathbf{J} = \mathbf{0}$, with $\delta = 0.05$ and $\tilde{\rho} = 30$. The remaining parameters of the model are $\nu = \mu/\rho_0 = 2 \times 10^{-3}$, $\rho_0 = 1$, $c_v = 1$, $c_s = 8$, $c_h = 2$ and $\tau_2 = 4 \times 10^{-3}$. The characteristic Mach number of the flow resulting from this setup is $M = 0.1$. The numerical simulations are carried out with all new HTC schemes proposed in this paper until $t = 1.8$. The HTC finite volume scheme is run on a computational grid of 4000×4000 elements, while the HTC DG schemes of type I and II use a coarser mesh of 1024×1024 control volumes with a polynomial approximation degree of $N = 3$. The numerical viscosity is set to $\epsilon = 1 \times 10^{-6}$ in all cases. In Fig. 7 the results obtained with the new HTC FV scheme for the time evolution of the distortion field component A_{12} are shown. The results agree very well with those reported in Busto et al. [61], where also a validation against an incompressible Navier–Stokes solver [72,79] was provided. The initial shear layers develop into several vortices, as already described in more detail in Dumbser et al. [64], Boscheri et al. [71], Bermúdez et al. [72], Busto et al. [73], Bell et al. [76]. Almost identical results are obtained for this test problem also with the HTC DG schemes of type I and II, see Figs. 8 and 9. Overall, we can therefore conclude that the methods proposed in this paper allow the reliable simulation of complex flows in the fluid limit of the GPR model, leading to numerical results that are essentially independent of the underlying mesh and numerical method, once a sufficiently fine mesh has been used.

6.6. Solid rotor

Here, we apply our new thermodynamically compatible schemes to the solid rotor problem proposed in Busto et al. [61], Boscheri et al. [71]. Choosing $\tau_1 = \tau_2 = 10^{20}$ the governing PDE system (1) describes the dynamics of a nonlinear hyperelastic solid. We define the two-dimensional domain as $\Omega = [-1, +1]^2$ with transmissive boundary conditions everywhere. As initial conditions for density, pressure, distortion field and thermal impulse we set $\rho = 1$, $p = 1$, $\mathbf{A} = \mathbf{I}$ and $\mathbf{J} = \mathbf{0}$, the initial velocity field is given by $v_1 = -y/R$, $v_2 = +x/R$ and $v_3 = 0$ within the circle $\|\mathbf{x}\| \leq R$ of radius $R = 0.2$, while for $r > R$ the velocity is $\mathbf{v} = 0$. The remaining parameters of the model are $\gamma = 1.4$, $c_s = 1.0$ and $c_h = 1.0$. The final simulation time is set to $t = 0.3$ in all cases. We run this test using the HTC finite volume scheme on 512×512 control volumes as well as the HTC DG schemes of type I and II with 128×128 elements and a polynomial approximation degree of $N = 5$. In all cases the artificial viscosity is set to $\epsilon = 5 \times 10^{-4}$. The reference solution is provided by a second order MUSCL-Hancock scheme on 512×512 control volumes, solving the total energy conservation law (1f) rather than the entropy inequality (1c), as also done in Dumbser

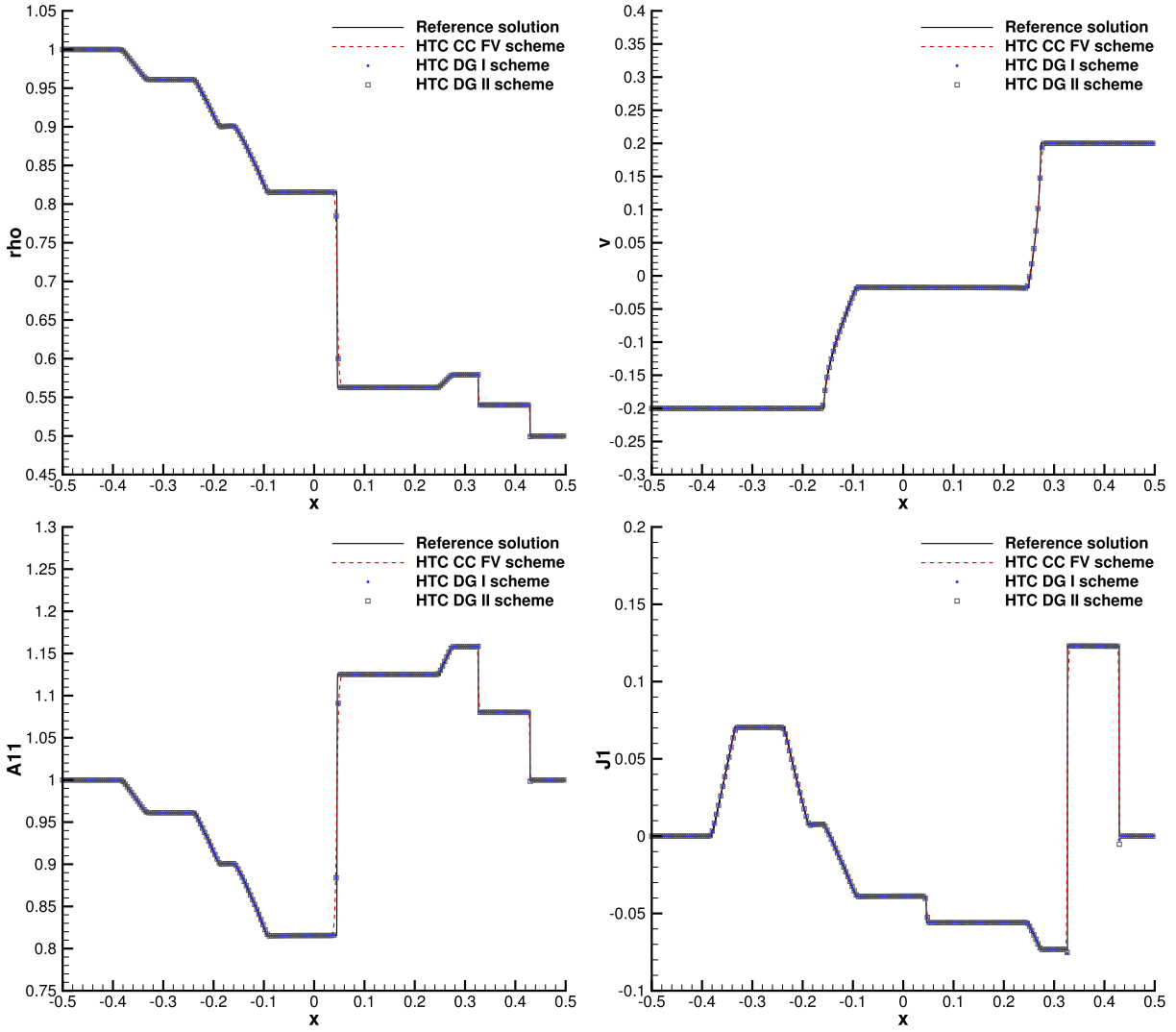

Fig. 5. Results for the density for Riemann problem RP5 ($x_c = 0$) at time $t = 0.2$, obtained using the new thermodynamically compatible cell-centered HTC FV scheme (6144 cells) and the HTC DG schemes of type I and II ($N = 5$, 1024 elements) applied to the GPR model in the solid limit ($\tau_1 = \tau_2 = 10^{20}$).

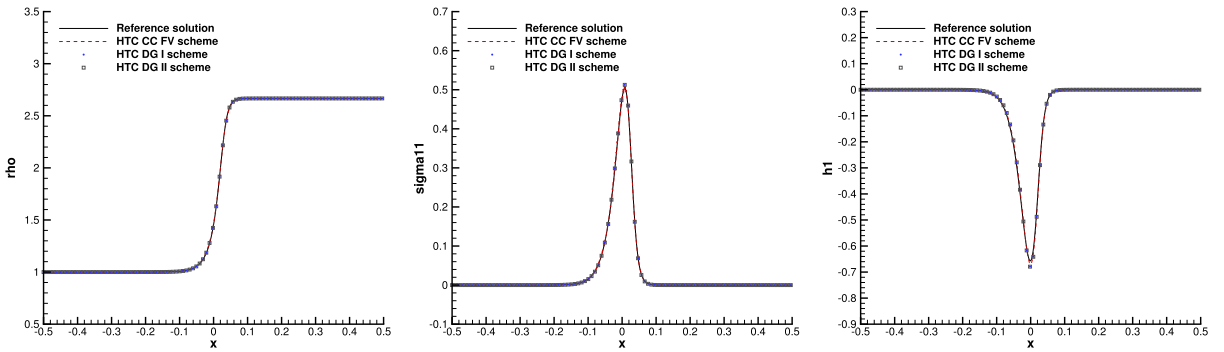

Fig. 6. Viscous shock at $Re_s = 100$, $M_s = 2$ and $Pr = 0.75$. Numerical solution obtained with the new thermodynamically compatible cell-centered HTC FV scheme (1536 cells) and the new HTC DG schemes of type I and II (256 elements, $N = 5$) applied to the GPR model. Comparison with the exact solution from the compressible Navier–Stokes equations. Density (left), stress σ_{11} (center) and heat flux h_1 (right) at time $t = 0.25$.

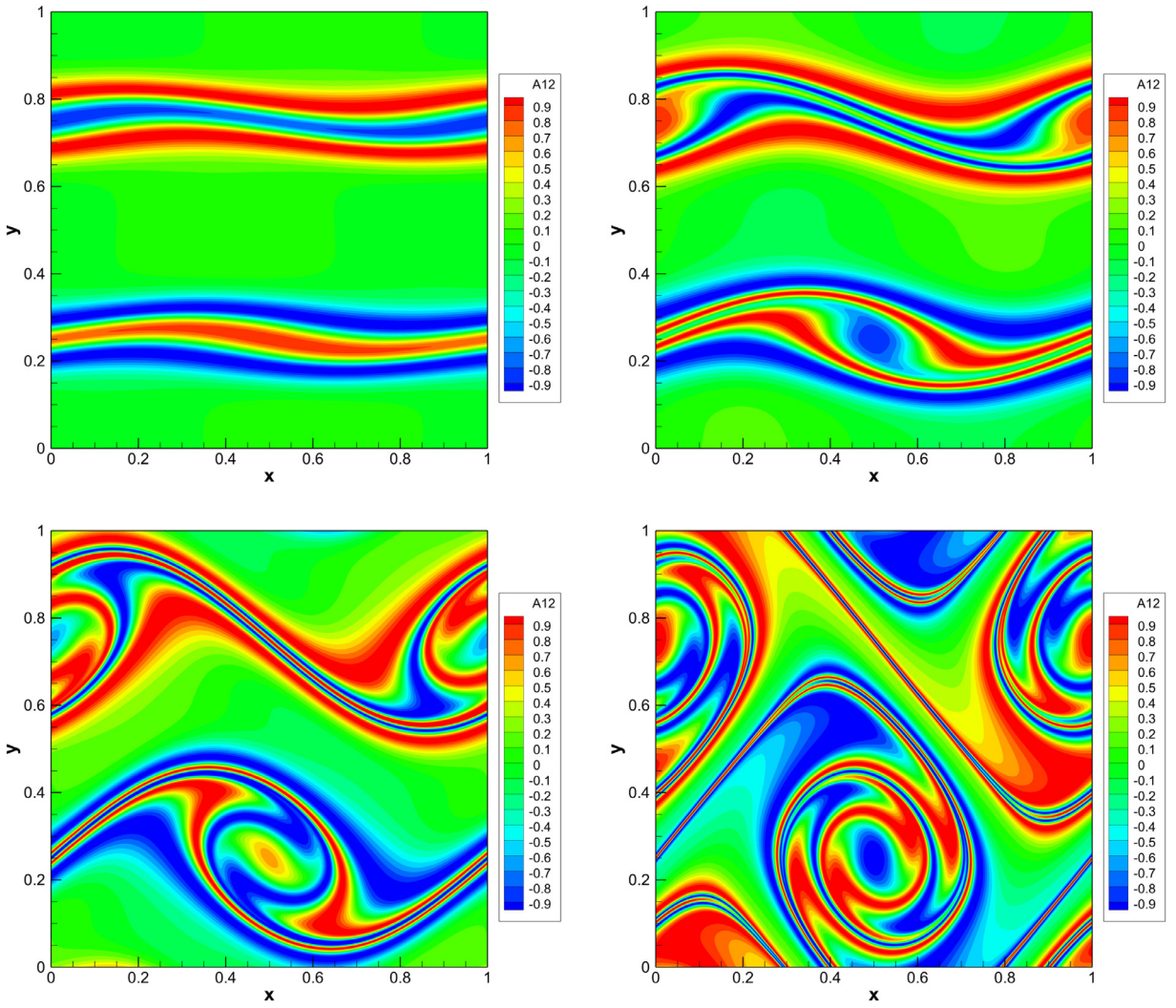

Fig. 7. Numerical solution obtained for the double shear layer problem with the new thermodynamically compatible cell-centered HTC finite volume scheme applied to the GPR model with $\mu = 2 \cdot 10^{-3}$. Distortion field component A_{12} at times $t = 0.4$ (top left), $t = 0.8$ (top right), $t = 1.2$ (bottom left) and $t = 1.8$ (bottom right).

et al. [64]. In Fig. 10 the computational results of the HTC schemes are compared with each other and with the reference solution, obtaining an excellent agreement among all of them.

6.7. Lid-driven cavity

The final test problem is the lid-driven cavity benchmark, see [80], which is also well-suited to validate numerical schemes in the low Mach number limit of the compressible Navier–Stokes equations, see e.g. [72,73,78]. This test case was already successfully solved with different numerical schemes applied to the GPR model in Busto et al. [61], Dumbser et al. [64], Boscheri et al. [71]. The two-dimensional computational domain is the unit square $\Omega = [0, 1] \times [0, 1]$ and the initial condition reads $\rho = 1$, $\mathbf{v} = \mathbf{0}$, $p = 10^2$, $\mathbf{A} = \mathbf{I}$ and $\mathbf{J} = \mathbf{0}$. According to Busto et al. [61] the remaining model parameters are $\gamma = 1.4$, $c_v = 1$, $c_s = 8$, $\rho_0 = 1$ and $c_h = 2$, $\tau_2 = 10^{-2}$ and $\mu = 10^{-2}$, hence the characteristic Reynolds number of the flow based on the lid velocity $\mathbf{v} = (1, 0, 0)$ is $Re = 100$. Apart from the lid, all boundaries are no-slip wall boundaries with zero velocity. The characteristic Mach number of this test problem based on the lid velocity is about $M = 0.08$. All HTC schemes use a mesh composed of 256×256 elements and the HTC DG schemes of type I and II employ a polynomial approximation degree of $N = 3$. The final time for all simulations is $t = 10$. We have always used a constant artificial viscosity of $\epsilon = 10^{-3}$, apart from the DG scheme of type II, for which we set $\epsilon = 1.5 \times 10^{-3}$. All numerical results are summarized in Fig. 11 and compared against the reference solution available in Ghia et al. [80]. We can observe an excellent agreement between the

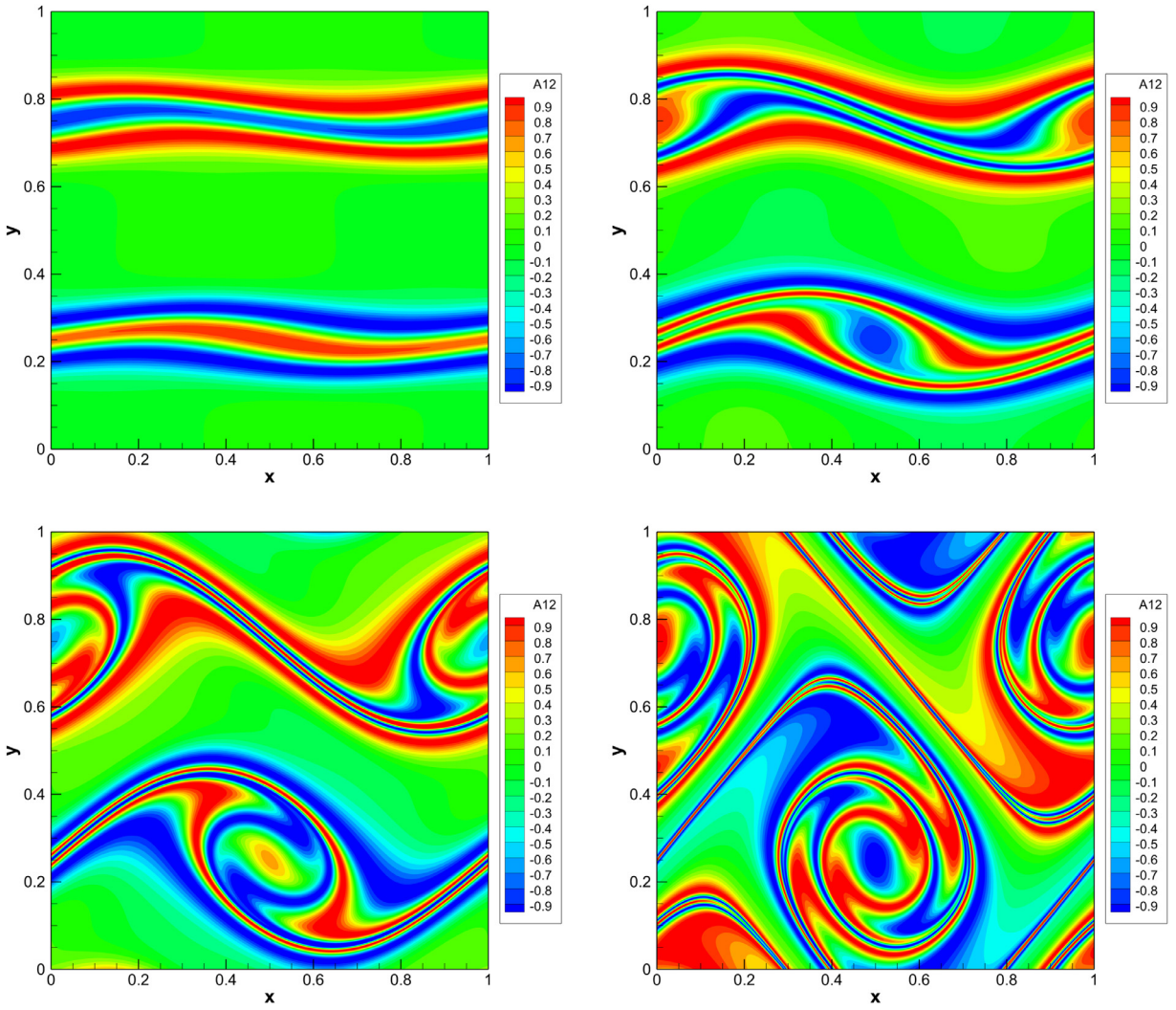

Fig. 8. Numerical solution obtained for the double shear layer problem with the new HTC DG scheme of type I applied to the GPR model with $\mu = 2 \cdot 10^{-3}$. Distortion field component A_{12} at times $t = 0.4$ (top left), $t = 0.8$ (top right), $t = 1.2$ (bottom left) and $t = 1.8$ (bottom right).

solution approximated by solving the GPR model with the new HTC schemes and the reference solution for the incompressible Navier–Stokes equations.

In order to obtain stable results for the DG schemes of type II the artificial viscosity needed to be increased in this test problem compared to the other two schemes. The authors conjecture that the problem is related to the no-slip wall boundary conditions, which are non-trivial for the lid driven cavity in general, due to the discontinuous velocity field on the boundary, and for the GPR model in particular, see [71] for a detailed discussion. The lid-driven cavity generates pressure peaks in the upper corners of the domain, which may require more limiting in the case of DG schemes of type II compared to the other two methods. Further and more detailed investigations on the behaviour of DG schemes of type II in the presence of no-slip wall boundaries are needed in the future.

7. Conclusions

In this paper we have presented three new semi-discrete thermodynamically compatible schemes for the GPR model of continuum mechanics: one scheme of the cell-centered finite volume type and two different high order DG schemes. All three methods have in common that they discretize the *entropy density* as a primary evolution quantity, in contrast to standard methods for hyperbolic systems, while total energy conservation is obtained as a mere consequence of the thermodynamically compatible discretization. All methods satisfy a discrete cell entropy inequality *by construction* and can be proven to be nonlinearly stable in the energy norm. For all schemes we have shown numerical results for several benchmarks in both the solid and fluid limit of the GPR model. In all cases a very good agreement with exact or numerical

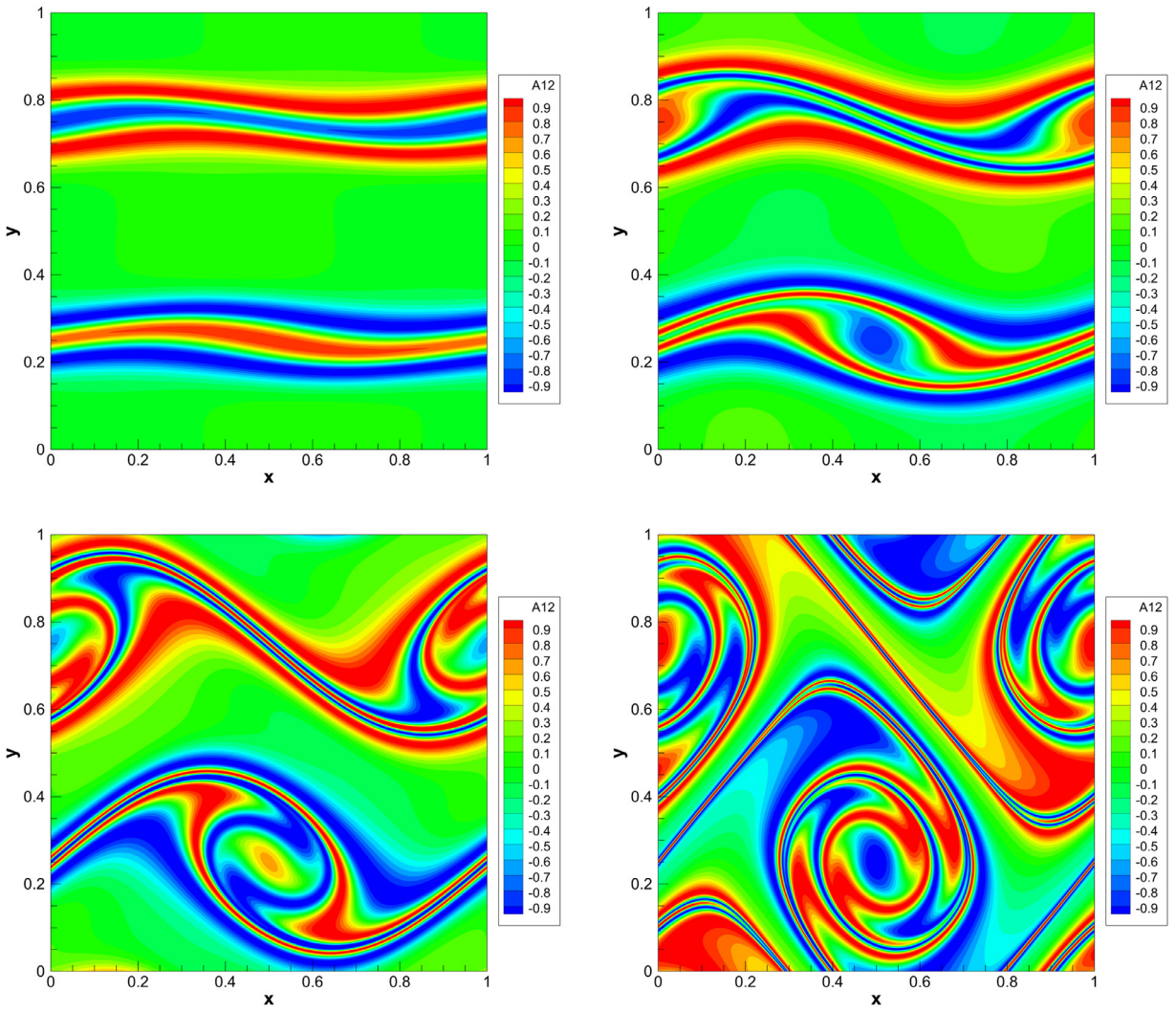

Fig. 9. Numerical solution obtained for the double shear layer problem with the new HTC DG scheme of type II applied to the GPR model with $\mu = 2 \cdot 10^{-3}$. Distortion field component A_{12} at times $t = 0.4$ (top left), $t = 0.8$ (top right), $t = 1.2$ (bottom left) and $t = 1.8$ (bottom right).

reference solutions was obtained. Compared to previous work on similar schemes presented in Busto et al. [59], Busto and Dumbser [60], Busto et al. [61], Busto and Dumbser [62] the new numerical methods introduced in this paper were shown to be computationally more efficient and simpler to implement, since no path-integrals need to be computed in order to obtain a thermodynamically compatible flux for the inviscid Euler subsystem. Furthermore, the new family of numerical schemes discussed in this paper does *not* require an underlying Godunov parametrization of the physical flux in terms of a generating potential, unlike the thermodynamically compatible schemes forwarded in Busto et al. [59], Busto and Dumbser [60], Busto et al. [61], Busto and Dumbser [62]. The finite volume schemes are clearly the most simple schemes presented in this paper. They only only require the calculation of compatible fluxes and jump terms. DG methods of type I are simple straightforward extensions of the former to the DG framework. The new DG schemes of type II proposed in this paper do not need a special compatible discretization of terms related to the distortion field **A** and to the specific thermal impulse **J**. Simple arithmetic averages are enough to construct a baseline scheme and subsequently the entire correction leading to thermodynamic compatibility, including numerical quadrature errors, is achieved in the calculation of the element-wise scalar correction factor α^i.

Future work will consider an extension of the approach proposed in this paper to the MHD equations, to turbulent shallow water flows [81,82] and to the conservative SHTC system of compressible two-fluid flows proposed by Romenski et al. in Romenski et al. [10], 11], which was already studied numerically and analytically in Lukácová-Medvidóvá et al. [83], Thein et al. [84]. In the future, we also plan an extension of the methodology outlined in this paper to the fully discrete case as well as to *staggered* Cartesian and unstructured meshes, in order to combine it with involution-preserving semi-implicit discretizations [71,85] and semi-implicit hybrid finite-volume / finite-element schemes [72,73,79] on staggered meshes. All

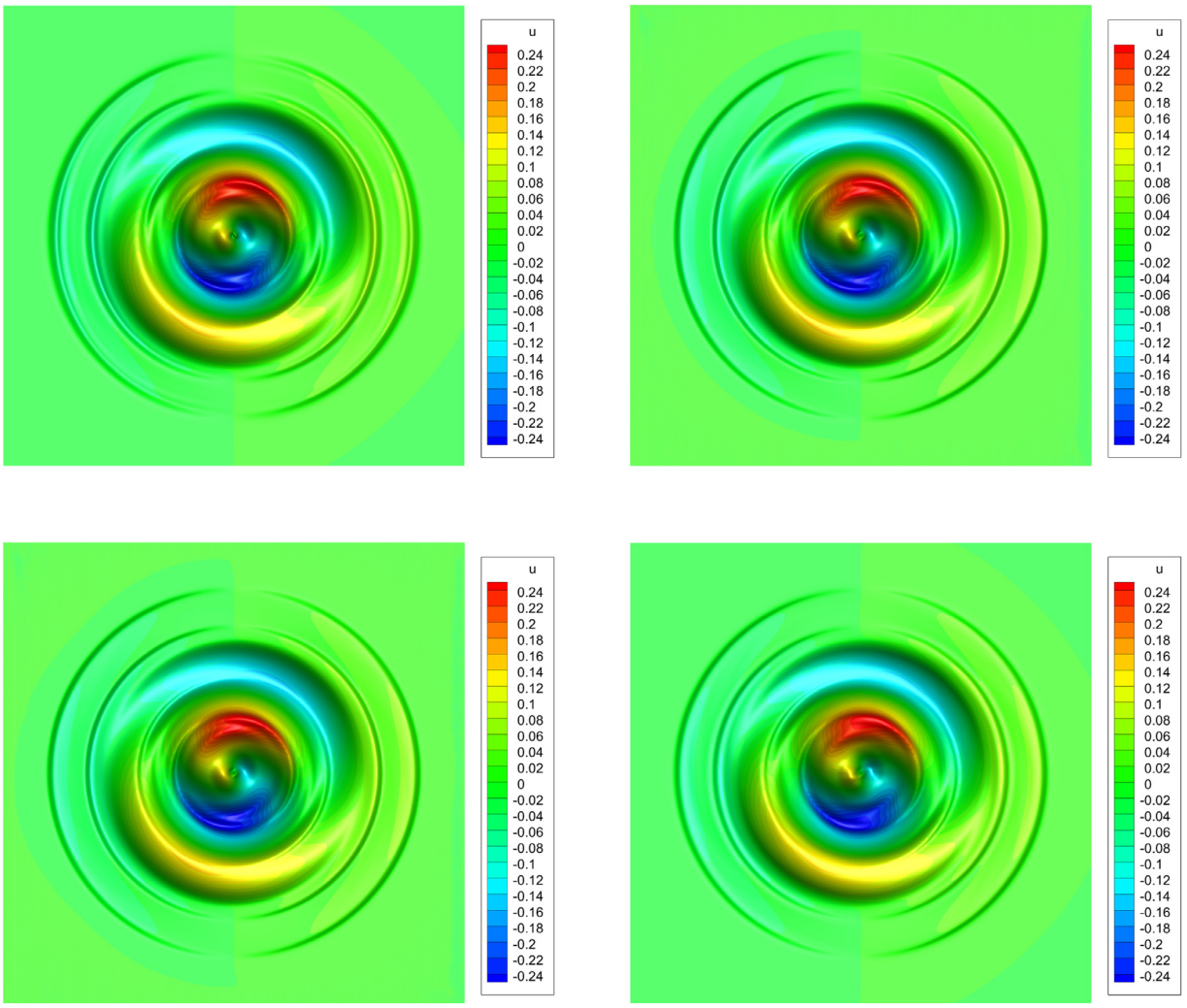

Fig. 10. Contour colours of the velocity component v_1 for the solid rotor problem obtained solving the GPR model in the solid limit up to time $t = 0.3$. Thermodynamically compatible HTC FV scheme (top left), HTC DG scheme of type I (top right), HTC DG scheme of type II (bottom left) and reference solution obtained with a classical second order MUSCL-Hancock scheme (bottom right).

schemes presented in this paper have been analyzed in the semi discrete setting. For a possible extension to the fully discrete case, at least for the Euler subsystem, see e.g. [61,86–88]. We will also consider the use of conservative and symplectic time integrators, such as those forwarded in Brugnano and Iavernaro [89], 90], in order to preserve the conservation of total energy of our semi-discrete schemes exactly also in a fully discrete setting. The incorporation of limiters in the DG scheme was out of scope of this work. We will therefore also consider proper limiters for DG schemes in the future, such as slope and moment limiters [91,92], positivity preserving limiters [93], or the use of the cell-centered thermodynamically compatible finite volume schemes presented in this paper as *a posteriori* subcell FV limiter of the DG schemes of type I and II, following the ideas on subcell limiting for DG schemes outlined in Rueda-Ramírez et al. [41], Sonntag and Munz [94], Dumbser et al. [95], Sonntag and Munz [96].

Dedication

The new numerical methods introduced in this paper are dedicated to Prof. Eleuterio Francisco Toro at the occasion of his 75th birthday and in honor of his groundbreaking scientific contributions to the field of numerical methods for hyperbolic PDE.

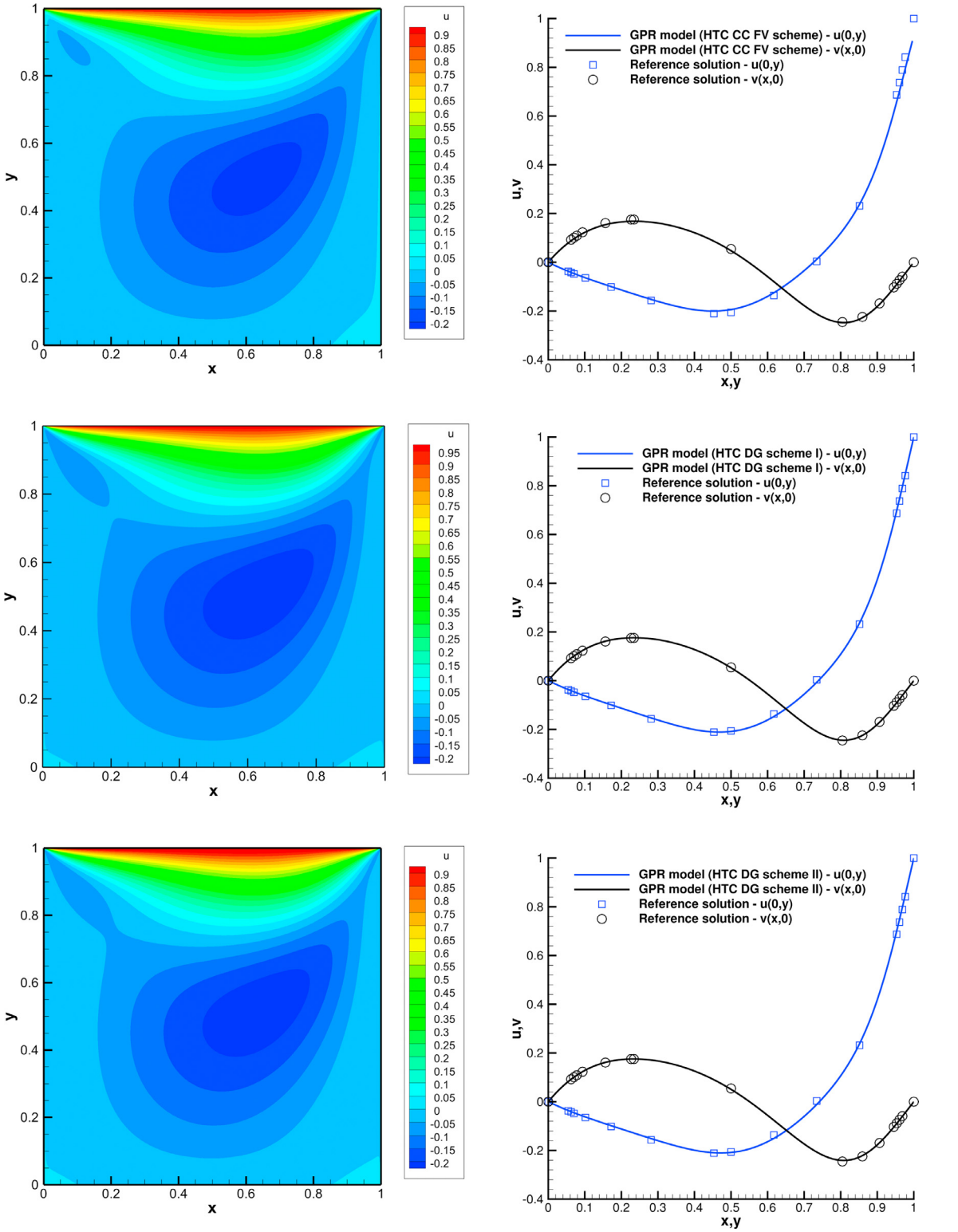

Fig. 11. Results for the lid-driven cavity test at $Re = 100$ using the first order hyperbolic GPR model in entropy formulation. Results obtained at time $t = 10$ on 256×256 elements using the new thermodynamically compatible cell-centered HTC finite volume scheme (top row), the HTC DG scheme of type I (middle row) and the HTC DG scheme of type II (bottom row). Left column: colour contours of the velocity component v_1. Right column: comparison of v_1 and v_2 along the 1D cuts $x = 0.5$ and $y = 0.5$ with the reference solution provided in Ghia et al. [80].

Data Availability

Data will be made available on request.

Acknowledgements

S.B. and M.D. are members of the INdAM GNCS group and acknowledge the financial support received from the Italian Ministry of Education, University and Research (MIUR) in the frame of the PRIN 2017 project *Innovative numerical methods for evolutionary partial differential equations and applications* and from the Spanish Ministry of Science and Innovation, grant number PID2021-122625OB-I00. S.B. was also funded by INdAM via a GNCS grant for young researchers and by an *UniTN starting grant* of the University of Trento. R.A. was partially funded by SNFS grant #200020_204917. The authors would like to acknowledge support from the Leibniz Rechenzentrum (LRZ) in Garching, Germany, for granting access to the SuperMUC-NG supercomputer under project number pr63qo and to the CESGA in Santiago de Compostela, Spain, for the access to the FT3 supercomputer. The Authors also would like to thank the Universidade de Vigo/CISUG for the funding of the open access charge.

The authors would like to thank the anonymous referee for the very useful and constructive comments, which helped to improve the quality and clarity of this paper.

References

[1] R. Abgrall, A general framework to construct schemes satisfying additional conservation relations. Application to entropy conservative and entropy dissipative schemes, J. Comput. Phys. 372 (2018) 640–666.
[2] K. Friedrichs, Symmetric positive linear differential equations, Commun. Pure Appl. Math. 11 (1958) 333–418.
[3] S. Godunov, An interesting class of quasilinear systems, Dokl. Akad. Nauk SSSR 139 (3) (1961) 521–523.
[4] K. Friedrichs, P. Lax, Systems of conservation equations with a convex extension, Proc. Natl. Acad. Sci. USA 68 (1971) 1686–1688.
[5] G. Boillat, Sur l'existence et la recherche d'équations de conservation supplémentaires pour les systèmes hyperboliques, C. R. Acad. Sci. Paris Sér. A 278 (1974) 909–912.
[6] T. Ruggeri, A. Strumia, Main field and convex covariant density for quasilinear hyperbolic systems. Relativistic fluid dynamics, Ann. Inst. H. Poincaré Sect. A (N.S.) 34 (1981) 65–84.
[7] H. Freistühler, Relativistic barotropic fluids: a Godunov–Boillat formulation for their dynamics and a discussion of two special classes, Arch. Ration. Mech. Anal. 232 (2019) 473–488.
[8] S. Godunov, Symmetric form of the equations of magnetohydrodynamics, Numer. Methods Mech. Contin. Media 3 (1) (1972) 26–31.
[9] S. Godunov, E. Romenski, Nonstationary equations of the nonlinear theory of elasticity in Euler coordinates, J. Appl. Mech. Tech. Phys. 13 (1972) 868–885.
[10] E. Romenski, A. Resnyansky, E. Toro, Conservative hyperbolic formulation for compressible two-phase flow with different phase pressures and temperatures, Q. Appl. Math. 65 (2007) 259–279.
[11] E. Romenski, D. Drikakis, E. Toro, Conservative models and numerical methods for compressible two-phase flow, J. Sci. Comput. 42 (2010) 68–95.
[12] S.K. Godunov, Thermodynamic formalization of the fluid dynamics equations for a charged dielectric in an electromagnetic field, Comput. Math. Math. Phys. 52 (2012) 787–799.
[13] E. Romenski, I. Peshkov, M. Dumbser, F. Fambri, A new continuum model for general relativistic viscous heat-conducting media, Philos. Trans. R. Soc. A 378 (2020) 20190175.
[14] I. Peshkov, E. Romenski, M. Dumbser, Continuum mechanics with torsion, Contin Mech. Thermodyn. 31 (2019) 1517–1541.
[15] I. Peshkov, M. Pavelka, E. Romenski, M. Grmela, Continuum mechanics and thermodynamics in the Hamilton and the Godunov-type formulations, Contin. Mech. Thermodyn. 30 (6) (2018) 1343–1378.
[16] E. Romenski, Hyperbolic systems of thermodynamically compatible conservation laws in continuum mechanics, Math. Comput. Model. 28 (10) (1998) 115–130.
[17] S. Godunov, E. Romenski, Elements of Continuum Mechanics and Conservation Laws, Kluwer Academic/Plenum Publishers, 2003.
[18] N. Favrie, S. Gavrilyuk, A rapid numerical method for solving Serre–Green–Naghdi equations describing long free surface gravity waves, Nonlinearity 30 (2017) 2718–2736.
[19] F. Dhaouadi, N. Favrie, S. Gavrilyuk, Extended Lagrangian approach for the defocusing nonlinear Schrödinger equation, Stud. Appl. Math. 142 (2019) 336–358.
[20] E. Tadmor, The numerical viscosity of entropy stable schemes for systems of conservation laws I, Math. Comput. 49 (1987) 91–103.
[21] F. Ducros, V. Ferrand, F. Nicoud, C. Weber, D. Darracq, C. Gacherieu, T. Poinsot, Large-eddy simulation of the shock/turbulence interaction, J. Comput. Phys. 152 (1999) 517–549.
[22] F. Ducros, F. Laporte, T. Soulères, V. Guinot, P. Moinat, B. Caruelle, High-order fluxes for conservative skew-symmetric-like schemes in structured meshes: application to compressible flows, J. Comput. Phys. 161 (2000) 114–139.
[23] T. Fisher, M. Carpenter, J. Nordström, N. Yamaleev, C. Swanson, Discretely conservative finite-difference formulations for nonlinear conservation laws in split form: theory and boundary conditions, J. Comput. Phys. 234 (2013) 353–375.
[24] T. Fisher, M. Carpenter, High-order entropy stable finite difference schemes for nonlinear conservation laws: finite domains, J. Comput. Phys. 252 (2013) 518–557.
[25] M. Carpenter, T. Fisher, E. Nielsen, S. Frankel, Entropy stable spectral collocation schemes for the Navier–Stokes equations: discontinuous interfaces, SIAM J. Sci. Comput. 36 (2014) B835–B867.
[26] M. Carpenter, D. Gottlieb, S. Abarbanel, The stability of numerical boundary treatments for compact high–order finite–difference schemes, J. Comput. Phys. 108 (1993) 272–295.
[27] M. Carpenter, J. Nordström, D. Gottlieb, Revisiting and extending interface penalties for multi–domain summation–by–parts operators, J. Sci. Comput. 45 (2010) 118–150.
[28] J. Nordström, M.H. Carpenter, Boundary and interface conditions for high–order finite–difference methods applied to the Euler and Navier–Stokes equations, J. Comput. Phys. 148 (1999) 621–645.
[29] S. Pirozzoli, Generalized conservative approximations of split convective derivative operators, J. Comput. Phys. 229 (2010) 7180–7190.
[30] S. Pirozzoli, Stabilized non–dissipative approximations of Euler equations in generalized curvilinear coordinates, J. Comput. Phys. 230 (2011) 2997–3014.

[31] B. Sjögreen, H. Yee, High order entropy conservative central schemes for wide ranges of compressible gas dynamics and MHD flows, J. Comput. Phys. 364 (2018) 153–185.
[32] B. Sjögreen, H. Yee, Entropy stable method for the Euler equations revisited: central differencing via entropy splitting and SBP, J. Sci. Comput. 81 (2019) 1359–1385.
[33] H. Yee, B. Sjögreen, Recent advancement of entropy split methods for compressible gas dynamics and MHD, Appl. Math. Comput. (2022).
[34] J. Reiss, J. Sesterhenn, A conservative, skew–symmetric finite difference scheme for the compressible Navier–Stokes equations, Comput. Fluids 101 (2014) 208–219.
[35] U.S. Fjordholm, S. Mishra, E. Tadmor, Arbitrarily high-order accurate entropy stable essentially nonoscillatory schemes for systems of conservation laws, SIAM J. Numer. Anal. 50 (2) (2012) 544–573.
[36] M.J. Castro, U.S. Fjordholm, S. Mishra, C. Parés, Entropy conservative and entropy stable schemes for nonconservative hyperbolic systems, SIAM J. Numer. Anal. 51 (3) (2013) 1371–1391.
[37] A. Hiltebrand, S. Mishra, Entropy stable shock capturing space-time discontinuous Galerkin schemes for systems of conservation laws, Numer. Math. 126 (1) (2014) 103–151.
[38] G. Gassner, A. Winters, D. Kopriva, A well balanced and entropy conservative discontinuous Galerkin spectral element method for the shallow water equations, Appl. Math. Comput. 272 (2016) 291–308.
[39] D. Derigs, A.R. Winters, G. Gassner, S. Walch, M. Bohm, Ideal GLM-MHD: about the entropy consistent nine-wave magnetic field divergence diminishing ideal magnetohydrodynamics equations, J. Comput. Phys. 364 (2018) 420–467.
[40] G. Schnücke, N. Krais, T. Bolemann, G.J. Gassner, Entropy stable discontinuous Galerkin schemes on moving meshes for hyperbolic conservation laws, J. Sci. Comput. 82 (3) (2020).
[41] A.M. Rueda-Ramírez, S. Hennemann, F.J. Hindenlang, A.R. Winters, G.J. Gassner, An entropy stable nodal discontinuous Galerkin method for the resistive MHD equations. Part II: subcell finite volume shock capturing, J. Comput. Phys. 444 (2021) 109935.
[42] S. Hennemann, A.M. Rueda-Ramírez, F.J. Hindenlang, G.J. Gassner, A provably entropy stable subcell shock capturing approach for high order split form DG for the compressible euler equations, J. Comput. Phys. 426 (2021).
[43] T. Cheng, C. Shu, Entropy stable high order discontinuous Galerkin methods with suitable quadrature rules for hyperbolic conservation laws, J. Comput. Phys. 345 (2017) 427–461.
[44] Y. Liu, C. Shu, M. Zhang, Entropy stable high order discontinuous Galerkin methods for ideal compressible MHD on structured meshes, J. Comput. Phys. 354 (2018) 163–178.
[45] P. Chandrashekar, C. Klingenberg, Entropy stable finite volume scheme for ideal compressible MHD on 2-D Cartesian meshes, SIAM J. Numer. Anal. 54 (2) (2016) 1313–1340.
[46] D. Ray, P. Chandrashekar, U.S. Fjordholm, S. Mishra, Entropy stable scheme on two-dimensional unstructured grids for Euler equations, Commun. Comput. Phys. 19 (5) (2016) 1111–1140.
[47] D. Ray, P. Chandrashekar, An entropy stable finite volume scheme for the two dimensional Navier–Stokes equations on triangular grids, Appl. Math. Comput. 314 (2017) 257–286.
[48] J. Chan, C.G. Taylor, Efficient computation of Jacobian matrices for entropy stable summation-by-parts schemes, J. Comput. Phys. 448 (2022) 110701.
[49] J. Chan, Y. Lin, T. Warburton, Entropy stable modal discontinuous Galerkin schemes and wall boundary conditions for the compressible Navier–Stokes equations, J. Comput. Phys. 448 (2022) 110723.
[50] E. Gaburro, P. Öffner, M. Ricchiuto, D. Torlo, High order entropy preserving ADER-DG schemes, Appl. Math. Comput. (2022).
[51] U. Fjordholm, S. Mishra, Accurate numerical discretizations of non-conservative hyperbolic systems, ESAIM Math. Model. Numer. Anal. 46 (1) (2012) 187–206.
[52] R. Abgrall, P. Bacigaluppi, S. Tokareva, A high-order nonconservative approach for hyperbolic equations in fluid dynamics, Comput. Fluids 169 (2018) 10–22.
[53] R. Abgrall, P. Öffner, H. Ranocha, Reinterpretation and extension of entropy correction terms for residual distribution and discontinuous Galerkin schemes: application to structure preserving discretization, J. Comput. Phys. 453 (2022).
[54] R. Abgrall, J. Nordström, P. Öffner, S. Tokareva, Analysis of the SBP-SAT stabilization for finite element methods. I: linear problems, J. Sci. Comput. 85 (2) (2020) 28, doi:10.1007/s10915-020-01349-z.
[55] R. Abgrall, R. Nordström, P. Öffner, S. Tokareva, Analysis of the SBP-SAT stabilization for finite element methods part II: entropy stability, Commun. Appl. Math. Comput. (2021), doi:10.1007/s42967-020-00086-2.
[56] E. Caramana, R. Loubère, The force/work differencing of exceptional points in the discrete, compatible formulation of Lagrangian hydrodynamics, J. Comput. Phys. 216 (2006) 1–18.
[57] A. Bauera, D.E. Burton, E. Caramana, R. Loubère, M. Shashkov, P. Whalen, The internal consistency, stability, and accuracy of the discrete, compatible formulation of Lagrangian hydrodynamics, J. Comput. Phys. 218 (2006) 572–593.
[58] P. Maire, I. Bertron, R. Chauvin, B. Rebourcet, Thermodynamic consistency of cell-centered Lagrangian schemes, Comput. Fluids 203 (2020) 104527.
[59] S. Busto, M. Dumbser, S. Gavrilyuk, K. Ivanova, On thermodynamically compatible finite volume methods and path-conservative ADER discontinuous Galerkin schemes for turbulent shallow water flows, J. Sci. Comput. 88 (2021) 28.
[60] S. Busto, M. Dumbser, A new thermodynamically compatible finite volume scheme for magnetohydrodynamics, SIAM J. Numer. Anal. (2022). in press
[61] S. Busto, M. Dumbser, I. Peshkov, E. Romenski, On thermodynamically compatible finite volume schemes for continuum mechanics, SIAM J. Sci. Comput. 44 (2022) A1723–A1751.
[62] S. Busto, M. Dumbser, On thermodynamically compatible discontinuous Galerkin methods for continuum mechanics and turbulent shallow water flows, J. Sci. Comput. 93 (56) (2022), doi:10.1007/s10915-022-02017-0.
[63] I. Peshkov, E. Romenski, A hyperbolic model for viscous Newtonian flows, Contin. Mech. Thermodyn. 28 (2016) 85–104.
[64] M. Dumbser, I. Peshkov, E. Romenski, O. Zanotti, High order ADER schemes for a unified first order hyperbolic formulation of continuum mechanics: viscous heat–conducting fluids and elastic solids, J. Comput. Phys. 314 (2016) 824–862.
[65] F. Dhaouadi, M. Dumbser, A first order hyperbolic reformulation of the Navier–Stokes–Korteweg system based on the GPR model and an augmented Lagrangian approach, J. Comput. Phys. 470 (2022) 111544.
[66] E. Toro, Riemann Solvers and Numerical Methods for Fluid Dynamics, Springer, 2009.
[67] G. Gassner, F. Lörcher, C. Munz, A contribution to the construction of diffusion fluxes for finite volume and discontinuous Galerkin schemes, J. Comput. Phys. 224 (2007) 1049–1063.
[68] G. Jiang, C. Shu, On a cell entropy inequality for discontinuous Galerkin methods, Math. Comput. 62 (1994) 531–538.
[69] S. Gottlieb, C. Shu, Total variation diminishing Runge–Kutta schemes, Math. Comput. 67 (1998) 73–85.
[70] C. Hu, C. Shu, Weighted essentially non-oscillatory schemes on triangular meshes, J. Comput. Phys. 150 (1999) 97–127.
[71] W. Boscheri, M. Dumbser, M. Ioriatti, I. Peshkov, E. Romenski, A structure-preserving staggered semi-implicit finite volume scheme for continuum mechanics, J. Comput. Phys. 424 (2021) 109866.
[72] A. Bermúdez, S. Busto, M. Dumbser, J. Ferrín, L. Saavedra, M. Vázquez-Cendón, A staggered semi-implicit hybrid FV/FE projection method for weakly compressible flows, J. Comput. Phys. 421 (2020) 109743.
[73] S. Busto, L.D. Rio, M. Vázquez-Cendón, M. Dumbser, A semi-implicit hybrid finite volume / finite element scheme for all Mach number flows on staggered unstructured meshes, Appl. Math. Comput. 402 (2021) 126117.
[74] R. Becker, Stosswelle und detonation, Physik 8 (1923) 321.
[75] A. Bonnet, J. Luneau, Aérodynamique. Théories de la Dynamique des Fluides, Cepadues Editions, Toulouse, 1989.
[76] J.B. Bell, P. Coletta, H.M. Glaz, A second-order projection method for the incompressible Navier–Stokes equations, J. Comput. Phys. 85 (1989) 257–283.

[77] M. Tavelli, M. Dumbser, A staggered space–time discontinuous Galerkin method for the incompressible Navier–Stokes equations on two–dimensional triangular meshes, Comput. Fluids 119 (2015) 235–249.
[78] M. Tavelli, M. Dumbser, A pressure-based semi-implicit space-time discontinuous Galerkin method on staggered unstructured meshes for the solution of the compressible Navier–Stokes equations at all Mach numbers, J. Comput. Phys. 341 (2017) 341–376.
[79] S. Busto, J. Ferrín, E. Toro, M. Vázquez-Cendón, A projection hybrid high order finite volume/finite element method for incompressible turbulent flows, J. Comput. Phys. 353 (2018) 169–192.
[80] U. Ghia, K.N. Ghia, C.T. Shin, High-Re solutions for incompressible flow using Navier–Stokes equations and multigrid method, J. Comput. Phys. 48 (1982) 387–411.
[81] S. Gavrilyuk, K. Ivanova, N. Favrie, Multi-dimensional shear shallow water flows: problems and solutions, J. Comput. Phys. 366 (2018) 252–280.
[82] K. Ivanova, S. Gavrilyuk, Structure of the hydraulic jump in convergent radial flows, J. Fluid Mech. 860 (2019) 441–464.
[83] M. Lukácová-Medvidóvá, G. Puppo, A. Thomann, An all Mach number finite volume method for isentropic two-phase flow, J. Numer. Math. (2022), doi:10.1515/jnma-2022-0015. In press
[84] F. Thein, E. Romenski, M. Dumbser, Exact and numerical solutions of the Riemann problem for a conservative model of compressible two-phase flows, J. Sci. Comput. (2022). in press
[85] M. Dumbser, D. Balsara, M. Tavelli, F. Fambri, A divergence-free semi-implicit finite volume scheme for ideal, viscous and resistive magnetohydrodynamics, Int. J. Numer. Methods Fluids 89 (2019) 16–42.
[86] H. Ranocha, L. Dalcin, M. Parsani, Fully discrete explicit locally entropy-stable schemes for the compressible Euler and Navier–Stokes equations, Comput. Math. Appl. 80 (5) (2020a) 1343–1359.
[87] H. Ranocha, M. Sayyari, L. Dalcin, M. Parsani, D.I. Ketcheson, Relaxation Runge–Kutta methods: fully discrete explicit entropy-stable schemes for the compressible Euler and navier-Stokes equations, SIAM J. Sci. Comput. 42 (2020b) A612–A638.
[88] D. Mitsotakis, H. Ranocha, D. Ketcheson, E. Suli, A conservative fully discrete numerical method for the regularized shallow water wave equations, SIAM J. Sci. Comput. 43 (2) (2021) B508–B537.
[89] L. Brugnano, F. Iavernaro, Line Integral Methods for Conservative Problems, Chapman et Hall/CRC, Boca Raton, 2016.
[90] L. Brugnano, F. Iavernaro, Line integral solution of differential problems, Axioms 7 (2) (2018) 36.
[91] L. Krivodonova, J. Xin, J.-F. Remacle, N. Chevaugeon, J. Flaherty, Shock detection and limiting with discontinuous Galerkin methods for hyperbolic conservation laws, Appl. Numer. Math. 48 (3–4) (2004) 323–338.
[92] D. Kuzmin, Hierarchical slope limiting in explicit and implicit discontinuous Galerkin methods, J. Comput. Phys. 257 (Part B) (2014) 1140–1162.
[93] X. Zhang, C. Shu, On positivity-preserving high order discontinuous Galerkin schemes for compressible Euler equations on rectangular meshes, J. Comput. Phys. 229 (23) (2010) 8918–8934.
[94] M. Sonntag, C. Munz, Shock Capturing for discontinuous Galerkin methods using Finite Volume Subcells, in: J. Fuhrmann, M. Ohlberger, C. Rohde (Eds.), Finite Volumes for Complex Applications VII, Springer, 2014, pp. 945–953.
[95] M. Dumbser, O. Zanotti, R. Loubère, S. Diot, A posteriori subcell limiting of the discontinuous Galerkin finite element method for hyperbolic conservation laws, J. Comput. Phys. 278 (2014) 47–75.
[96] M. Sonntag, C. Munz, Efficient parallelization of a shock capturing for discontinuous Galerkin methods using finite volume sub-cells, J. Sci. Comput. 70 (2017) 1262–1289.